NATIONAL COOPERATIVE HIGHWAY RESEARCH PROGRAM REPORT **52**

MEASUREMENT OF PAVEMENT THICKNESS BY RAPID AND NONDESTRUCTIVE METHODS

HIGHWAY RESEARCH BOARD
NATIONAL RESEARCH COUNCIL
NATIONAL ACADEMY OF SCIENCES—NATIONAL ACADEMY OF ENGINEERING

/MEASUREMENT OF PAVEMENT
THICKNESS BY RAPID AND
NONDESTRUCTIVE METHODS

S. D. HOWKINS
IIT RESEARCH INSTITUTE
CHICAGO, ILLINOIS

SUBJECT CLASSIFICATION
   CONSTRUCTION
   GENERAL MATERIALS

NATIONAL COOPERATIVE HIGHWAY RESEARCH PROGRAM

Systematic, well-designed research provides the most effective approach to the solution of many problems facing highway administrators and engineers. Often, highway problems are of local interest and can best be studied by highway departments individually or in cooperation with their state universities and others. However, the accelerating growth of highway transportation develops increasingly complex problems of wide interest to highway authorities. These problems are best studied through a coordinated program of cooperative research.

In recognition of these needs, the highway administrators of the American Association of State Highway Officials initiated in 1962 an objective national highway research program employing modern scientific techniques. This program is supported on a continuing basis by funds from participating member states of the Association and it receives the full cooperation and support of the Bureau of Public Roads, United States Department of Transportation.

The Highway Research Board of the National Academy of Sciences-National Research Council was requested by the Association to administer the research program because of the Board's recognized objectivity and understanding of modern research practices. The Board is uniquely suited for this purpose as: it maintains an extensive committee structure from which authorities on any highway transportation subject may be drawn; it possesses avenues of communications and cooperation with federal, state, and local governmental agencies, universities, and industry; its relationship to its parent organization, the National Academy of Sciences, a private, nonprofit institution, is an insurance of objectivity; it maintains a full-time research correlation staff of specialists in highway transportation matters to bring the findings of research directly to those who are in a position to use them.

The program is developed on the basis of research needs identified by chief administrators of the highway departments and by committees of AASHO. Each year, specific areas of research needs to be included in the program are proposed to the Academy and the Board by the American Association of State Highway Officials. Research projects to fulfill these needs are defined by the Board, and qualified research agencies are selected from those that have submitted proposals. Administration and surveillance of research contracts are responsibilities of the Academy and its Highway Research Board.

The needs for highway research are many, and the National Cooperative Highway Research Program can make significant contributions to the solution of highway transportation problems of mutual concern to many responsible groups. The program, however, is intended to complement rather than to substitute for or duplicate other highway research programs.

FOREWORD

By Staff

Highway Research Board

This report considers the feasibility of various acoustic (sonic), nuclear, and electrical techniques for nondestructive measurement of portland cement and bituminous concrete pavement thickness both during and after construction. Recommendations are made for equipment development and field testing of three specific methods that could potentially result in such measurements with the desired degree of speed and accuracy. Theoretical background information and details of laboratory experimental work leading to the recommended measurement techniques are included as appendix items of the report. Due to the increasing emphasis on acceptance testing and documentation of results in the highway construction field, highway construction, testing, and materials engineers, as well as testing equipment manufacturers, should find this a worthwhile reference document.

During recent years, more than 75,000 lane-miles of new portland cement and bituminous concrete pavements have been built per year on the primary state highway systems of this country. The thickness of the pavement sections, as constructed, must be measured to determine compliance with plans and specifications. The general current practice is to take one or two cores of the pavement per lane-mile for measurement as documentary evidence of contract performance. In extreme cases, as high as 10 cores per lane-mile may be required. When the tests indicate that a particular pavement section is outside of the tolerance limits for minimum thickness, the contract price is usually reduced in accordance with a predetermined schedule. To preclude this possibility, contractors may at times find it desirable to construct pavements to greater thicknesses than planned. Such practices must ultimately result in higher highway construction costs.

Rapid and nondestructive methods of measuring pavement thickness, both during and after construction, would have many advantages over the current procedure of taking cores from completed pavements. Such methods would permit a much larger number of thickness measurements per lane-mile, thus providing a more accurate basis for the determination of compliance with specifications. A large number of measurements would also make it possible to rely on statistical sampling procedures for product acceptance. Measurements during construction would permit the contractor to alter paving operations to meet specified tolerance limits and reduce the possibility of large portions of pavements being built to thicknesses other than originally planned.

The ultimate objective of the study, undertaken by IIT Research Institute, was to recommend a method or methods for the rapid and nondestructive measurement of pavement thickness that exhibits the greatest promise for eventual practical field application. The initial effort of the researchers was to review and evaluate all available literature pertaining to acoustic, nuclear, and electrical nondestructive

testing techniques being utilized outside of the highway industry. With this background, theoretical studies and laboratory experimental investigations were conducted involving a number of the feasible techniques that were considered new to the highway field.

The report recommends that research in this area be continued to further develop and field test the three new measurement methods found to hold the most promise for rapid and nondestructive determination of pavement thickness, both during and after construction. Instructions are given for the fabrication of a pair of large mosaic transducers for further laboratory testing and field evaluation of the thickness measurement technique considered most promising. If this procedure does not perform as anticipated, the IITRI researchers suggest certain modifications of a mechanical impact method as an alternate for field testing. Recommendations are also made for testing under field conditions a nuclear pellet technique which involves the spreading of a low-energy type of radioactive material at the base course-pavement interface during construction. A measure of activity at the pavement surface can be translated into pavement thickness.

Although unrelated to the research covered in this report, several procedures for pavement thickness measurement have been developed and are currently under field investigation. These include state-BPR-sponsored studies involving sonic devices to measure thickness of hardened and plastic concrete. A BPR in-house study is continuing to evaluate an electrical resistivity method for measurement of pavement thickness.

The majority of experimental work to date, other than that covered in this report, has dealt with hardened portland cement concrete pavements. There continues to be a need for rapid and nondestructive thickness measurements of both portland cement and bituminous pavements during and after construction. The need for continued research in this area is actually becoming more critical as highway construction costs continue to increase, pavement design procedures attain more sophistication, and the desirability of documentary data on contract performance becomes more prevalent.

CONTENTS

FIGURES

TABLES

MEASUREMENT OF PAVEMENT THICKNESS BY RAPID AND NONDESTRUCTIVE METHODS

SUMMARY   Three different techniques are recommended for thickness measurement, as follows:

1. Large mosaic ultrasonic transducers (estimated accuracy ±2 percent) can be used on any type of pavement under any conditions (that is, on bituminous or portland cement concrete pavements in either the plastic or hardened states and having a thickness of up to 10 in.) with an estimated measurement time of 30 sec. These units are suitable for operation by an unskilled man, and give digital read-out of thickness if required. The prototype has been designed but not yet constructed. Experimental data are available based only on small model experiments. The small model is also accurate to ±2 percent, but has poor beam collimation due to its small size, thus requiring a skilled operator.

2. The short mechanical impulse source with ultramicrometer detector (accuracy ±2 percent) can be used on any type of pavement in the hardened state, but difficulties are anticipated in attempts to apply the unit to unhardened concrete. The estimated measuring time is 30 sec, the unit being suitable for operation by a semi-skilled man, who should be capable of making a fine adjustment to an ultramicrometer. Digital read-out of thickness is available if required. Experimental tests of the system have been made on 10-in. slabs of portland cement concrete (a) air-backed and (b) on a gravel base course, as well as on 5-in. slabs of air-backed bituminous concrete. Tests gave satisfactory results except that weak signal strength made the system vulnerable to spurious signals on occasion. Future improvements could eliminate this problem.

3. Scattering of radioactive pellets prior to the laying of pavement is the most highly recommended technique for all future roads. It has an accuracy of ±1 percent and can be used on any type of pavement under any conditions (that is, on bituminous or portland cement concrete pavements in either the plastic or hardened states and having a thickness of up to 10 in.) The estimated measurement time is a few minutes. This is a simple and reliable system, suitable for operation by an unskilled man with no safety hazard involved. The cost of the pellets is estimated at $80 per lane-mile. The only disadvantages are that it cannot be applied to existing roads, and continuous measurement of thickness is not possible although frequent spot checks can be substituted.

All other techniques investigated in this work were found to be unsuitable or very limited in their application.

CHAPTER ONE

INTRODUCTION

A need exists to measure the in-situ thickness of both portland cement and bituminous concrete pavements. The objective of NCHRP Project 10-6 is to determine the feasibility of past, present, and possibly future nondestructive methods which will provide accurate and rapid thickness measurements.

Initially work on this project was directed toward determining the state-of-the-art in the use of acoustic (sonic or ultrasonic), nuclear, and electrical (including magnetic and electromagnetic) methods. The research approach included an extensive literature survey in conjunction with theoretical and experimental investigations of possible techniques.

After this initial research, attention was concentrated on new and original methods of applying each of the three disciplines (acoustics, nuclear physics, and electronics) to the measurement of pavement thickness. Because of the different approaches adopted by each of the three separate disciplines, the various chapters of this report are subdivided to present the three approaches under separate headings. In each of these approaches many different possibilities were investigated before three successful acoustic and nuclear techniques finally evolved. The results of the earlier investigations are important, however, in showing the necessity for the methods eventually employed in the final recommended techniques. For this reason the experimental approaches are described as far as possible in chronological sequence in the appendices, and details of the successful methods are included at the end of the appendices on acoustics and nuclear physics (Appendix A and Appendix B, respectively).

Of the more than 150 papers reviewed during this project, only about 6 were directly concerned with the nondestructive measurement of in-situ pavement thickness. With few exceptions, the present state-of-the-art has relied heavily upon direct application of existing nondestructive thickness-measuring techniques. Little attention has been given to the fact that these techniques were developed primarily for measuring homogeneous, fine-grained materials such as aluminum and steel. Because of the basic macrostructure of portland cement and bituminous concrete, in addition to the wide range of base courses upon which they are placed, many of the more common nondestructive measuring techniques are not directly applicable, if at all, to pavement thickness measurements.

The basic report includes only the results of the experimental work and the interpretation and appraisal of those results. The details of the work are presented in separate appendices for each of the three separate disciplines involved, as the technical difficulties encountered in each case were peculiar to these disciplines. Although this work has been conducted by specialists in each of the three fields, contact has been maintained with civil engineers and other personnel more familiar with highway problems, and advantage has been taken of opportunities to observe actual pavement-laying procedures in operation. Throughout this work, therefore, the needs peculiar to highway engineering have been considered before undertaking any experiment.

CHAPTER TWO

FINDINGS AND INTERPRETATION OF RESULTS

During the course of this research, several possible approaches to the problem of measuring highway thickness rapidly and nondestructively have been investigated. Of all the possibilities explored, only three techniques are finally recommended for being simply developed into a suitable thickness-measuring device that will satisfy the requirements discussed elsewhere in this report. The other techniques involve basic physical problems that would make their satisfactory incorporation in a practical thickness-measuring device difficult or impossible. It is believed

that even the negative results from this program are of importance in their indications of some fundamental limitations that may be encountered with other thickness-measuring techniques described in the literature.

In the following sections, therefore, the main findings (both positive and negative) and interpretation of the results of the research work conducted in this project are presented under the three headings "Acoustic Techniques," "Nuclear Techniques," and "Electrical Techniques."

ACOUSTIC TECHNIQUES

Early in the project the literature survey revealed some ultrasonic thickness-measuring techniques that were far from perfect. It was obvious that the limitation to these techniques could be found in the fundamental principles underlying their operation and that significant improvements could not be made by further sophistication of electronic circuitry. The orientation of this study, therefore, has been toward a more fundamental investigation of the principles that can be employed for thickness measurement. This type of basic investigation is best accomplished through the use of standard laboratory instruments, which have a much broader operating range and provide greater versatility and accuracy. Admittedly, this laboratory equipment is more sophisticated than would be required for actual field measurements. Suitable instruments with only necessary features, but with adequate accuracy, can be constructed at much lower cost. As an example, some instrumentation used to obtain velocity data in portland cement concrete is shown in Figure 1.

Furthermore, it should be noted that there are several well-known electronic techniques for processing data from transducers to give the final result in a simple form; e.g., a digital readout of thickness. The possibility of using some such system has been borne in mind continually for each technique investigated, although for obvious reasons of simplicity and versatility in the research no attempt has been made to include the necessary electronic circuitry in this study, as such work would have been outside the scope of this project. The final recommended methods are, however, easily adaptable for incorporation into a "black box" having a single dial or a digital readout of highway thickness.

Fundamentally, it is possible to make only two types of measurements using any type of sonic or ultrasonic
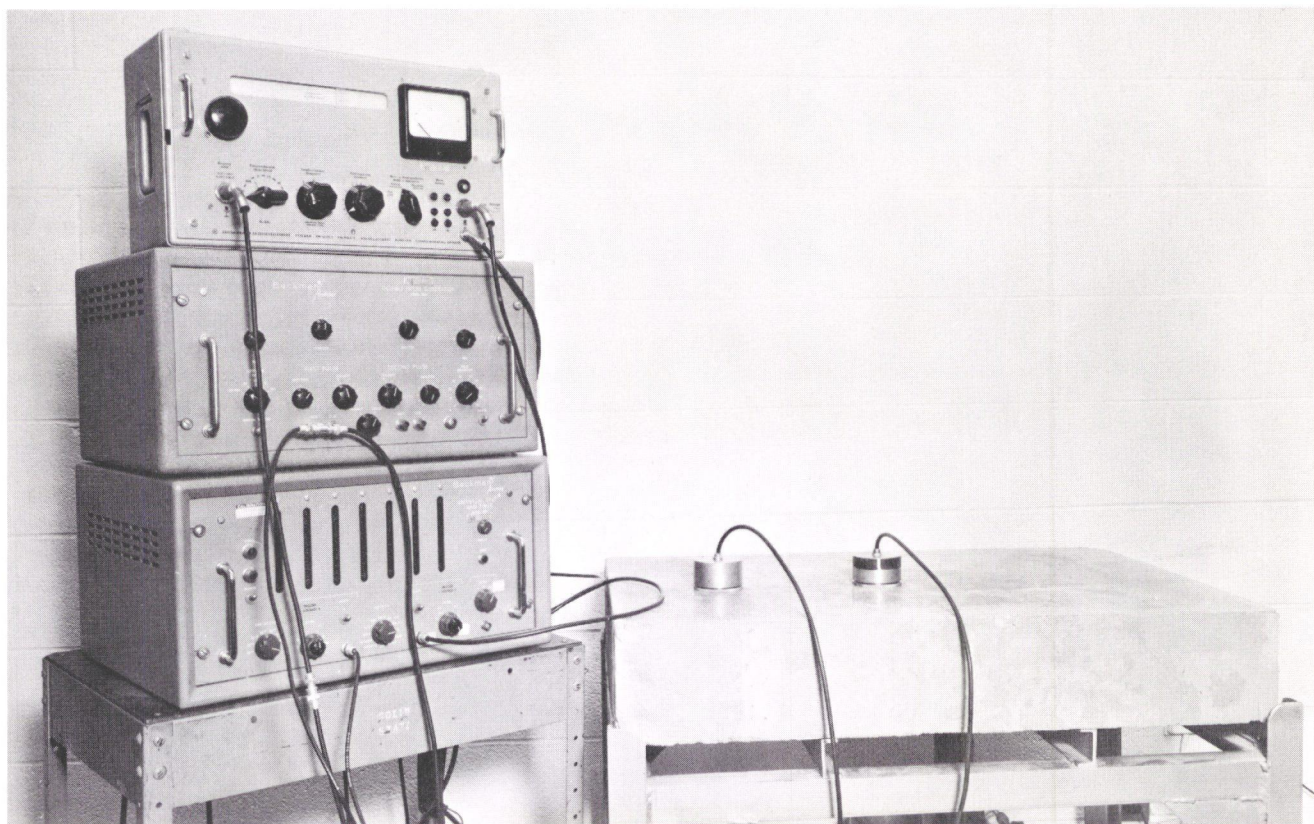
Figure 1. Instrumentation for measuring propagation time of an elastic wave. The instruments are (top) a broad-band, high-gain tunable amplifier; a double-pulse generator; and an electronic interval timer. Transmitter and receiver are shown on an experimental concrete slab at right.

apparatus. One is a measurement of sound velocity; the other, a measurement of attenuation. All other measurements of frequency, standing wave patterns, pulse time of flight, etc., can be regarded as being implicit measurements of attenuation or velocity. When considering the propagation of sound in concrete, the problem of measuring attenuation becomes formidable. There are two reasons for this. Experiments at IIT Research Institute (IITRI) and those of other researchers have shown that it is virtually impossible to remove a transducer from a concrete surface and then replace it without changing the degree of coupling of the sound energy between the transducer and the concrete; this is true for both transmitters and receivers. Secondly, for the case of sound waves in concrete where the wavelength is of the order of the aggregate size, the attenuation varies as the fourth power of the size of the aggregate. The attenuation would therefore fluctuate wildly from one point to another in the concrete. For these reasons it was decided early in the project to concentrate entirely on measurements of velocity.

In Appendix A some discussion is devoted to the problem of sound propagation in a bounded medium, such as a pavement slab, and to the effect of scattering from particles of aggregate. Without going into great technical detail, some of the results of this acoustical theory, together with some experimentally gained information, are summarized here because they are important and fundamental to any acoustic thickness-measuring technique developed.

1. An upper limiting frequency for ultrasonic propagation in concrete exists, owing to the sharp rise in attenuation with frequency. For the practical purpose of thickness measurement, this upper frequency limit is 150 to 200 kcps (kilocycles per second) for portland cement concrete.

2. Radiation of acoustic energy into the pavement is governed by diffraction theory and depends principally on the ratio of the wavelength to the diameter of the transducer. If the transducer is very small compared to the wavelength, energy will be radiated in a hemispherical pattern. (This assumes that the point source is mounted on a large, rigid baffle.) If, in contrast, the transducer is many wavelengths in diameter, radiation will occur in a narrow, well-collimated beam. At intermediate values of the diameter-wavelength ratio, the radiation pattern will be neither a hemisphere nor a collimated beam, but will consist of various lobes with relative amplitudes and directions dependent on the detailed geometry of the transducer.

3. Many different types of elastic waves can be generated in a bounded medium such as a pavement slab. Some of these waves can travel through the slab and others travel along the surface. Their velocities are, in general, all different and depend not only on the properties of the concrete, but also on the geometry and size relative to the wavelength. The mode or type of wave generated by a transducer on a concrete surface is determined by the angle of incidence of the sound. Therefore, unless the sound beam is perfectly collimated, many different angles of incidence will exist simultaneously, hence many spurious modes will be generated.

4. Two different ways of operating transducers in a thickness measurement are:

(a) Continuous-wave operation. This involves essentially a measurement of phase of the received signal. For a successful measurement of this type, it is necessary to reduce all spurious signals as far as possible. Difficulties are also encountered owing to multiple reflections occurring in the pavement slab. The problem of spurious mode generation can be overcome in practice if it is possible to produce a single well-collimated beam, which also serves to reduce the problem of multiple reflections. The multiple reflection problem can be further reduced by operating at normal incidence so that the wave is reflected at 90° from the bottom of the pavement or by operating near the upper frequency limit to get a maximum possible attenuation of unwanted waves. If it is possible to reduce unwanted signals to a reasonable level, sophisticated techniques (e.g., the modified sing-around system) have been developed to handle the phase measurement problem.

(b) Pulse operation. For this type of operation the transducer is excited either by a short rectangular pulse of electrical energy (referred to herein as a D-C pulse) causing it to "ring" mechanically, or a short burst of high-frequency energy * (referred to herein as an R.F. pulse) thus producing a damped wave train. Attempts can then be made to measure the time of flight for this wave train to be reflected from the bottom of the concrete. However, owing to the finite length of the pulse (wave train) produced, spurious surface waves arrive at the receiver before the desired reflected signal and mask the exact point in time at which the reflected signal comes in. As with the continuous-wave system, one way to overcome this problem is to suppress the surface waves by using a large transducer to generate a "collimated pulse." Owing to the wide spectrum of Fourier components present in a pulse, however, the problem of suppressing surface waves is even more severe than for the continuous-wave case. An alternative solution to the problem is to produce a pulse so short (i.e., very highly damped) that there will be a distinct time interval between the arrival of the surface pulse and the reflected pulse. The problem of producing very short pulses with conventional electromechanical transducers involves the construction of a transducer having a very low Q † factor (i.e., a highly damped transducer).

A further consideration with the pulse method is that the risetime of the pulse should be sufficiently short to reduce errors associated with identifying the start of the pulse. The risetime is controlled by the mechanical resonant frequency of the transducer and consequently this should be as

---

* In the limit, when the pulse length becomes long enough, standing waves can be established and one has, in effect, "continuous waves."
† The Q or quality factor of a transducer is the ratio of the mechanical energy stored to the mechanical energy dissipated during each cycle

high as possible. The upper limit is again imposed by the rapid rise of attenuation with frequency. For pulse methods, therefore, the optimum frequency is fixed in the range of 150 to 200 kcps.

5. The velocity of sound in concrete varies greatly in space and even slowly in time. Consequently, it must be assumed to be unknown and an independent measurement of sound velocity must be involved in any thickness measurement. In practice this means that two independent measurements must be made, either of time of flight or of phase. Furthermore, owing to velocity dispersion (i.e., the dependence of sound velocity on the mode of propagation and the dimensions of the concrete mentioned in item 3), care must be taken that the two measurements both refer to the same velocity. A question also arises concerning the constancy of the sound velocity throughout the section of pavement being measured. Experiments at IITRI and elsewhere have shown that in nearly all cases the velocity can be assumed to be uniform throughout the section. However, a theoretical analysis included in Appendix A shows that if the velocity cannot be assumed to be a constant throughout the thickness, further independent measurements can be used to provide progressively better approximations to compensate for the velocity variation.

As a summary of the previous items, it can be concluded that essentially the problem of measuring highway thickness has reduced to a problem of transducer design. The objectives are either to produce transducers generating a single mode in the concrete in the form of a continuous collimated wave, or to produce highly damped pulse transducers or, alternatively, pulse transducers in which the surface wave is suppressed.

In the following section the experiments that originally enabled these design objectives to be precisely formulated are presented in chronological order; then the experiments which finally lead to a successful design, and hence a successful thickness-measuring technique, are presented.

Description of Experiments

In order to obtain a general evaluation of acoustic measuring methods, some initial experimental work was carried out to determine some of the material properties of concrete, limitations of basic measuring techniques, and the design of electromechanical transducer devices. Each of these areas is considered in detail in the discussions given in Appendix A, and the results are summarized in the following.

MATERIAL PROPERTIES

Because of the nature of portland cement concrete and bituminous concrete, conventional nondestructive testing techniques that have been used for metals and other homogeneous materials cannot be used for highway thickness measurement without modification. The maximum frequency of ultrasonic waves that can be used is in the range of 150 to 200 kcps.

INITIAL MEASURING TECHNIQUES

Simple resonant techniques cannot be used without modification. Frequencies higher than 100 kcps must be used for pulse techniques.

ELECTROMECHANICAL TRANSDUCERS

Of the many types of electromechanical transducers available, the most suitable types for highway thickness measurement are magnetostrictive and electrostrictive. Lead zirconate titanate is recommended as a suitable electrostrictive material.

MODIFIED SING-AROUND TECHNIQUE

If other, more fundamental problems associated with the development of suitable transducers can be solved, the modified sing-around technique will provide a suitable way of electronically handling the data. It is also important in enabling high-frequency ultrasound to be used for resonance techniques.

RESONANCE METHODS

The resonance method described by the Portland Cement Association incorporates some erroneous assumptions. Basically the method is good and modifications introduced by the incorporation of the modified sing-around technique, and possibly the use of shear wave transducers or the application of a correction factor, would make it a useful method of measuring highway thickness. The use of the modified sing-around technique, however, is still based on the availability of suitable transducers.

SHEAR TRANSDUCER EXPERIMENTS

Shear waves can be propogated in concrete but cannot be used to eliminate surface waves by destructive interference. No method dependent on eliminating surface waves by destructive interference can be successful.

INITIAL PULSE TIME-OF-FLIGHT METHODS (DUAL-FREQUENCY METHOD)

The dual-frequency method is capable of enabling thickness measurements to be made with an accuracy of about ± 4 percent. It has the severe disadvantage, however, of requiring a skilled operator to first adjust the transducers to an optimum position with the aid of an oscilloscope and then to interpret the oscilloscope trace to determine the arrival point of the reflected pulse. Further transducer development in the direction of more highly damped transducers or larger transducers is necessary to obviate these disadvantages.

DAMPED ELECTROMECHANICAL TRANSDUCERS

This was an attempt to design very highly damped transducers for use in a pulse time-of-flight method as described.

The aim was to achieve sufficient damping for time separation between the unwanted surface wave and the reflected signal to be achieved. It was found that present damping techniques have reached the limit of the state-of-the-art in this direction. It will require an extensive research program to produce transducers that have significantly lower quality factors so that time separation in a pulse time-of-flight method could be used. Therefore, no further work in this direction is recommended.

MOSAIC TRANSDUCERS

Large mosaic transducers have been developed for use in conjunction with the pulse time-of-time technique. The resulting method is capable of being used to measure highway thickness to within ± 2 percent. It still requires a semiskilled operator to adjust the apparatus initially. The arrival point of the desired signal, however, is sharp enough to be handled electronically by a pulse sing-around system.

Predictions based on the performance of these mosaic transducers and linear array types have enabled a still larger transducer to be designed. It is predicted that this final transducer will be capable of being used by a completely unskilled person to measure highway thickness to an accuracy of ± 2 percent in a pulse sing-around technique. Tests may also show that a continuous-wave sing-around technique could be used in a resonance method. Such a method could have the advantage of being capable of still higher accuracies and of using less complicated, hence less costly, electronic equipment. This cannot be predicted until the transducer is built.

MECHANICAL IMPACT TECHNIQUE

A new type of method for producing short pulses by mechanical impact is capable of achieving pulses short enough for time separation methods to be used in a pulse time of flight technique. This method is capable of accuracies of ± 2 percent in a thickness measurement. It has one serious drawback, however, in that the detector used is an ultra-micrometer, an instrument which is delicate and needs careful adjustment. This instrument will have to be modified considerably, therefore, before it is suitable for use by an unskilled person in the field.

NUCLEAR TECHNIQUES

In considering the application of various nuclear techniques to the nondestructive measurement of in-situ pavement thickness, it was concluded that gamma rays and/or neutrons offer the most promise. Techniques involving the use of charged particles (i.e., electrons, protons, etc.) were ruled out because of their inherent lack of sufficient range. The selection of a given form of radiation or energy is rather straightforward, being based on energy levels, interaction phenomena, etc. However, the manner in which this energy is employed to give a measure of pavement thickness poses a question which requires considerable attention. Therefore, this investigation has included considerations of

various source geometries; i.e., the placement of that material from which radiation is ultimately detected and related to pavement thickness. (The word "source" is used herein to denote radioactive material.) Various approaches are briefly summarized as follows:

1. Attenuation of radiation through the pavement, using a source beneath the pavement. The source can be produced by (a) neutron activation of an inert material deposited prior to laying the pavement, (b) neutron capture in an inert material deposited prior to laying the pavement, or (c) spreading a radioactive isotope prior to laying the pavement.

2. Total intensity of radiation from sources distributed within the pavement. The sources can be produced by (a) neutron activation of an inert material mixed in the concrete, (b) neutron capture in an inert material mixed in the concrete, or (c) mixing a radioactive isotope with the concrete.

3. Backscattering of radiation from a source above the pavement.

The following section contains summarized discussions of these techniques. In some cases a rough analytic treatment is possible which aids in evaluating the potential of the technique. Calculations indicate that the first method (source beneath the pavement) shows the most promise and is more sensitive than the second (source distributed within the pavement) by approximately a factor of 20. Both techniques are relatively insensitive to the type of base course, because gamma rays scattered back into the detector from the base course will be reduced in energy and not counted by the detectors. The variation of the first method which employs materials that are initially inert rather than radioactive is preferred. This approach avoids the need for handling large quantities of radioactive isotopes and therefore poses no health hazards. Methods requiring the distribution or mixing of radioisotopes appear to present a formidable problem, even for the quantities estimated by this survey. Backscatter techniques appear to be applicable to bituminous pavements, but require further experimental evaluation.

The survey was limited by the need for (a) more information on pavement and roadbed composition, and (b) specification of the properties of the medium for neutron and gamma interactions based on this composition and the appropriate cross-sections. This additional information will aid in any further analysis of nuclear techniques. For those cases where an accurate analytical treatment is complex, experimental data are required to establish basic information on sensitivity and response.

Description of Experiments

Initial investigations into the nuclear properties of portland cement and bituminous concrete showed that no nuclear technique that did not require some sort of pre-preparation of the pavement could be used.* Techniques

* One exception to this is the possible method of activating the aluminum present in the concrete by a nuclear source on top of the pavement. This could only be used if the pavement were on a base course having a relatively low aluminum content

involving pre-preparation of the concrete are of two types—active and passive. The active techniques involve the spreading of a radioactive material in or under the pavement and the passive techniques involve the spreading of or doping of the pavement with a nonactive material (indium and cadmium are recommended) which is later made radioactive just prior to making a measurement by irradiation from a source above the pavement. Both of these techniques have been thoroughly investigated (details are given in Appendix B). They both have serious disadvantages associated with the large quantity of radioactive material that would be needed and with nuclear interactions in the concrete itself. However, further work in these areas is deemed not worthwhile owing to the discovery of the technique of radioactive pellets, which has none of these disadvantages.

The radioactive pellet technique is capable of an accuracy which increases with the counting time. For a counting time of a few minutes, pavement thickness can be measured to an accuracy of ± 1 percent. The technique is simple and can easily be used by an unskilled person. The measuring apparatus is basic and inexpensive, and the cost of pre-preparation of the pavement would be about $80 for a strip of concrete 15 ft wide and 1 mile long. The technique is equally applicable to portland cement concrete and bituminous concrete in both the plastic and the hardened states.

Even without any special precautions being taken, no real safety hazards are associated with this method, although it is recommended that the pellets should not be carried in the pocket. A simple automatic dispensing device would completely eliminate the need for handling the pellets at all.

Radioactive isotopes having a suitable half-life for the length of time over which thickness measurements are required can be chosen. For example, Co^{60} will enable thickness measurement to be made over a period of 10 to 20 years, whereas if the measurement is to be made within 1 month of laying the pavement Rb^{86} can be used.

Observations of practical road laying procedures have indicated that no difficulties would be entailed in the initial placement of the pellets. They can easily be made in a form so that they will remain at the base course-pavement interface after the concrete (either portland cement or bituminous) has been placed.

ELECTRICAL TECHNIQUES

If an electric current is caused to flow in a wire coil, a magnetic field will be produced which will vary in sympathy with the current. Now, if the coil is placed close to and with its axis normal to an electrically conducting surface (metal plate), circulating (eddy) currents will be induced in the plate. These eddy currents, in turn, produce a magnetic field of their own, which is in direct opposition to that of the coil. The net result, looking into the electrical

terminals of the coil, is a decrease in the coil self-inductance (Appendix C). For flat conducting surfaces or plates which are large compared to the coil diameter, the inductance of the coil is found to change in sympathy with the coil-plate separation; a decrease in separation results in a decrease of inductance. Hence, it is seen that this change in inductance can be used effectively to measure displacement. Several methods for electrically indicating this displacement to an accuracy of at least ± 1 percent are detailed in Appendix C.

Empirical data have been obtained to verify that the presence of either portland cement or bituminous concrete between the measuring coil and a conducting surface does not alter the variation of inductance with coil-plate spacing. Consequently, if the lower surface of the pavement rests on a conducting material and the coil is placed on or near the upper surface, the coil-plate spacing is related to the pavement thickness, and this thickness may be determined through measurements of coil self-inductance.

A typical conducting surface might be a 0.001-in. thick metallic foil on a 0.010-in. thick plastic film placed continuously along the roadbed as a vapor barrier. A thickness measurement, based on these principles, involves a comparison measurement. One coil is placed on the pavement surface. Separate from this measuring coil is an identical second coil mounted on a calibrated fixture which incorporates a large flat metallic reference plate. Because the coils are identical, the effect of the metallized film upon the measuring coil will be the same as the effect of the reference plate upon the reference coil at equal spacings. An electronic indicator (bridge circuit) is used to detect the difference in inductance between coils when the spacing, from their respective conductors, is unequal. By adjusting the reference coil-plate spacing until zero difference in inductance exists between coils, a direct reading of pavement thickness is obtained.

No electrical technique is recommended for the following reasons:

1. The research has shown that the electrical properties of concrete preclude the use of any direct technique which does not entail the placing of conducting foil prior to laying the pavement. A technique has reportedly been developed by the Time Engineering Laboratory which does not require pre-preparation, but evaluation of this method was not feasible under the project limitations.

2. Any method involving pre-preparation of the road by the placement of conducting foil is much more expensive than the nuclear pellet technique. The cost of pre-preparation would be about $675 for a 15-ft wide strip of concrete 1 mile long.

3. In order to avoid interference from the reinforcing mesh, an elaborate twin-coil technique is necessary. This technique does not have the simplicity, reliability, and accuracy of the nuclear pellet technique.

CHAPTER THREE

APPLICATION OF RESULTS

This chapter summarizes the results obtained from the point of view of how they could be used in the future for practical highway thickness measurements.

As previously noted, three successful techniques (two acoustic and one nuclear) have been experimentally and theoretically evaluated and are recommended for future application in a thickness-measuring apparatus. Of the two acoustic techniques, the mechanical impact method has been completely tested in the laboratory, but has a drawback in that it will require modification of the detector part of the equipment to make it suitable for application in the field. The other acoustic technique requires no modification, but a full-scale version of the equipment has not yet been constructed. Therefore, a complete experimental evaluation of its capabilities is not available. If, however, future tests with this equipment, when it is constructed, yield results in accordance with predictions, this acoustic technique will be recommended in preference to the other. In any case, acoustic techniques do not require any pre-preparation of the pavement before it is laid and are therefore recommended for all existing highways.

In the future it is recommended that all highways on which a thickness determination may be required should be seeded with nuclear pellets prior to the laying of the concrete. Large-scale mapping of the thickness can then be accomplished by the nuclear technique. Then, if a particular area needs more detailed small-scale mapping, an acoustic technique can be used.

CHAPTER FOUR

CONCLUSIONS AND SUGGESTED RESEARCH

As a result of the work performed in this project, it is possible to recommend three different techniques that could be used in equipment to measure highway thickness. Also as a result of the project studies, it is recommended that the following further research be performed:

1. The large mosaic transducers described in the final recommendations contained in Appendix A should be constructed according to the specifications given. Laboratory tests should be made to check the performance of the apparatus for measuring thickness (a) by means of a pulse time-of-flight system and incorporating the pulse sing-around technique, and (b) under continuous-wave conditions using the modified sing-around technique. A prototype instrument should then be built and tested under field conditions.

2. If, and only if, the tests with the large mosaic transducers, give negative results (this is believed to be unlikely), the ultramicrometer used in the mechanical impact technique should be modified for use under field conditions and the technique tested in the field.

3. The nuclear pellet technique should be tested under field conditions to determine the optimum size and shape of pellets. Isotopes having various half-lives should be used.

REFERENCES

1. MUENOW, R., "A Sonic Method to Determine Pavement Thickness." Portland Cement Assn.

2. BRADFIELD, G., and GATFIELD, E. N., "Determining the Thickness of Concrete by Mechanical Waves: Directed Beam Method." *Mag. Conc. Res.,* Vol. 16, No. 46, pp. 49-53 (Mar. 1964).

3. JONES, R., "Measurement of the Thickness of Concrete Pavements by Dynamic Methods: A Survey of the Difficulties." *Mag. Conc. Res.,* Vol. 1, No. 1, pp. 31-34 (Jan. 1949).

4. LESLIE, J. R., "Pulse Technique Applied to Dynamic Testing." *Proc. ASTM,* Vol. 50, pp. 104-116 (1950); *ASTM Spec. Tech. Publ. No. 101* (1951).

5. JONES, R., "A Vibration Method for Measuring the Thickness of Concrete Road Slabs In-Situ," *Mag. Conc. Res.,* Vol. 6, No. 6, pp. 97-102 (July 1955).

6. BRADFIELD, G., and WOODROOFE, E. P. H., "Determining the Thickness of Concrete Pavements by Mechanical Waves: Diverging Beam Method." *Mag. Conc. Res.,* Vol. 16, No. 46, pp. 45-48 (Mar. 1964).

7. CAMP, L., "Lamination Designs for Magnetostrictive Underwater Electroacoustic Transducers." *Jour. Acoust. Soc. Am.,* Vol. 20, No. 5, pp. 616-619 (Sept. 1948).

8. MAZARI, M., "Coefficients of Linear Absorption of Fast Neutrons in Concrete." *Rev. Mex. Fis.,* Vol. 6, pp. 1-8 (1957).

9. BOURGEOIS, J., ERTAUD, A., and JACKSQUESS, T., "Investigation of Several Special Shielding Concretes." *Jour. Phys. Radium,* Vol. 14, pp. 317-322 (May 1953).

10. BEAVER, J., Lane-Wells Company, Houston, Tex. (Private Communication).

11. TOLAN, J. H., and McINTOSH, W. T., "Investigations of Applications of Compton Backscatter." *Rep. NR-88,* Lockheed Nuclear Products, Marietta, Ga. (July 1960).

12. PRICE, B. T., HORTON, C. C., and SPINNEY, K. T., *Radiation Shielding.* Pergamon (1957).

13. *Reactor Physics Constants.* ANL-5800, 2nd Ed. Argonne Nat. Lab. (July 1963).

14. PLACZEK, G., "The Functions $E_n(X) = \int_1^\infty e^{-xu} u^{-n}\, dx$." *NRC No. 1547, MT-1,* Nat. Res. Council of Canada (1946).

15. HART, H., and KARSTENS, E., "Radioactive Isotopes in Thickness Measurement." *Vieb Vierial Tech.* (Berlin) (1958).

16. PLACZEK, G., "The Functions $E_n(X)$." *Nat. Res. Rep. NRC No. 1547,* Div. of Atomic Energy, Nat. Res. Council of Canada (Dec. 1946).

17. *American Institute of Physics Handbook,* pp. 8-104. McGraw-Hill (1957).

18. GRODSTEIN, G. W., "X-ray Attenuation Coefficients from 10 kev to 100 Mev." Nat. Bur. Stand. Circ. 583, U.S. Govt. Printing Off., Washington, D.C., 50 pp. (Apr. 30, 1957).

19. MANKE, P. G., and HEMPHILL, L., "Nondestructive Thickness Tests for Highway Pavements." *Res. Pub. No. 14,* School of Civil Eng., Oklahoma State Univ., pp. 9-24 (Bibliography of Nuclear Methods).

20. BAKER, P. E., "Density Logging with Gamma Rays." *Petrol. Trans. AIME,* Vol. 210, pp. 289-294 (Oct. 1957).

21. FEARON, R. E., "Gamma-Ray Well Logging." *Nucleonics,* Vol. 7, No. 4, pp. 67-75 (Apr. 1949).

22. CAREY, W. N., JR., and REYNOLDS, J. F., "Some Refinements in Measurement of Surface Density by Gamma Ray Absorption." *HRB Spec. Rep. 38* (1958) pp. 1-23.

23. COLE, E. K., and DAVIS, R. G., "Backscatter Measuring Gauges." Brit. Patent No. 814,286 (June 3, 1959).

24. PURTNAM, J. L., "Development Control and Automation." Vol. 2, No. 11, pp. 417-421 (Nov. 1955).

25. HAMMOND, E., and ROBSON, T. D., "Comparison of the Electrical Properties of Various Kinds of Cement and Concrete." *The Engineer,* Vol. 199, No. 5165 (Jan. 21, 1955), pp. 78-80; No. 5166 (Jan. 28, 1955), pp. 114-115.

26. BALACHANDRAN, M., "Measurements of Dielectric Constants and Loss Tangents of Building Materials." (in German), *Zeits. für Angerwandte Phys.,* Vol. 7, No. 12, pp. 588-593 (Nov. 1955).

27. CUMING, W. A., "Materials for RF Shielded Chambers and Enclosures." Digest of Fourth Nat. Symp. on Radio Frequency Interference (June 1962).

28. *Reference Data for Radio Engineers.* American Book —Stratford Press, N.Y., 4th Ed. (1956).

29. REED, H. R., "Propagation Data for Interference Prediction." *RADC-TN-59-218,* Vol. 11, pp. 55-109, DDC No. AD 233-387 (Jan. 1960).

30. COHN, G. I., and EBSTEIN, B., "A Microwave Noncontacting Tracing Technique for Automatic Contour-Following Machines." *Proceedings,* National Electronics Conference (October 1956).

APPENDIX A

ACOUSTIC TECHNIQUES

ACOUSTIC WAVE PROPAGATION IN SOLIDS

In order to reduce the reader's effort in referring to other sections of this report and to other literature, the various modes or propagation of acoustic (elastic) waves in solids are defined.

1. *Longitudinal waves,* sometimes called *compressional* or *dilatational waves,* have the characteristic of oscillatory particle motion in the direction of propagation. Normally, distinction is made between two extreme boundary conditions:

(a) Propagation in a solid of infinite extent normal to the direction of propagation. This approximation is valid if the lateral dimensions are greater than a few wavelengths. In this case, lateral strains vanish. Propagation velocity in an isotropic solid is

$$C_l^2 = B/\rho \qquad \text{(A-1)}$$

in which C_l is the propagation velocity, B is the plate modulus, and ρ is the density;

(b) If the lateral dimensions are small (wire or slender bar), the lateral stresses must vanish and the governing modulus is Young's modulus, or

$$C_l^2 = E/\rho \qquad \text{(A-2)}$$

2. If vibrations are at right angles to the direction of propagation, the wave is known as a *shear wave,* and its velocity of propagation is governed by the shear modulus, μ; that is,

$$C_s^2 = \mu/\rho \qquad \text{(A-3)}$$

3. *Rayleigh waves* or *surface waves* are observed on a free surface of a solid. Particle motion is elliptical, reducing exponentially with distance beneath the surface. The Rayleigh wave velocity is somewhat lower (approximately 5 percent) than the shear wave velocity, depending primarily on the shear modulus, with other moduli modifying the velocity slightly; that is,

$$C_r = kC_s \qquad \text{(A-4)}$$

The constant, k, may be computed in terms of Poisson's ratio, σ, by the approximate relation

$$k \simeq (0.87 + 1.126\sigma)(1 + \sigma) \qquad \text{(A-5)}$$

Wavelengths must be less than the slab thickness; otherwise, these waves become Lamb waves.

4. *Lamb waves* in a sheet or slab of material are bending waves of the slab as a whole; wavelengths are greater than the slab thickness. Velocity is governed by both material elastic moduli and slab thickness.

All the different types of waves may be generated by a simple length expander transducer placed on the surface.

Let a coordinate system be designated as shown in Figure A-1, in which the base of the slab is in the x,y plane, and the top of the slab is in the $z = Z$ plane, Z being the thickness of the slab.

Transducers are placed at $(-X, 0, Z)$. Longitudinal transducers will produce motion at the interface in the z-direction. Waves propagating in the block will all have a component in the vertical (z) direction. Waves normal to the slab surface will be purely longitudinal. At other angles shear waves are also produced. On reflection at the lower surface, mode conversion takes place for all except the perpendicular direction of incidence. In other words, an incident longitudinal wave gives rise to both a reflected longitudinal and a reflected shear wave and similarly both types are produced by a pure shear wave in which there is a vibration component in the z-direction. In addition, a Rayleigh (surface) wave is produced along the upper surface.

For the case of pure shear transducers in which the direction of propagation is in the y-direction, only pure shear waves are transmitted between transducers, lying with their centers on a line parallel to the x-axis.

For shear transducers vibrating along a line parallel to the x-direction, a component of motion in this direction is to be expected. Therefore, a longitudinal wave in this direction must be anticipated. This longitudinal wave near the surface would seem to be particularly convenient for measuring the longitudinal wave velocity in this direction.

THEORETICAL METHOD OF CORRECTING FOR VARIATION OF VELOCITY WITH DEPTH IN CONCRETE

Let it be assumed initially that the velocity of sound, v_2, is constant throughout the concrete. Let the velocity of sound in the material above the concrete be v_1, the angle of incidence θ_1, the angle of refraction θ_2, and the thickness of the concrete D (Fig. A-2).

Let L be the half-distance spacing between the points of entrance into and exit of the sound from the concrete. Then

$$(\sin \theta_1)/v_1 = (\sin \theta_2/v_2 \qquad \text{(A-6)}$$

and

$$\cos \theta_2 = D/(L^2 + D^2)^{\frac{1}{2}} \qquad \text{(A-7)}$$

If τ is the half-time of travel in the concrete,

$$\tau = (L^2 + D^2)^{\frac{1}{2}}/v_2 \qquad \text{(A-8)}$$

In Eqs. A-6, A-7, and A-8, τ, L, θ_1, and v_1 are known experimentally and v_2, θ_2, and D are unknowns. These three equations can therefore be solved to give
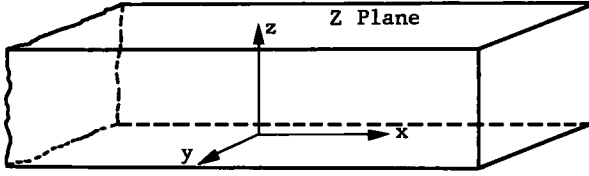
Figure A-1. Coordinate system for wave measurements.
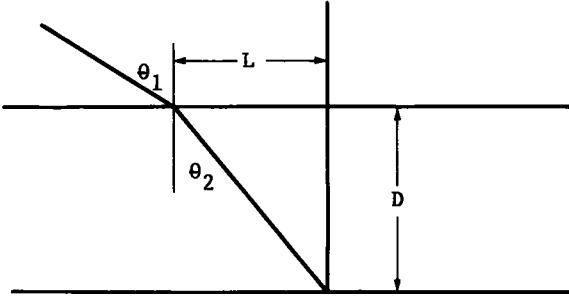
Figure A-2.

Figure A-3.

$$D = \left(\frac{L \tau v_1}{\sin \theta_1} - L^2 \right)^{\frac{1}{2}} \qquad (A-9)$$

To obtain a better approximation to a continuously varying sound velocity in the concrete, it may be assumed initially that the top half of the concrete has a velocity v_2 and the bottom half a velocity v_3 (Fig. A-3). Then

$$(\sin \theta_1)/v_1 = (\sin \theta_2)/v_2 \qquad (A-10)$$

$$(\sin \theta_2)/v_2 = (\sin \theta_3)/v_3 \qquad (A-11)$$

$$\cos \theta_2 = \frac{D/2}{[(D/2)^2 + L_1^2]^{\frac{1}{2}}} \qquad (A-12)$$

$$\cos \theta_3 = \frac{D/2}{[(D/2)^2 + L_2^2]^{\frac{1}{2}}} \qquad (A-13)$$

$$L_1 + L_2 = L_3 \qquad (A-14)$$

$$\tau = \frac{[(D/2)^2 + L_1^2]^{\frac{1}{2}}}{v_2} + \frac{[(D/2)^2 + L_2^2]^{\frac{1}{2}}}{v_3} \qquad (A-15)$$

In Eqs. A-10 through A-15 the unknowns are v_2, v_3, θ_2, θ_3, L_1, L_2, and D. In order to solve for D, therefore, an additional equation is needed. This may be obtained by using another pair of transducers and obtaining the time-of-flight for another set of angles (θ_1', θ_2' and θ_3') and corresponding displacements (L_1' and L_2'). This will give, in all, 12 equations with 11 unknowns, which can be used to determine D.

A better approximation can then be obtained by dividing the pavement into n strips, and by using $2n$ pairs of transducers the equations can be solved in each case to give D. The variation in velocity (v_1, v_2, . . ., v_n) can also be obtained.
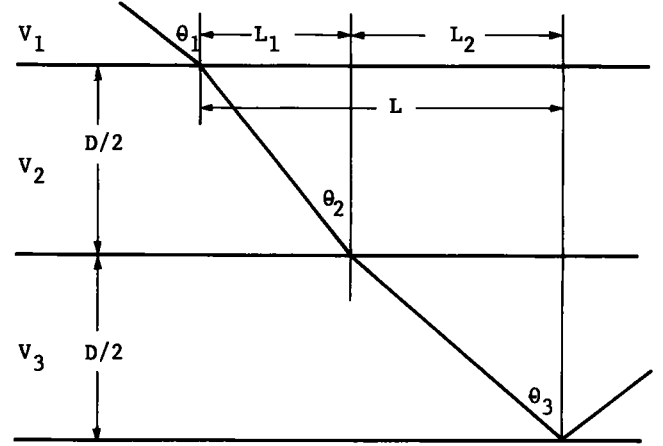
CONVENTIONAL SING-AROUND TECHNIQUES

Pulse Sing-Around

Many methods are available for measuring transit times with high accuracy. One of the best such methods is the pulse sing-around technique. In this method a pulse is sent into the material by one transducer and is detected by a second transducer. The received pulse from the second transducer is used to trigger the next transmitted pulse. Thus, a continuous series of pulses is generated, with the pulse repetition frequency being inversely proportional to the sum of the acoustic transit time and the electronic delays. The pulses can be either pulsed modulation of a high-frequency wave, or a DC pulse. Normally, the delays occurring in the electronic apparatus are small in comparison to the acoustic transit time.

This conventional sing-around method is subject to one major disadvantage—the transducers used to convert electrical to acoustic energy must have relatively low Q's (high mechanical damping), because each pulse is made up of a large number of spectral components. The low-Q transducers result in low sensitivity, and therefore require much greater electrical power for adequate results. Cumulative errors will be introduced unless the coupling between the transducers and the pavement is held constant.

CW Sing-Around

The CW sing-around technique utilizes a simple, positive, feedback loop comprising a transmitter and a detector, with the signal from the detector going via an amplifier and a limiting circuit to drive the transmitter. In such a system the circuit goes into self-oscillations at a frequency corresponding to the total delay time, T, in the whole system. T is made up of the acoustic delay, τ, and an electronic delay time, t, which is a known constant. The frequency, f, of the self-oscillations is given by

$$f = 1/(nT) = 1/[n(\tau + t)] \qquad (A-16)$$

in which n is a positive integer.

The system is thus only semi-stable and can either ring at the fundamental frequency, $1/T(n = 1)$, or it can be tripped into the higher harmonics. This simple system thus has no real advantages over the direct phase-comparison method and cannot be used for measuring concrete thickness for the same reasons.

STANDING WAVES IN A PAVEMENT

Consider two arrays of transducers mounted on a slab. Elements of each array are between adjacent pairs of the other array and the elements of each array are spaced less than one-quarter slab thickness apart. One array is fed with an oscillatory signal such that the wavelength of a sound wave in the slab is exactly twice the thickness of the slab. Assuming that the lower surface is essentially a free surface, a reflected signal from this surface will arrive at the upper surface in phase with the next transmitted cycle.

Now let the amplitude of the reflected wave be $b(< 1)$ times the original amplitude so that the amplitude of the wave which has been reflected n times is b^n.

If tuning is not exact, the amplitude of the received wave will be the sum of many multiple reflected waves, making allowance for the phase shift. In other words, the received signal will be of the form

$$A \cos(\omega t - \theta) = b \cos(\omega t - 2kx) +$$
$$b^2 \cos(\omega t - 2 \times 2\,kx) + \ldots + b^j \cos(\omega t - jkx) \quad (A\text{-}17)$$

To improve readability, write $\beta = 2kx$, and for easier manipulation, use complex notation. Then

$$A e^{i(\omega t - \theta)} = \sum_{j=1}^{\infty} b^j e^{i\omega t} e^{-ij\beta} \quad (A\text{-}18)$$

or

$$A e^{-i\theta} = \lim_{n \to \infty} \sum_{j=1}^{n} b^j e^{-ij\beta} \quad (A\text{-}19)$$

$$b e^{-i\beta} A e^{-i\theta} = \lim_{n \to \infty} \sum_{j=2}^{n-1} b^j e^{-ij\beta} \quad (A\text{-}20)$$

Therefore,

$$(1 - b e^{-i\beta}) A e^{-i\theta} = \lim_{n \to \infty} b e^{-i\beta}(1 - b^n e^{-in\beta}) \quad (A\text{-}21)$$

But

$$-b^{n+1} e^{i(n+1)\beta} \to b e^{-i\beta} \quad (b < 1) \quad (A\text{-}22)$$

Therefore,

$$A^{-1} e^{i\theta} = \frac{e^{i\beta}}{b} - 1 \quad (A\text{-}23)$$

$$A^{-1} \cos\theta = b^{-1} \cos\beta - 1 \quad (A\text{-}24)$$

$$A^{-1} \sin\theta = b^{-1} \sin\beta \quad (A\text{-}25)$$

$$A^{-2} = b^{-2} + 1 - 2b^{-1} \cos\beta \quad (A\text{-}26)$$

$$\cot\theta = \cot\beta - b \operatorname{cosec}\beta \quad (A\text{-}27)$$

Thus, the amplitude of the received wave is

$$A = 1/(1 + b^2 - 2b^{-1} \cos\beta)^{\frac{1}{2}} \quad (A\text{-}28)$$

which has a maximum value when

$$\beta = 2n\pi \quad (A\text{-}29)$$

and the phase shift between the received and transmitted wave is

$$\theta = \cot^{-1}(\cot\beta - b \operatorname{cosec}\beta) \quad (A\text{-}30)$$

(Note: when $\beta = 2n\pi$, $\theta = 2n\pi$.)

Consequently, maximum amplitude does not occur for a phase difference between transmitted and received waves of $2n\pi + \pi/4, n = 0, 1, 2 \ldots$. This is in direct contrast to the Portland Cement Association method.

An effective Q for the slab is derived by finding the frequency shift for a 3-db reduction in amplitude. Thus,

$$A^2_{max} = 2A_1^2 \quad (A\text{-}31)$$

$$A^2_{max} = (1 - b^{-1})^{-2} \quad (A\text{-}32)$$

$$2A_1^2 = 2(1 + b^2 - 2b^{-1} \cos\beta_1)^{-1} = (1 - b^{-1})^{-2} \quad (A\text{-}33)$$

hence

$$1 + b^2 - 2b^{-1} \cos\beta_1 = 2(1 - b^{-1})^2 \quad (A\text{-}34)$$

$$(1 - b^{-1})^2 - 2b^{-1}(\cos\beta_1 - 1) = 2(1 - b^{-1})^2 \quad (A\text{-}35)$$

$$2b^{-1}(\cos\beta_1 - 1) = -(1 - b^{-1})^2 \quad (A\text{-}36)$$

$$\cos\beta_1 = +1 - \frac{(1 - b^{-1})^2}{2b^{-1}} = 1 - (b - 1)^2/2b \quad (A\text{-}37)$$

Now

$$\beta = 2kx = \pi f x/c \quad (A\text{-}38)$$

$$\beta_0 = 2\pi \quad (A\text{-}39)$$

$$\beta_0/\beta_1 = f_0/f_1 \quad (A\text{-}40)$$

$$Q = \frac{f_0}{2(f_0 - f_1)} = \frac{\pi}{(2\pi - \beta_1)} \quad (A\text{-}41)$$

For small values of b tables are used; for values of b approaching unity further approximations can be made, as

$$\cos(2\pi - \beta_1) = +\cos\beta_2 \doteq 1 - \frac{(b - 1)^2}{2b} \simeq 1 - \frac{\beta_2^2}{2} \quad (A\text{-}42)$$

$$\beta_2^2 \simeq (b - 1)^2/b \quad (A\text{-}43)$$

$$\beta_2 = (1 - b)/b \quad (A\text{-}44)$$

$$Q = \frac{\pi}{\beta_2} = \frac{\pi\sqrt{b}}{(1 - b)} \quad (A\text{-}45)$$

from which it follows that for reflection, b, of 0.172, 0.2, 0.4, 0.6, 0.8, 0.9, 0.95, and 0.99, the effective Q is 1.0, 1.4, 3.61, 6.02, 14.0, 28.7, 60.5, and 308.0 respectively.

The question has arisen as to why a 90° phase shift was observed by Muenow (1) at resonance. It has been shown in the foregoing that maximum amplitude occurs when the thickness is an integral multiple of half wavelengths or when the phase shift is $2n\pi$ radians. A second wave could easily have been introduced through electrical leakage or Rayleigh wave transmission. It is then possible to get a 90° phase shift if the extraneous signal is near the desired signal in amplitude. However, the 90° phase shift occurs at the antiresonant point, and not for the resonant condition.

The phase shift might have been due to the transducers themselves and would explain the difficulty of repeating this technique with more conventional and more powerful transducers.

As a final point, and this is really mentioned only from an academic point of view, it should be noted that a 90°

phase shift can be attained if the attenuation in the concrete or base course is sufficiently large. The complex reflection coefficient, R, at the pavement-base course interface is given by

$$R = (\bar{z}_2 - \bar{z}_1)/(\bar{z}_2 + \bar{z}_1) \qquad \text{(A-46)}$$

in which $\bar{z}_1$ is the complex acoustic impedance of the concrete and $\bar{z}_2$ is the complex acoustic impedance of the base course.

The expression for the complex impedance is given by

$$\bar{z} = \rho c(1 - j\,a/k) \qquad \text{(A-47)}$$

in which ρ is the density of the medium, c is the velocity of sound, a is the attenuation coefficient, and k is the wave number (subscripts 1 and 2 refer to the pavement and base course, respectively).

Examination of Eqs. A-46 and A-47 shows that if a_1 is small, the phase change upon reflection is 0 if $\rho_2 c_2 \ll \rho_1 c_1$ (i.e., R is real and positive if the base course has much lower acoustic impedance than the pavement) and the phase change is 180° if $\rho_1 c_1 \ll \rho_2 c_2$ (i.e., R is real and negative if the base course has a much higher acoustic impedance than the pavement). In fact, unless a_1 is very large the phase change will always be nearly 0 or 180°. The attenuation would have to be much higher than it is known to be for the concrete samples tested so far in order to give a 90° phase shift. However, the attenuation coefficient, a_2, for the base course could well be very large and give rise to any value for the phase change. The phase change would, in fact, depend on a_2 and the relative magnitudes of $\rho_1 c_1 k_1$ and $\rho_2 c_2 k_2$ and would be accordingly completely unknown if a is small (as it is in most cases at 10 kcps). The phase change could only be determined by extensive field tests—it may be found for the normal types of base course used that it would always be the same or it may vary greatly. This cannot be predicted theoretically.

GENERAL THEORETICAL CONSIDERATIONS OF ACOUSTIC TECHNIQUES OF THICKNESS MEASUREMENT

The following is a brief review of some acoustic theory necessary for comprehension of some of the problems associated with ultrasonic thickness-measuring techniques.

The propagation of elastic waves, sonic or ultrasonic, is governed by the elastic wave equation. In an electric medium of infinite extent, all elastic waves obey the general wave equation

$$(\lambda + 2\mu)\nabla^2(\bar{\nabla}\phi) + \mu\nabla^2(\bar{\nabla} \times \psi) = \rho\frac{\partial^2}{\partial t^2}(\bar{\nabla}\phi + \bar{\nabla} \times \bar{\psi})$$

$$\text{(A-48)}$$

in which λ is the Lamé constant, μ is the shear modulus, ρ is the density, ϕ is the scalar potential, and $\bar{\psi}$ is the vector potential.

The quantities $\bar{\nabla}\phi$ and $\bar{\nabla} \times \bar{\psi}$ are the dilatational and shear particle displacements associated with the wave motion. The stresses, particle velocities, or variations in density may be calculated from these displacements. The wave equation combines Newton's laws and the continuity equation with the equation of state for the material.

Wave propagation is also controlled by boundary conditions. If an elastic wave impinges upon the interface between two materials having different densities or elastic constants, part of the energy will be reflected and part transmitted. Both the reflected and transmitted portions will, in general, be composed of longitudinal and shear modes. In addition, Rayleigh waves, Lamb waves, or any other mode that exists with special boundary conditions, may also be generated. The laws of optical reflection and refraction are obeyed by elastic waves, but must be extended to include mode conversion at interfaces.

The reflection of elastic waves at an interface between two materials of different properties permits the most direct measurement of thickness. If a short pulse is directed downward through the pavement, part will be reflected at the pavement-base course interface and return to the surface. A measurement of the time of flight and a knowledge of velocity permits calculation of the thickness.

If longitudinal waves are propagated in a material, the transverse dimensions of the material may alter their velocity. As an example, a steel rod excited longitudinally at a frequency such that the sound wavelength is many times the rod diameter will have a phase velocity given by $(E/\rho)^{\frac{1}{2}}$. If now a high frequency is used, so that the rod diameter is much greater than a wavelength, the velocity will be given by $(\lambda + 2\mu/\rho)^{\frac{1}{2}}$, which is equivalent to $[E(1 - \sigma)/\rho(1 + \sigma)(1 - 2\sigma)]^{\frac{1}{2}}$, in which σ is Poisson's ratio. This second expression is about 10 percent greater than $(E/\rho)^{\frac{1}{2}}$ for such metals as steel and aluminum. Similar effects would be noted for concrete. Therefore, when the transverse dimensions of a pavement are large in comparison to a sound wavelength, as would occur when an elastic wave propagates normal to the surface, the velocity will be greater than if the longitudinal wave propagates parallel to the surface.

Inasmuch as elastic waves are periodic disturbances, they obey the laws of diffraction. Waves are commonly generated by conversion of electrical energy to mechanical energy through the use of a transducer. The radiation of acoustic energy into the pavement is governed by diffraction theory and depends principally on the ratio of the wavelength to the diameter of the transducer. If the transducer is very small compared to the wavelength, energy will be radiated in a hemispherical pattern; if it is infinitely large compared to the wavelength, the energy will be radiated in a parallel beam. For the case of the transducers used for pavement thickness measurement, this latter condition can only be approximated and one has to consider optical diffraction theory to obtain the radiation pattern. This theory was used in the design of the large mosaic transducer described in the final recommendation for an acoustic technique.

The chief results of diffraction theory for a piston radiating in an infinite baffle are summarized in Figure A-4. Near to the source (in the Fresnel zone) the beam may be considered to be almost parallel for a distance $4a^2/\lambda$ where a is the diameter of the piston and λ is the acoustic wavelength. Up to this point the beam will have a succession of maxima and minima of intensity along its axis due to interference of rays from different parts of
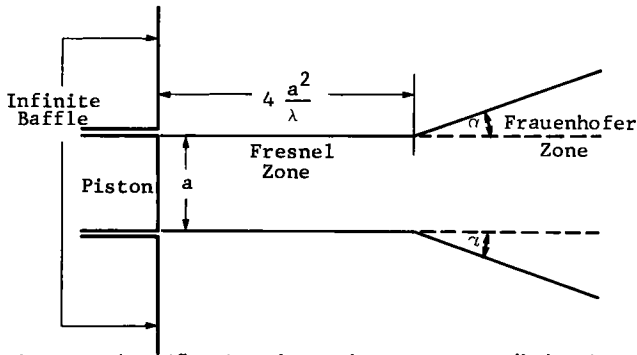
Figure A-4. Diffraction theory for a piston radiating in an infinite baffle.

Figure A-5. Polar plot of intensity as a function of angle.

the piston. The last minimum point occurs at a distance along the axis of $2a^2/\lambda$ and the last maximum at a distance of $4a^2/\lambda$, when the beam enters the Frauenhofer zone. The axial intensity then falls off according to an inverse square law with distance and diverges with a semi-angle, a, given by

$$a = \sin^{-1} 1.22 \lambda/a \qquad (A\text{-}49)$$

The angle a defines the edge of the main beam and is the angular distance to the first minimum of intensity. For larger angles one finds side lobes of energy being radiated in many directions (Fig. A-5).

In general, the greater the ratio, a/λ, the greater is the suppression of the side lobes and the more the total radiated energy is confined to the main beam.

This theory was worked out for a circular piston radiating in an infinite baffle, which is not strictly the case for many of the transducers used in the experiments. The general results, however, are still applicable in at least a qualitative way.

The upper operating frequency for pavement thickness measurements will be dictated by attenuation considerations. There exist in concrete several mechanisms by which elastic energy is dissipated. Probably the most significant is scattering.

Concrete is a distribution of rather coarse aggregate in a matrix with different acoustic properties. The elastic wave equation is derived on the basis that the medium through which the wave propagates is homogeneous. As frequency is increased and the wavelength approaches the dimensions of the aggregate, the assumption of homogeneity is violated. In effect, each interface between the matrix and the aggregate forms a reflecting surface. The random orientation of the surfaces causes reflection in all directions. Instead of coherent wave motion, the randomly reflected components of the wave recombine with random phases and directions of propagation to produce a greatly attenuated wave.

For wavelengths less than about three times the aggregate size, the attenuation varies inversely as the fourth power of wavelength. A damped progressive stress wave may be represented by
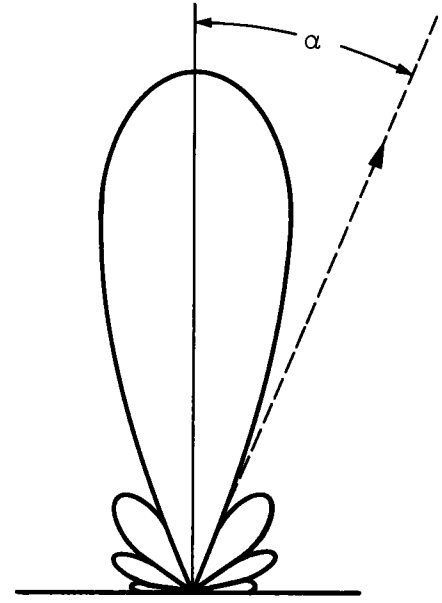
$$P = P_0 e^{a^i} e^{j(\omega t - kx)} \qquad (A\text{-}50)$$

in which a is the attenuation; x is the distance; ω is the angular frequency, related to the frequency, f, by $\omega = 2\pi f$; and k is the wave number, related to the wavelength, l, by $k = 2\pi/l$. Because a varies inversely as the fourth power of frequency and because it appears as an exponent, a small increase in frequency can produce a large decrease in amplitude.

At frequencies such that the wavelength is from three times to one-third the aggregate size, the attenuation varies inversely as the square of the frequency, and at higher frequencies the scattering losses are independent of frequency.

The minimum frequency that should be used for thickness measurements is determined by the instrumentation available and by the accuracy required of the measurement. Two separate difficulties are introduced by using excessively low frequencies; one is associated with the increased percentage accuracy of phase or frequency measurement, the other with transducer performance. Measuring thickness with a wave of known velocity then involves the measurement of time. Alternately, the reciprocal of time, frequency, may be measured. Another alternative is the measurement of phase. If a resonance technique is used with the third harmonic of the fundamental resonant frequency, the relative phases of the reflected and incident waves need be adjusted with only one-third the accuracy required using the fundamental for the same thickness accuracy.

The second effect of excessively low frequencies is that transducer rise times become long. If two transducers, operating at substantially different frequencies, each have

an identical quality factor, Q, the number of cycles required for the vibrational amplitude to build up will be the same. The absolute time is directly proportional to the period, and thus inversely proportional to the frequency. When the accuracy of a measurement depends on the precise identification of the beginning of a pulse, short rise times are necessary to permit this precise identification.

In principle, any frequency between the upper and lower limits as determined may be used. As high a frequency as possible, consistent with adequate acoustic transmission, should be selected. By selecting a high frequency, wavelengths are reduced and transducers of reasonable size then become many wavelengths wide. Use of a large transducer diameter-wavelength ratio will prevent generation of spurious modes that can confuse the empirical measurement. If the transducer radiates a nondirectional wave, the wave will then approach the boundary surfaces of the pavement over a large range of angles. The conditions for generation of other modes will be satisfied and these spurious waves will propagate with different velocities and in a variety of directions. Some of these spurious waves will reach the detecting transducer, be reconverted into the desired type of wave, and interfere with the desired wave to produce an uninterpretable result.

REFRACTION

Any acoustic wave arriving at an interface between two media having different sound velocities will, in general, give rise to two reflected and two refracted waves (Fig. A-6). Both longitudinal waves and shear waves (polarized in a plane normal to the interface) will emanate from the intersection of this incident wave and the interface.

The amplitude relations of the various waves are rather complicated; they are not reproduced here because they may be found in textbooks. The directions of the various waves are simply related by Snell's law,

$$c_n/\sin \theta_n = \text{constant} \qquad (A\text{-}51)$$

in which c_n is the velocity of the wave under consideration and θ_n is the angle this wave makes with the normal to the interface.

Whenever conditions arise so that $c_n/\text{constant} > 1$, no transmission takes place. Because the longitudinal wave velocity is always greater than the shear wave velocity, it is possible to generate only shear waves.

When the angle of incidence, θ, is adjusted so that

$$c_t/\sin \theta_t = c_{\text{Rayleigh}} \qquad (A\text{-}52)$$

Rayleigh waves only are produced and these are particularly strong for this condition.

The foregoing consideration assumes plane waves, which implies a plane wave of infinite extent in the direction normal to their propagation direction. At the edge of the sound beam departure from plane wave, conditions arise and the propagation direction and incidence angles are ill defined.

It is possible to generate acoustic waves in particular directions in concrete using a wedge of material having a low sound velocity between the transducer and the specimen. Adjustable wedges using a liquid coupling medium have been used by us and others. An alternate system using quadrants of cylinders with a sliding shoe have been described in the literature (2).

It is theoretically possible to obtain pavement thickness with adjustable wedges using a triangulation method. Response peaks, however, are very broad and both the desired precision and simplicity are difficult to obtain. The method does show promise if used in conjunction with some time-of-flight method.

By suitable adjustment of the angle of the wedge of each transducer, each of the following waves may be given primary emphasis in order of decreasing angle of incidence:

(i) Rayleigh wave.
(ii) Shear wave parallel to surface.
(iii) Longitudinal wave parallel to surface.
(iv) Shear wave reflected off lower surface.
(v) Longitudinal wave reflected off lower surface.

The following equations will then hold:

$$\sin \theta_{(i)} = c_\omega/c_t; \; c_t = L/T_{(i)} \qquad (A\text{-}53)$$

$$\sin \theta_{(ii)} = c_\omega/c_s; \; c_s = L/T_{(ii)} \qquad (A\text{-}54)$$

$$\sin \theta_{(iii)} = c_\omega/c_l; \; c_l = L/T_{(iii)} \qquad (A\text{-}55)$$

$$\sin \theta_{(iv)} = \sin \theta_c \, (c_\omega/c_s) = 1 + 2D^2 L^{-2})^{-\frac{1}{2}} \, (c_\omega/c_s);$$
$$L^2 + 2D^2 = c_s \, T_{(iv)} \qquad (A\text{-}56)$$

$$\sin \theta_{(v)} = (1 + 2D^2 L^{-2})^{-\frac{1}{2}} \, (c_\omega/c_s);$$
$$L^2 + 2D^2 = c_l \, T_{(v)} \qquad (A\text{-}57)$$

Once the sound velocity, c_ω, in the wedge is known, the velocities of the Rayleigh, shear, and longitudinal waves in the concrete may be determined, as well as the thickness, D.

Individual measurements of angles require excessive transducer dimensions to generate a sharply defined beam. However, the critical angle measurements serve as a check on measurements of flight time and signal variation, because
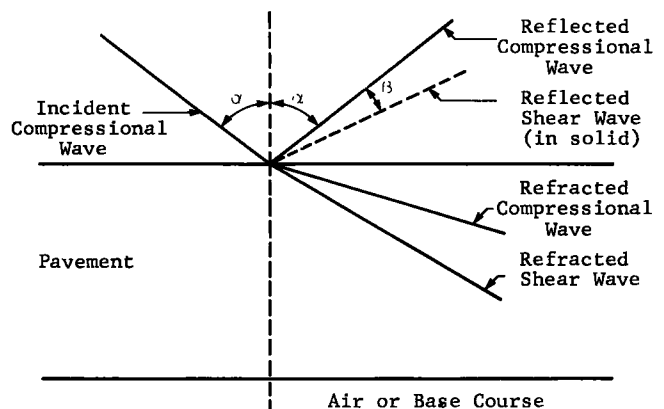
Figure A-6. Mode conversion at interface of two solid media having different sound velocities.

the angle will indicate to an experimenter which part of a signal is due to each particular wave.

This combination of techniques is thus suitable for the independent velocity determination required in the resonance method.

SPACING OF TRANSDUCERS IN SHEAR WAVE INTERFERENCE TECHNIQUES

The following calculation was made to determine the optimum spacing distances, l_1 and l_2, of the shear transducers. Figure A-7 shows the positions of the transmitters (T_1 and T_2) and the receiver (R). The receiver has an image (R′), as shown. The thickness of the concrete is denoted by D and the velocity of shear waves by c.

Assume that at a time $t = 0$ a negative pulse starts out from T_1 and at a time t_2 ($= l_1/c$) a positive pulse starts out from T_2. Waves traveling along the surface will therefore cancel.

The time, t_3, of arrival of the reflected pulse at R from T_1 is then given by

$$t_3 = 1/c \sqrt{(l_1 + l_2)^2 + (2D)^2}$$
$$= 2D/c \sqrt{1 + (l_1/2D + l_2/2D)^2} \qquad \text{(A-58)}$$

Now let

$$a = l_1/2D \qquad \text{(A-59)}$$

and

$$b = l_2/2D \qquad \text{(A-60)}$$

Then

$$t_3 = \frac{2D}{c} \sqrt{1 + (a + b)^2} \qquad \text{(A-61)}$$

The arrival time, t_4, of the reflected pulse from T_2 is given by

$$t_4 = t_2 + \frac{1}{c} \sqrt{l_2^2 + (2D)^2}$$
$$= \frac{l_1}{c} + \frac{2D}{c} \sqrt{1 + b^2}$$
$$= \frac{2D}{c} (a + \sqrt{1 - b^2}) \qquad \text{(A-62)}$$

The difference in arrival time, therefore, is given by

$$t_4 - t_3 = \frac{2D}{c} [a + \sqrt{1 + b^2} - \sqrt{1 + (a + b)^2}] \qquad \text{(A-63)}$$

For maximum reinforcement of the reflected signals,

$$t_4 - t_3 \simeq \frac{1}{2f} \qquad \text{(A-64)}$$

in which f is the resonant frequency of the shear transducers. Thus,

$$\frac{1}{2f} = \frac{2D}{c} [a + \sqrt{1 + b^2} - \sqrt{1 + (a + b)^2}] \qquad \text{(A-65)}$$

For this case,

$$(a + b)^2 \ll 1 \qquad \text{(A-66)}$$

so Eq. A-65 simplifies somewhat to

$$\frac{1}{2f} = \frac{2D\,a}{c} \left[1 - \frac{a}{2} - b \right] \qquad \text{(A-67)}$$

Hence,

$$b = 1 - \frac{c}{4aD\,f} - \frac{a}{2} \qquad \text{(A-68)}$$

Substituting Eqs. A-59 and A-60 in Eq. A-68 gives

$$l_1 = 4D - \frac{2c\,D}{l_1\,f} - 2l_2 \qquad \text{(A-69)}$$

Using the value of $D = 25$ cm, $f = 10^5$ c/s (100 kcps), and $c = 2.2 \times 10^5$ cm per sec, gives the values in Table A-1 of l_1 for values of l_2 between 0 and 10 cm.

METHOD OF DUAL-FREQUENCY EXCITATION

By exploiting a generally adverse characteristic of most electrostrictive ceramic transducers (i.e., large Poisson's coupling), two signals of different frequency can be simultaneously generated by a single transducer element. The basic concept involves the use of ceramic disc-type elements which have a high-frequency (250 to 400 kcps) thickness mode resonance and a low-frequency (40 to 90 kcps)
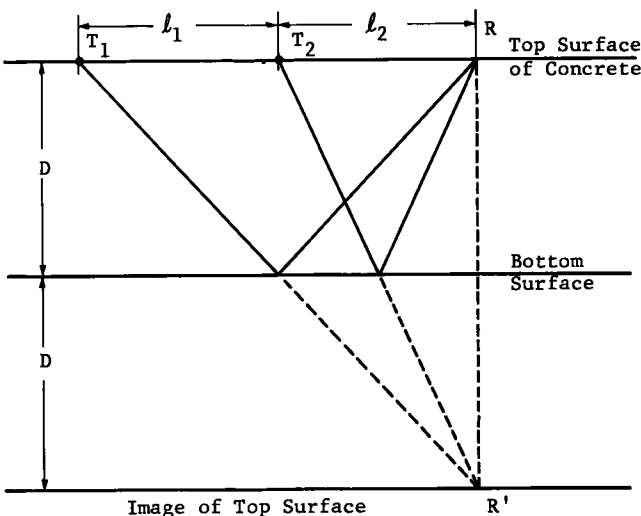
Figure A-7.

TABLE A-1

VALUES OF l_1 FOR SELECTED VALUES OF l_2 IN EQ. 69

l_2 (cm)	l_1 (cm)
1	1.14
2	1.20
3	1.25
5	1.37
7	1.53
10	1.83

radial mode resonance. When such an element is excited with a large-amplitude nonresonant electric pulse, analogous to hitting the transducer element with a hammer, the element will tend to vibrate in all its possible modes. In the case of the selected disc, the radial and thickness modes predominate. Because of large Poisson coupling, the element will simultaneously vibrate both radially and in thickness at both frequencies; i.e., the thickness mode of vibration will include both low and high frequencies. Similarly, radial vibrations will be of two frequencies. Thus, the transducer is generating two acoustic signals of different frequencies. Both signals are coupled into the pavement and propagate as longitudinal, Rayleigh, and shear waves.

MATERIAL PROPERTIES

As discussed in Chapter Two, an accurate measurement of pavement thickness is predicated upon independent and accurate measurements of sound velocity and time. However, a review of the literature has indicated that sound velocities over different paths in a given specimen can vary considerably, due to the presence of velocity gradients through the thickness (3). These velocity gradients would necessarily be associated with variations in density, moisture content, aggregate distribution, and even boundary conditions.

Measurements were carried out on a $3 \times 2 \times 0.5$-ft specimen of Type 1A* portland cement concrete. The specimen was constructed under controlled conditions using standard construction practices.

Initially, the velocity was measured in the orthogonal

---
* Composition: 13 3% high early strength portland cement, 24 2% No 2 torpedo sand, 49.7% 1½-in. aggregate, 12.8% water.

direction, as shown in Figure A-8, using 2-in. diameter ceramic transducers resonant at 300 kcps. A large-amplitude electrical impulse, of variable width and repetition rate, was applied to one transducer (on the surface of the concrete specimen) and simultaneously to the counter. At the same instant that the elastic wave was generated in the concrete, the counter was turned on. The wave propagated to the second transducer, where it was detected and this received signal was used to turn the counter off. Hence, the time of flight was measured directly; with the transducer spacing known, the velocity was readily calculated. Comparison of the velocities so obtained showed less than 1 percent variation, indicating that the frequency was sufficiently high to avoid induced velocity dispersion. In addition, these measurements indicated the absence of anisotropy.

A second series of measurements was made to determine the degree to which the laboratory specimen exhibited settling of aggregate. Figure A-9 shows both the relative placement of the transducers and the experimental results. The dimensions of the transmitting transducer were small compared to a wavelength so as to provide a point source. The radiation pattern was then assumed to be hemispherical. The transmitter was first mounted at position A and then at position B on the slab. The pulsed sound energy introduced into the concrete was assumed to propagate over a straight-line path to the receiving transducer, as shown. The velocity was again measured over a range of path lengths by varying the position of the receiving transducer. The empirical velocity data determined from this measurement were also found to differ by less than 1 percent from the sound velocity measured over a path between transducers diametrically opposite. If it can be assumed
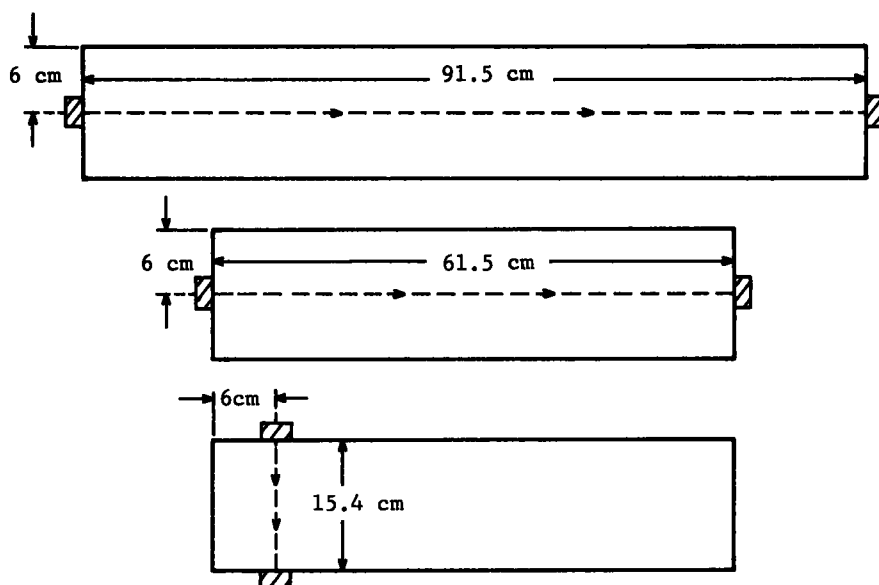
Figure A-8. Transducer arrangement for investigating geometrically induced velocity dispersion and degree of anisotrophy. The acoustic transducers are 2-in. diameter PZT discs having a resonant frequency of approximately 400 kcps.
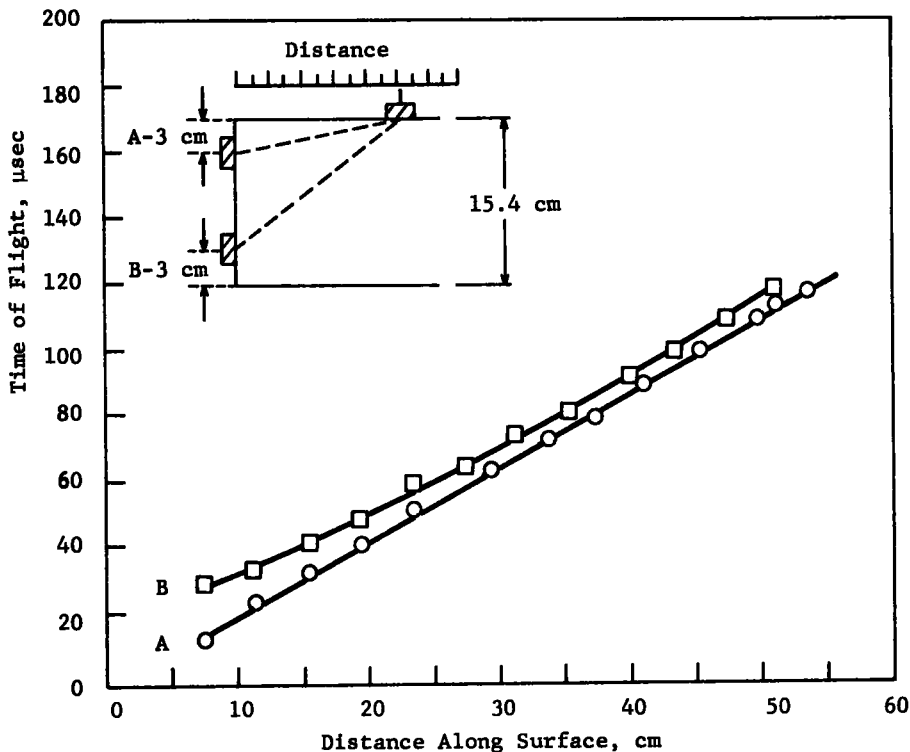
Figure A-9. Measurement of composition nonuniformity in Type 1A portland cement concrete specimen. The transverse dimension of the transmitting transducer was small compared to a wavelength to produce a point source with a hemispherical radiation pattern.

that the test specimen is typical of concrete pavement structures, it is safe to assume that velocity gradients in standard portland cement pavements are negligible. This particular specimen was made using construction techniques under laboratory conditions; the concrete in its plastic state was vibrated according to accepted practice. However, if a concrete pavement is placed on a base course material that has an excessively high moisture content, or if the pavement is placed without due regard to standard construction techniques, it is questionable whether the foregoing conclusions are, in fact, valid.

The apparatus shown in Figure A-10 was used to evaluate the upper frequency limits for concrete measurements. A typical measurement is shown in Figure A-11. The ultrasonic frequency is approximately 500 kcps, with a pulse width of 2.0 μsec. The electrical pulse applied to the transmitting transducer is shown in the upper trace and the received acoustic signal, after traveling through 6 in. of Type 1A concrete, is seen in the lower trace. Careful study of the lower trace shows that:

(a) The mechanical Q of the transducer is rather high, thereby causing "ringing" in both the transmitting and receiving transducers, and precludes rapid risetimes of the pulse.

(b) The wavelength is small compared to aggregate size. It therefore produces scattering or reverberation, as noted by the interference in the lower trace.

(c) The attenuation is such that the start of the received pulse is lost in the electrical noise and prevents accurate time-of-flight measurements.

These observations are in complete agreement with the theory of elastic wave propagation.

INITIAL MEASURING TECHNIQUES

Low-frequency measurements were initially the subject of experimental investigation. Resonant measurements were tried, as discussed under "Resonance Methods," but indications were that further transducer development is required. One of the major difficulties in low-frequency velocity measurements is the generation of spurious modes at a frequency of about 20 kcps (the transducer diameter was about one-fourth wavelength). Consequently, a broad radiation pattern resulted and the wave approached the concrete surfaces over a wide range of angles. Spurious modes were generated, which, after multiple reflection and mode reconversion, interfered with the desired signal. The detected composite signal then became uninterpretable.

Indications were found in the literature (4) that pulsed techniques had been used at low ultrasonic frequencies. The wisdom of attempting low-frequency pulse methods for pavement thickness measurements is questioned, because neither sufficiently fast risetimes nor short pulses can be obtained below about 100 kcps. Although these limita-
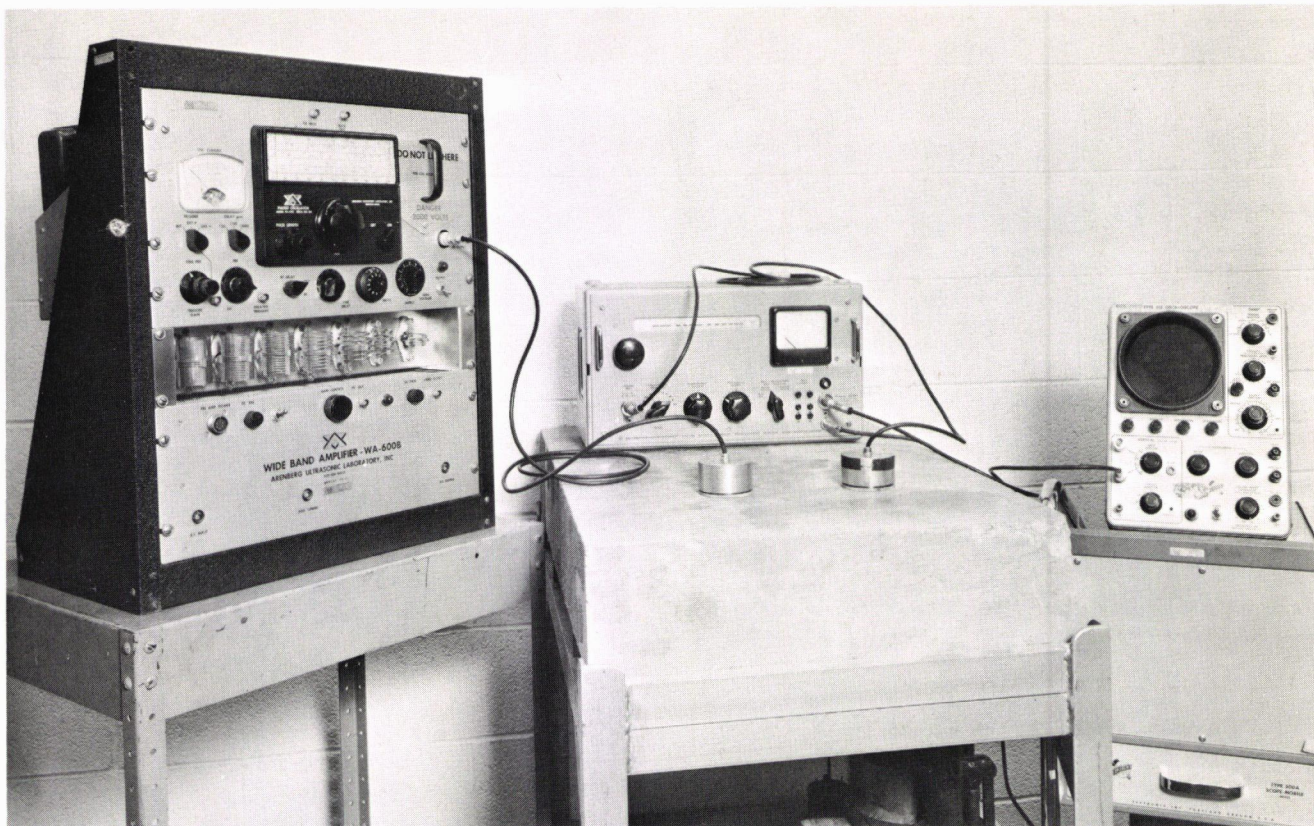
Figure A-10. Apparatus for determining the upper frequency limits for concrete thickness measurements. The instrument at left is a high-power, high-frequency (200 kcps to 100 mcps) pulsed oscillator, which is used to drive a 500-kcps ceramic transducer.

tions, based on transducer theory, were expected, empirical confirmation was obtained.

Several papers reviewed in the literature survey (*1, 5*) refer to resonance techniques for thickness measurements. Various methods have been employed which yield a wide range of results.

The instruments shown in Figure A-12 include a complex impedance locus plotter, which provides a measure of both the real and imaginary components of transducer impedance over a wide frequency range. Although not specifically designed for this purpose, the instrument can be used to obtain a measure of wave propagation time. Instead of directly measuring the time required for an acoustic wave to propagate through a sample pavement and return, the resonant frequency is measured. Resonance occurs when the pavement thickness is an integral number of half wavelengths. Under these conditions, the acoustic impedance presented to the transducer and appearing at its electrical terminals, in parallel with its purely electrical impedance, is a minimum. This is true only when the inherent resonant modes of the transducer alone are far removed from the frequency range of interest, or when the transducer is of low-Q design. Then, the acoustic impedance minimum and the resonant frequency can be obtained directly from the impedance plotter and electronic frequency counter. The success of this technique depends largely on the mechanical

Q of the concrete structure; excessive mechanical damping will render this technique useless. (The effect of losses is not considered here.)

ELECTROMECHANICAL TRANSDUCER DEVICES

All acoustic techniques depend on the conversion of electrical energy to mechanical and/or vice versa. In addition, the ultimate feasibility of an acoustic measurement of in-situ pavement thickness is strongly dependent on the development of suitable transducer devices, as implied in the previous sections. Although this program did not allow an extensive investigation of transducer development, several devices were constructed and tested on concrete specimens to determine future design considerations.

Energy conversion can be accomplished in a variety of ways. However, the more promising techniques would appear to be through the use of "electrostrictive" or "magnetostrictive" materials. Suitable electrostrictive materials are barium titanate and the lead zirconate titanate (PZT) ceramics. These materials become stressed with the application of an electrical potential, or, conversely, generate a voltage when stressed. The more common magnetostrictive materials are pure nickel, permendur, and nickel-iron ferrite. These materials experience a change in dimension when exposed to a magnetic field; the predominant
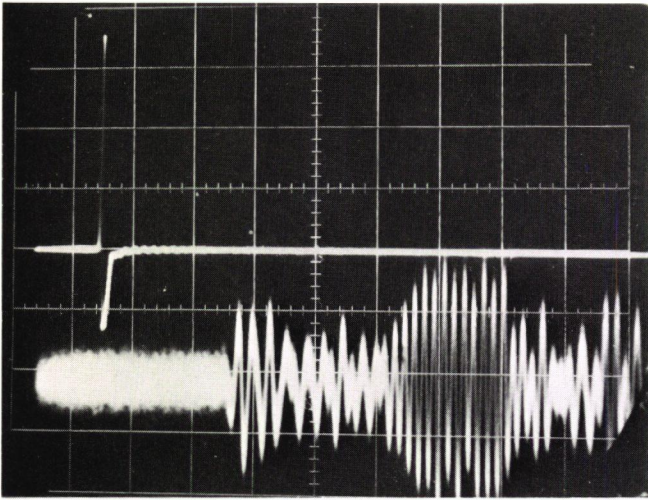
Figure A-11. Oscillograph presentation of a high-frequency time-of-flight measurement. The upper trace is a 2-μsec wide, 500-kcps electrical pulse applied to the transmitter transducer. The lower sweep is the received pulse after propagation through 6.0 in. of Type IA concrete.

under an applied stress). Various electrostrictive and magnetostrictive transducer configurations are shown in Figure A-13. Two magnetostrictive "window" transducers are shown at the right of the photo. A third, low-frequency (15 kcps) water-cooled magnetostrictor is shown at the top of the photo. This transducer is coupled to an exponential horn, which allows the generation of extremely large sound intensities; acoustic intensity is in excess of 100 watts/cm². The remaining transducer configurations are electrostrictive ceramics. All are either thickness (for the plates) or length (for the rods and bars) vibrators. The particular construction is dictated by performance requirements. As an example, the ceramic transducer shown upper center consists of 43 barium titanate rods, having a length resonance of 200 kcps, bonded in an epoxy base. This mosaic transducer was constructed to give low mechanical Q and yet provide a large active area. A pair of highly damped, 300 kcps, ceramic transducers are shown in Figure A-14. Damping here is accomplished through bonding a cone-shaped, lead-and-brass-impregnated epoxy backing to the ceramic disc. The lead and brass chips provide a high loss media to the sound wave radiated from the back surface of the transducer and the cone shape prevents reflection of the wave back to the transducer surface. The presence of the damping material (high mechanical resistance) reduced the mechanical Q of the ceramic elements from approximately 2,000 to 15. This resulted in a change of bandwidth from about 150 cps to 20 kcps.

dimension changes occur in the dimension parallel to the applied field. These materials also exhibit an inverse magnetostrictive effect (i.e., the generation of a magnetic field
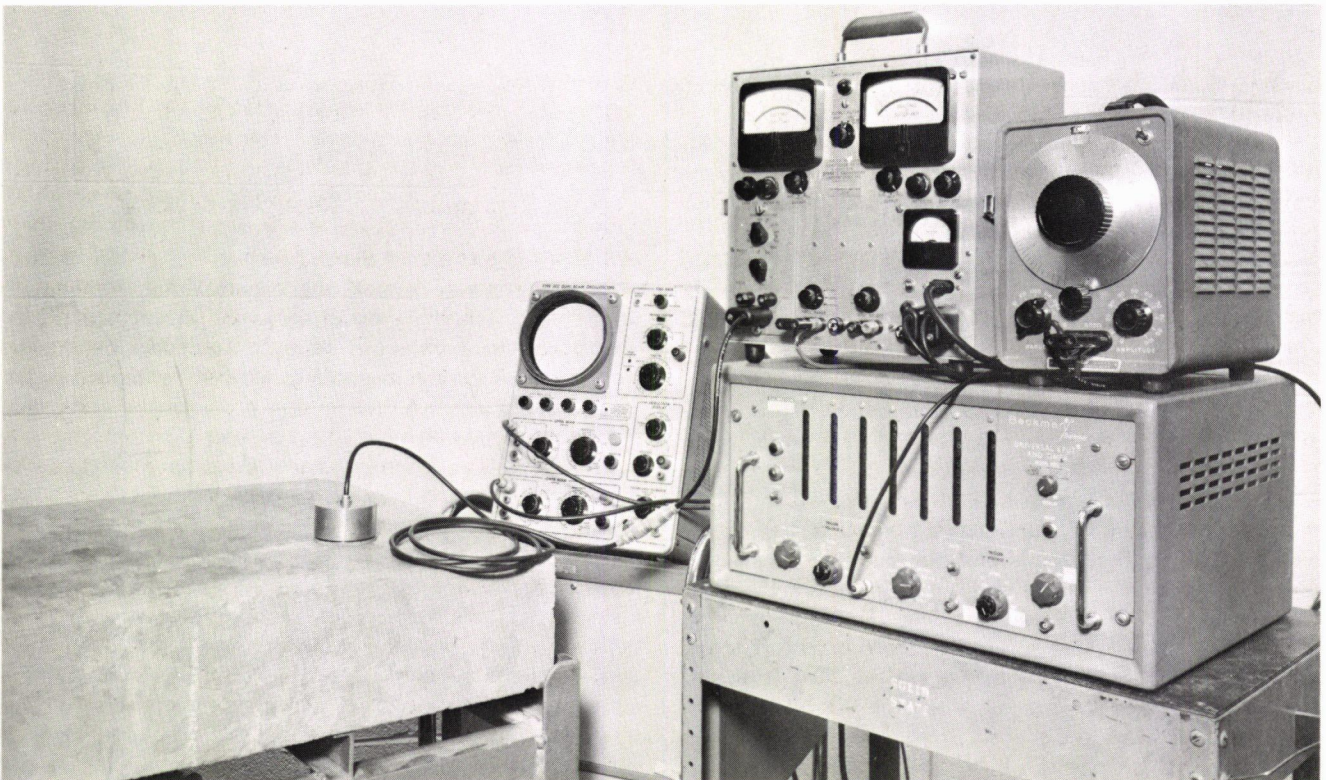
Figure A-12. Instruments for measuring pavement thickness using resonant techniques. The instrument in upper center is a complex impedance locus plotter, which is used to indicate pavement resonance through a measure of the acoustic impedance.
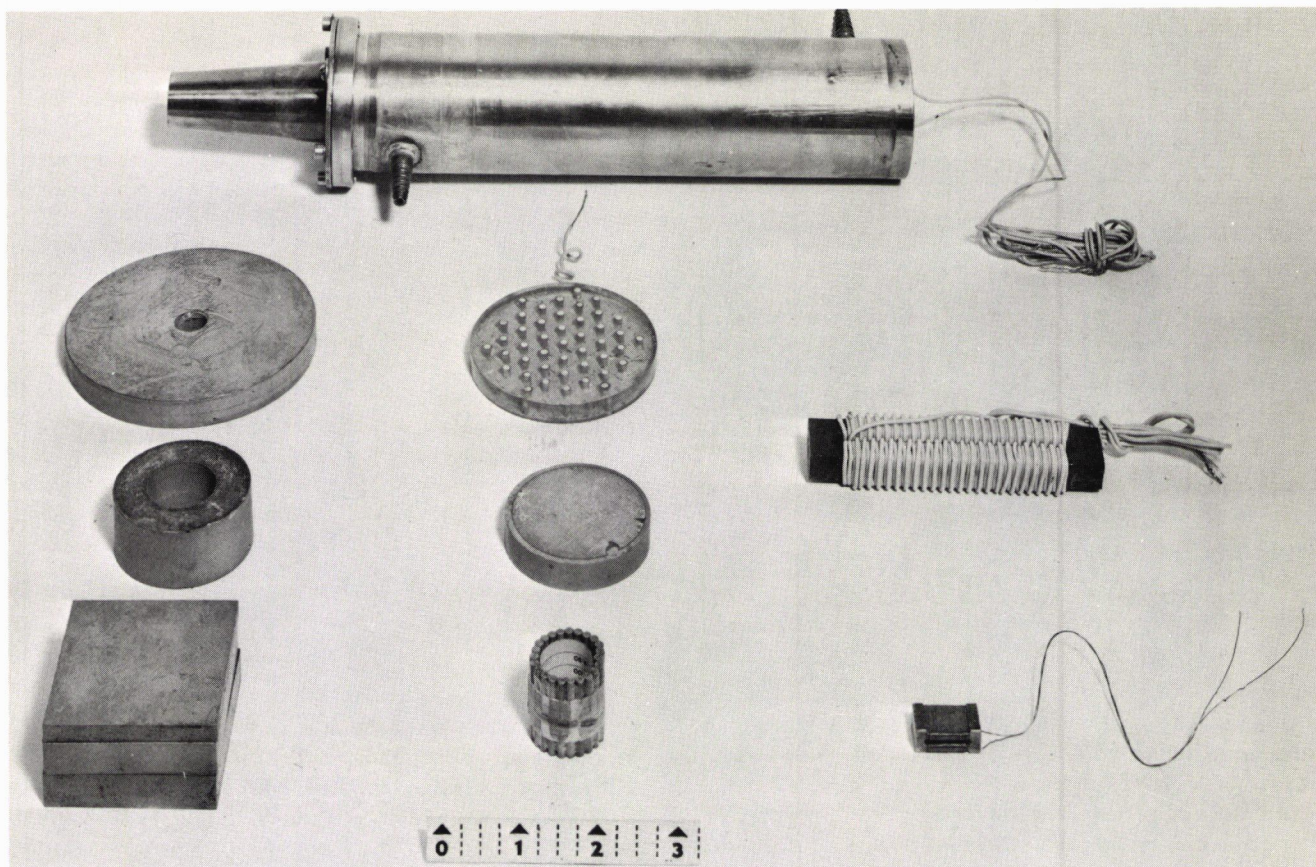
Figure A-13. Experimental electrostrictive and magnetostrictive transducer devices.

The increased bandwidth allows the generation of much narrower acoustic pulses having significantly faster rise-times.

The transducers shown in Figure A-15 were constructed for use in obtaining the measurements discussed previously under "Material Properties." The transducers were designed to allow operation over a range of frequencies (using different ceramic elements) in addition to providing repeatable coupling to concrete surfaces. A layer of castor oil was maintained between the ceramic element and a rubber diaphragm. A slight excess pressure on the diaphragm caused it to extend slightly beyond the metallic face. Under normal use, a thin layer of cellulose gum is used between the rubber diaphragm and the concrete surface. It will be noted that the interior of the transducer housing is also cone shaped and designed to accept various liquid loads.

As was mentioned in the previous section, methods have been investigated for measuring phase differences when continuous-wave techniques are used. One of the most promising of these methods has been the modified sing-around technique.

MODIFIED SING-AROUND TECHNIQUE

It should be emphasized at the beginning that the modified sing-around technique is not a method for overcoming some of the basic difficulties discussed earlier in connection with continuous-wave systems. The use of this technique assumes that the basic problems of transmitting a single well-collimated beam into the concrete have been solved. The problem, then, reduces to one of measuring the phase difference between the transmitted and received signals. This can be done by using the modified sing-around technique very accurately and quickly and in such a way that ambiguities of multiples of 2π associated with conventional phase measurements are eliminated. In order to understand this more clearly, it is helpful to first consider conventional techniques.

Consider the simple transmit-receive system shown in Fig. A-16. If it is known that the frequency, f, of the ultra-sound is low enough for the wavelength to be greater than the total path length, $2X$, of the sound in the pavement, then X, and hence the thickness, can be calculated unambiguously from the measured phase difference, δ; that is,

$$X = \delta c / 2\pi f \tag{A-70}$$

in which c is the ultrasonic velocity, determined from another measurement (e.g., by using the same apparatus with a different angle of transmission).

If, however, the frequency, f, is not low enough, there
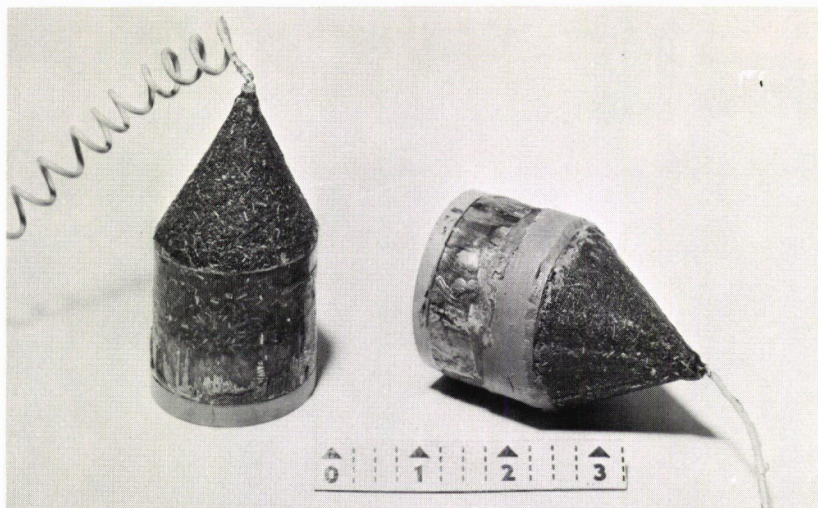
Figure A-14. Experimental low-Q ceramic transducers. The ceramic disc is mass-loaded with a lead-and-brass-impregnated epoxy cone.

is an ambiguity in the value of X. In fact, X can be any value given by

$$X = \left(\frac{\delta}{2\pi} + n \right) \frac{c}{f} \qquad (A-71)$$

in which n is zero or any positive integer.

This simple method of measurement of phase thus requires that only low-frequency ultrasonic energy be used. For a 10-in. thick slab of portland cement concrete, the maximum possible frequency would be about 10 kcps. Such a limitation completely precludes the possibility of operating with collimated beams. It is this severe limitation that is obviated by means of the modified sing-around technique.

Originally the term "sing-around" was given to automatic pulse triggering systems and later to a direct positive feedback loop using continuous waves. These systems are described in the earlier section on "Conventional Sing-Around Techniques," but do not offer a solution in this case. For this reason the modified sing-around technique was developed at IITRI on another program. The mode of operation is shown in Figure A-17.

A modulated continuous wave is used to excite a generating transducer coupled to the concrete. After propagating to the lower surface and returning, the acoustic wave is detected by a second transducer. The electrical output is demodulated and the modulation is used to amplitude (or frequency) modulate the carrier applied to the generating transducer. If the phase shift in the demodulator and other electronic components is an even multiple of 2π radians and independent of frequency, the frequency of modulation will be such that the phase shift of the modulation envelope will be a multiple of 2π radians in the acoustic path. In effect, the modulation frequency will be controlled by the acoustic phase shift, inasmuch as positive feedback is required to maintain the modulation. The path length, $2X$, in the pavement is then computed from the

product of the known sound velocity and one-half the period of the modulation envelope.

The modified sing-around method using amplitude modulation has been used experimentally in IITRI laboratories for air-path experiments. The use of resonant transducers increased the overall sensitivity by a factor of 10 and permitted measurements over appreciably greater air paths than was possible with the conventional method. Applied to pavement thickness measurements, the modulated continuous wave permits selection of an optimum carrier frequency (e.g., 150 kcps) without regard for the requirements of phase measurement at this frequency. The use of a relatively high carrier permits better wavelength-transducer diameter ratios. This, in turn, provides better collimation of the transmitted wave and results in reduced spurious mode generation. The measurement of modulation frequency, rather than time, may be accomplished using any one of a large number of available instruments.

Initial experiments to demonstrate the feasibility of this technique in concrete were made with transducers set up on either side of a 10-in. thick slab of portland cement concrete so that the ultrasound was propagated directly through the thickness of the slab. Separate tests using the same technique were also performed with a 5-in. thick bituminous slab. This, of course, was not intended to represent a realistic thickness measurement, but was merely a method of testing the system in the absence of spurious surface waves. The results of both sets of tests were very good (the thickness was measured with an accuracy of $\pm$ 0.2 percent) and demonstrated that if the problem of spurious signals could be eliminated by better beam collimation the modified sing-around technique would be an ideal way of measuring phase. The tests also showed that some of the difficulties of acoustic noise encountered in "air" tests were absent in the concrete thickness measurement. By using a 150-kcps carrier wave, the ratio of carrier wave frequency to modulation frequency (10 kcps) was
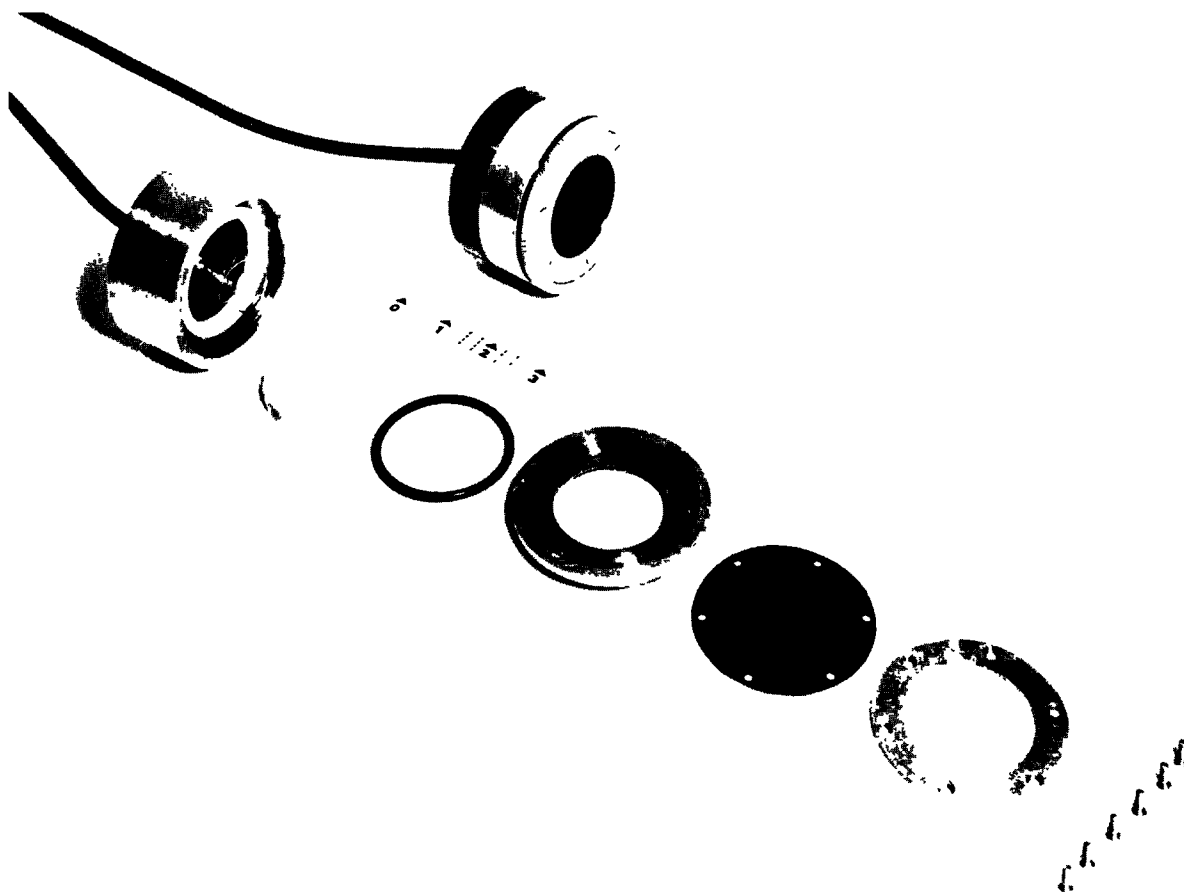
Figure A-15. Variable-frequency transducers. The transducers are designed to accept ceramic elements over a wide frequency range, in addition to providing a stable coupling medium between the transducer and the concrete surface.

sufficiently large to be handled by the detector circuit constructed for this application. The measured modulation frequency was found to be very steady, thus enabling accurate measurements to be made.

During the literature survey, a thickness measuring technique developed at the Portland Cement Association (*1*) was evaluated. Close examination of this technique showed it to have serious disadvantages that would make measurements with this apparatus very suspect under certain conditions. A description of this technique is included in the following section, as it serves also to illustrate a statement made in the previous section to the effect that it is necessary to perform two independent measurements in any thickness measurement because the velocity also must be considered to be an unknown.

RESONANCE METHODS

Resonance methods are essentially a special case of phase-measuring methods using continuous waves. Instead of measuring phase directly, the frequency is varied until a certain phase relationship corresponding to resonance is obtained. In fact, the resonance thickness measurement

consists of transmitting a continuous wave in and normal to the surface of a pavement and adjusting the frequency, f, until the sound wavelength, λ, in the slab is exactly twice its thickness. The thickness, D, of the pavement is then obtained from

$$D = c/2f \qquad (A-72)$$

However, the wave velocity, c, must be determined by an independent measurement. The determination of the half-wavelength condition can be obtained by either of two methods. One method relies upon tuning of the transmitter for a maximum signal response in a receiving transducer placed adjacent to the transmitter. Although a Portland Cement Association publication (*1*) claims reliable thickness measurement using this technique, tests made at IITRI show that there are certain reservations to be considered prior to adopting this method for field use by personnel unskilled in ultrasonics and uncertain of the pavement thickness prior to measurement. These reservations are as follows:

1. The signal response maximum is quite broad, and therefore requires considerable technical background to

24
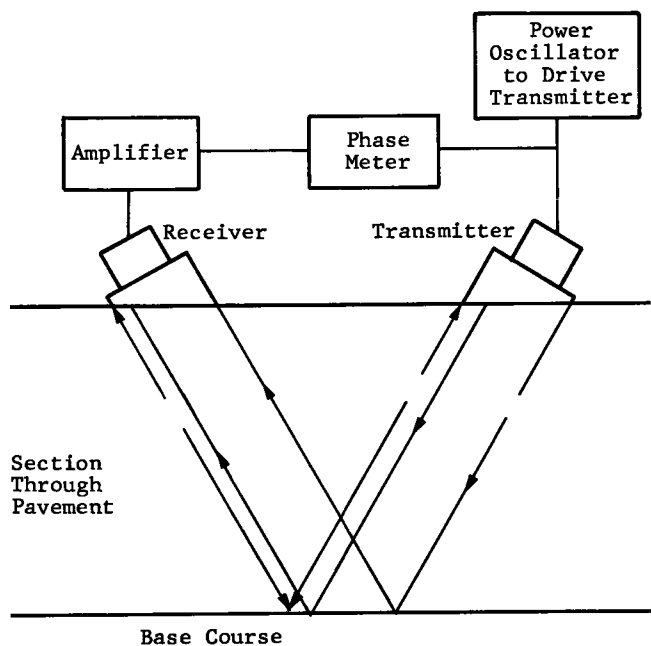
Figure A-16. Conventional phase-measuring technique for thickness measurement using continuous waves.

ments at IITRI have shown that with the following modifications some of the difficulties enumerated could be overcome:

1. Shear waves were used instead of longitudinal waves for both resonance and velocity measurements. These shear waves were generated without also generating Rayleigh waves, so that the interaction problem with spurious waves was overcome. The propagation of horizontally polarized shear waves also assisted with separate velocity determination, because their velocity is not affected by geometry.

2. Use of the modified sing-around technique (see previous section) would have the benefits associated with using a high-frequency carrier wave, which would introduce the following advantages:

(a) The phase shift at the pavement-base course layer is believed to be an unknown quantity and not 90°. At high frequencies it would not be necessary to know the phase shift.

(b) Phase shifts in the transducers would be negligible, so transducers could be used at their resonant frequency.

(c) The high-frequency waves would be highly attenuated, so reflections from remote points, such as the edge of the slab or joints, could be neglected.

(d) The independent velocity measurement could be

evaluate. This was discussed further in the earlier section on "Standing Waves in a Pavement."

2. Original measurements made with this technique showed that the point of maximum response can be recognized by a 90° phase shift. This is believed to be in part fortuitous and can lead to significant errors. This factor is also further discussed in the section on "Standing Waves in a Pavement."

3. The technique is susceptible to additional error because several response maxima, due to the interaction of different waves arising through mode conversion, are also present. This is especially true if measurements are made near an edge or a joint in the pavement. However, if an approximate thickness of the pavement is known use of Eq. A-72 will generally allow identification of the proper resonance provided it is not masked by resonance effects of Rayleigh (surface) waves.

4. An independent method of measuring the wave velocity is open to question also. A frequency (11 kcps) that was below the resonant frequency of the pavement was used for measuring the velocity in a length direction; i.e., parallel to the surface of the pavement. This means that the condition for a large dimension normal to the propagation direction (see section on "General Theoretical Considerations of Acoustic Techniques of Thickness Measurements") was not satisfied and geometrically induced dispersion can occur. In addition, Rayleigh waves and reflections from the bottom may also interact, making phase measurements (i.e., location of half-wavelength or wavelength nodes of continuous waves) questionable.

Although criticisms of this resonance method have been presented, the technique is, in principle, a good one. Experi-

Figure A-17. Block diagram for modified sing-around technique.

done at the same frequency without introducing the mode errors due to the finite slab thickness.

Such a modification, of course, would fundamentally change the method altogether. The possibility of actually using this technique is discussed further under the sections on "Modified Sing-Around Technique" and "Mosaic Transducers (Final Recommendation)."

3. Apart from using shear transducers, another possible way of circumventing the velocity dispersion mentioned in the fourth reservation would be to apply a correction factor to the velocity measured in the surface. This correction factor would be calculated from the elastic constants of the concrete and an initial approximate knowledge of the pavement thickness to about 10 percent. In order to perform this calculation, it would be necessary to know both Young's modulus of elasticity and Poisson's ratio for the concrete. This information could be readily obtained from a combination of a measurement of shear wave velocity and longitudinal velocity in the surface. It is known from the experiments made with shear waves that both of these velocities are readily obtainable. With the application of a correction factor calculated in this way, longitudinal propagation could still be used. Generally speaking, all acoustic techniques have the same common problem of a need for two independent measurements. This arises because instead of thickness being measured directly, it is the quotient of thickness and sound velocity that is measured, and inasmuch as the sound velocity varies from pavement to pavement, it must be considered to be an unknown. Thus, an independent measure of sound velocity is needed to obtain an accurate thickness measurement. In all other cases considered, this problem has been solved satisfactorily by making two separate measurements at two different angles of incidence. It is only in this technique, where normal incidence only would be used, that the problem of velocity dispersion arose.

Other solutions were also shown to exist for the independent measurement needed in resonance techniques. Apart from the possibility of using shear waves, for which there is no velocity dispersion, the measurement of Rayleigh wave velocity is particularly easy, because these waves are usually produced with large amplitude. Rayleigh wave velocity is closely related to shear velocity, so that even an appreciable error in the determination or assumption of the value of Poisson's ratio (see section on "General Theoretical Considerations of Acoustic Techniques of Thickness Measurement") gave a measure of shear wave velocity to a resonably high degree of precision (within 2 or 3 percent).

A second method for determining pavement resonance relies upon measuring the change with frequency of the electrical input impedance of the transmitting transducer. In particular, all acoustic transducers exhibit a marked change in their impedance at electromechanical resonance. When a transducer is mechanically coupled to another medium that also exhibits a mechanical resonance (which need not be the same as that of the transducer), the electrical impedance at the terminals of the transducer will also change. By using a transmitting transducer which has its fundamental resonant frequency far above the resonant frequencies normally expected in typical pavements, and measuring the change in the real (resistive) portion of the transducer impedance, the resonant frequency of the pavement can be accurately determined. The typical resonance curve shown in Figure A-18 was obtained on a 7-in. thick, air-back, reinforced portland cement concrete slab. The transducer (Fig. A-19) consisted of 16 ceramic rods having a resonance of 50 kcps. The resonant frequency of this slab is seen to be 14 kcps. Although an oscilloscope display of resonant amplitude versus frequency is shown with the plotted curve, the maximum signal amplitude and corresponding resonant frequency can be measured to better than 2 percent with sensitive meters.

At this state of development it was evident that use of any type of continuous wave system would require development of transducers capable of producing well-collimated beams with a marked suppression of surface waves. Attention was then turned toward the possibility of using shear transducers to produce a single mode of propagation.
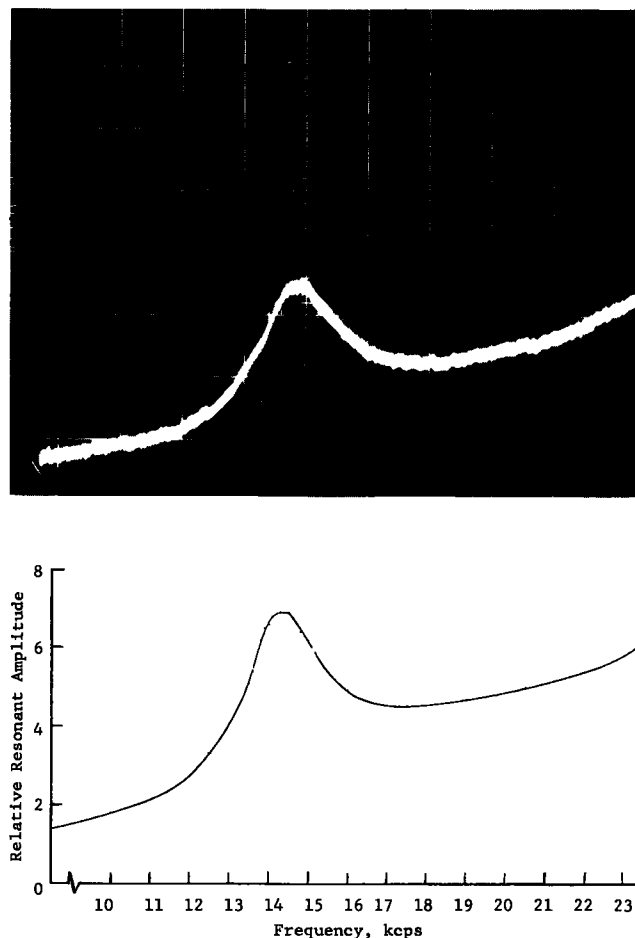
Figure A-18. Resonance frequency (kcps) response of a 7-in. reinforced portland cement concrete slab. The resonance curve shows the change in electrical resistance with frequency for a 50-kcps transducer coupled to the slab.
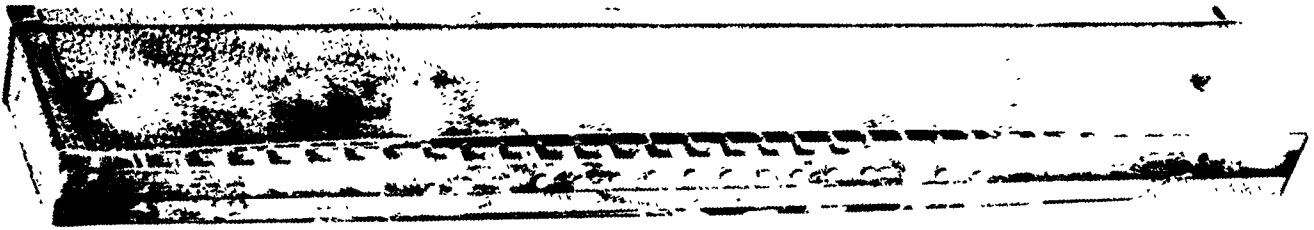
Figure A-19. In-line transducer array developed for resonance and time-of-flight measurements. The transducer consists of 16 ⅛-in. diameter ceramic rod transducers, each resonant at 50 kcps.

SHEAR TRANSDUCER EXPERIMENTS

Shear wave transducers recommended themselves because wedge couplers could be designed to eliminate longitudinal waves but not shear waves (see earlier section on "Refraction" for a more complete discussion of this point). Thus it was hoped that a transducer could be designed which would generate only one mode of propagation, so that the surface wave could be eliminated by destructive interference. In order to conduct initial feasibility tests with the shear transducers, it was decided to use pulses, as the transducers were too small to produce collimated continuous waves.

At this point it should be noted that previous attempts had been made to eliminate the surface wave by setting up two transmitting transducers and one receiving transducer on the concrete surface. With experimental conditions properly arranged, it should then have been possible to cause destructive interference to occur between the two surface wave pulses. However, this dipole transmitter arrangement was shown to be unsuccessful in producing surface wave cancellation when longitudinal transducers were used. The reason for this lack of interference was that many different modes of propagation, each traveling at a different velocity, were produced by the longitudinal transducers. The use of shear wave transducers, generating only one mode of propagation, should have thus obviated this difficulty. For these experiments, small rectangular (1½ in. × ⅜ in. × ¼ in.) PZT ceramics were obtained, which were polarized for shear wave propagation. Initial experiments with these transducers showed that the shear wave being propagated through the top surface of the concrete was larger in amplitude than the shear wave being reflected from the bottom. For this reason, it was decided to arrange two transmitters spaced at an optimum distance from each other and from the receiver (Fig. A-20) so that the surface waves generated by each would destructively interfere and the desired waves traveling through the concrete would constructively interfere. Experimental attempts to determine the optimum positions were not successful, owing to the number of separate variables involved. Therefore, a theoretical calculation was made, as given in the earlier section on "Spacing of Transducers in Shear Wave Interference Techniques."

To avoid confusion, the transducer holders and associated electronics for the shear wave "interference" method are not shown in Figure A-20. However, the method of excitation was to use two pulses from a Beckman double-pulse generator. One pulse was delayed in time by a variable amount, t, with respect to the other, the later pulse being used to excite the transmitter nearest the receiver. By adjusting the delay to a value calculated from the earlier section on "Spacing of Transducers . . .," optimum interference effects could be obtained. Separate attenuators were included for both pulses so that their amplitudes could be independently varied and complete interference could be produced.

Prior to the use of the shear transducers some difficulty was anticipated with coupling problems. For this reason, various coupling systems were tried experimentally and a thermosetting resin was found which has proved to be successful as a coupling agent.

The arrangement of the transducers is shown schematically in Figure A-21. The three transducers were spaced at optimum distances, l_1 and l_2, as calculated in the earlier section on "Spacing of Transducers. . . ." A short positive electrical pulse having a duration of 5 μsec was applied to transmitter T_1. After a further interval corresponding to the time taken for a surface wave pulse to propagate from T_1 to T_2, a second negative electrical pulse was applied to transmitter T_2. Under these conditions the surface waves from T_1 and T_2 should have destructively interfered and, provided l_1 and l_2 corresponded to the values calculated previously, there should have been constructive interference between the two reflected waves.

The results of these experiments, however, showed that it was not possible to obtain destructive interference over the whole length of the surface pulse. The reason for this was that due to the increase of attenuation with frequency, the higher frequency Fourier components of the pulse were attenuated more rapidly; hence, the surface pulse changed its shape in traveling from T_1 to T_2. Varying the delay time and the amplitude of the two signals applied separately to T_1 and T_2 enabled various portions of the surface wave to be cancelled out, but under no conditions could the whole surface wave be cancelled. The experiments were carried out using a dipole receiver as well as a dipole transmitter. Even in this case, however, the same objection still applied and it was found impossible to get complete cancellation of the surface signals.
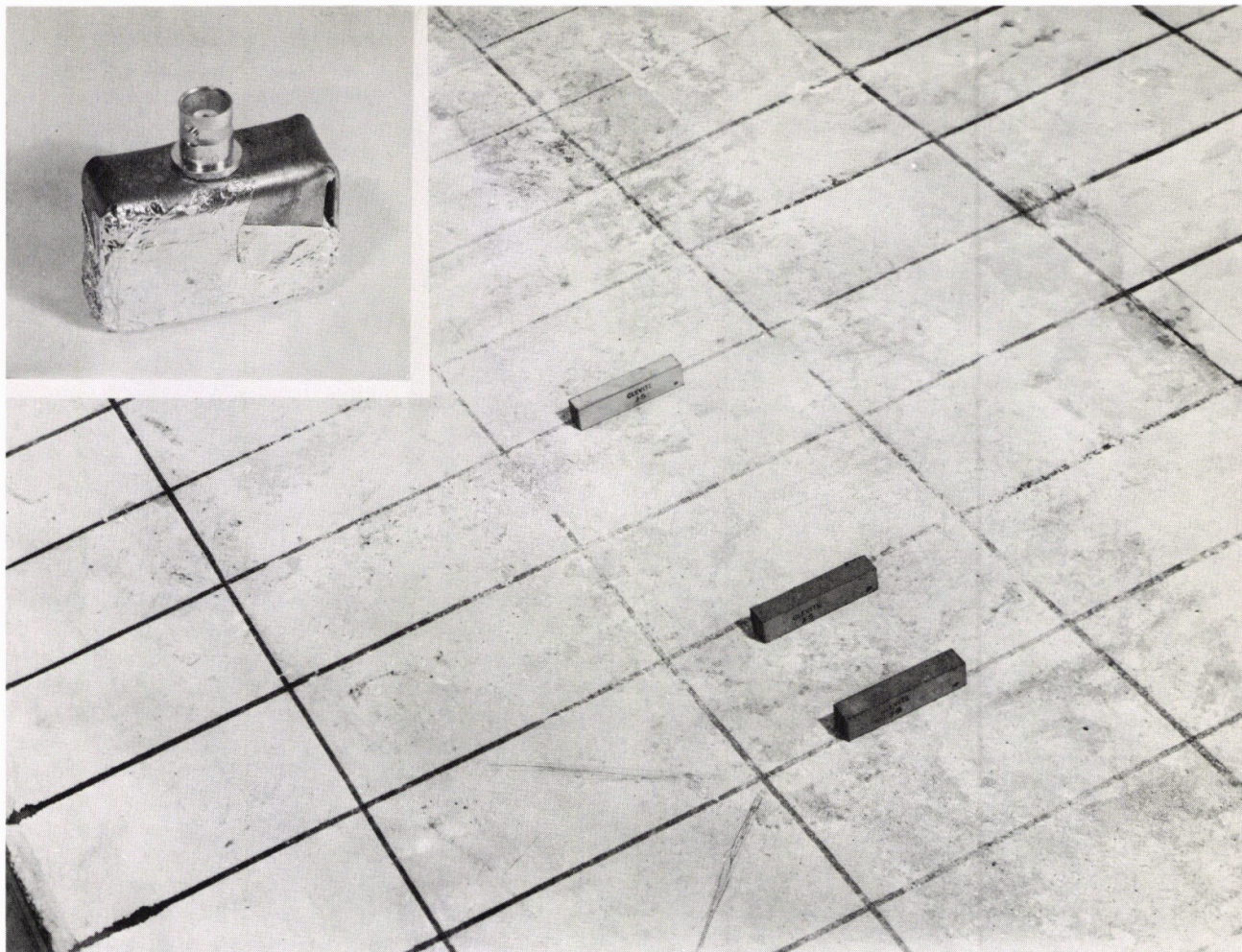
Figure A-20. Shear transducers (two transmitters and one receiver) removed from their holders. Insert shows unit wrapped as used in actual service.

Prior to the commencement of these experiments this difficulty due to dispersion had been anticipated, but the difficulty of theoretically calculating the change in shape of a pulse traveling through concrete under these particular conditions made the experimental evaluation necessary. It has therefore been decided that any type of interference effect cannot be used to advantage (i.e., to produce cancellation of the surface wave signal) either using shear wave transducers or with any other type of transducer.

Another attempt was made, however, to measure the time of flight of the shear wave being propagated downward into the concrete at 90° to the concrete surface by using the transmitting transducer as the receiver as well. It will be remembered that such an arrangement was ruled out for the case of longitudinal waves; because it is necessary to measure two independent times of flight in the concrete, both times of flight had to be measured for waves propagating down at nearly normal incidence, as for smaller angles of incidence geometrical dispersion effects introduced errors. For shear waves, however, there is no geometrical disper-
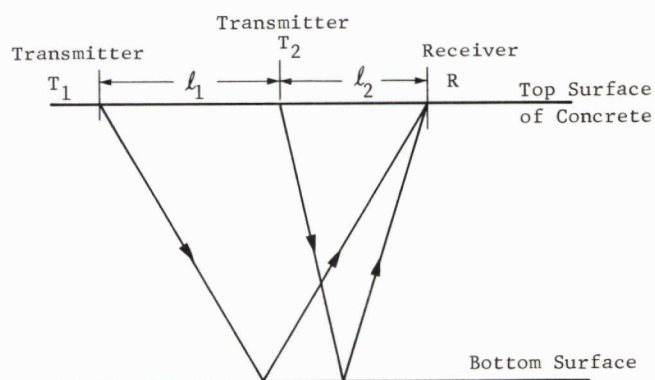
Figure A-21. Relative positions of two transmitting and single receiving shear transducers. Distances l_1 and l_2 are selected to produce destructive interference between the surface waves received at R, and constructive interference between the two waves reflected from the bottom surface.

sion. Theoretically, therefore, it should be sufficient to measure the normal reflected time of flight and the time of flight along the surface of the concrete. A single shear transducer was therefore set on the surface of the concrete and, with the aid of an electronic transmit/receive switch, the crystal was excited with a short electrical pulse and then used to look for the return of the reflected signal from the bottom. It was found, however, that even when used under these conditions the transducer continued to ring mechanically for a sufficient length of time to totally obscure any reflected signal from the bottom. This was found to be the case for tests with both portland cement concrete and bituminous concrete.

In conclusion, therefore, it may be said that although shear wave transducers enable an accurate measurement to be made of shear wave velocity, they suffer from the same disadvantages as longitudinal transducers for measuring the time of flight of the reflected wave. Also, owing to a continuous change in the shape of the surface wave pulse, pulse interference techniques cannot be used.

At this stage in the program it was evident that if continuous-wave systems were to be used, well-collimated beams and single-mode propagation would be necessary. This could be achieved only by the construction of transducers having a large diameter/wavelength ratio. Attention was then diverted to pulse time-of-flight techniques and, as was subsequently discovered, pulse techniques also required large diameter/wavelength ratio transducers if electromechanical transducers were to be used. Experiments with these large transducers are therefore discussed in the following sections.

INITIAL PULSE TIME-OF-FLIGHT METHODS

Basically, the pulse time-of-flight method involved propagation of a short wave train into the concrete and measuring the time taken for the reflected pulse to return from the bottom. Initially, tests were made with 7- and 10-in. thick air-backed slabs of portland cement concrete. Later the tests were found to be repeatable both with a 10-in. slab of portland cement concrete on a typical 4-in. thick base course, and with a 5-in. slab of air-backed bituminous concrete. Initially encountered with this technique in portland cement concrete were limitations imposed by attenuation of the high-frequency components by the concrete. This meant that pulse risetimes were long, thus making the precise start of the pulse hard to determine. This was particularly true in the case of inspection from only one side of the slab. The received signal consisted of a combination of many waves propagating by different modes (i.e., longitudinal, shear, Rayleigh, etc.) and reflected from many irregularities off the lower surface. It was possible to pick out the longitudinal wave having traveled the shortest distance to the opposite surface and back, by the fact that it arrived first. However, when a reflection technique of this kind was used, some component of the wave was scattered inside the material at the aggregate interfaces. These waves may have traveled a shorter distance and thus arrived before the main pulse. Although small in amplitude, these waves seriously hampered a precise identification of the start of the main pulse. After much practice,

the arrival of the main pulse could be discerned. Bradfield and Woodroofe (5) have reported successful results measuring the thickness of a slab of concrete using this method. They plotted the square of the spatial separation, L^2, of two transducers against the square of the delay time, T^2, of the arrival of the pulse, the intercept on the T^2 axis giving the square of the slab thickness, D^2, from

$$c^2 T^2 = L^2 + D^2 \qquad (A-73)$$

A preliminary evaluation of this technique was carried out in the following way. Two in-line transducer arrays (see Fig. A-19) having a resonance of 50 kcps were mounted on a 7-in. thick portland cement concrete slab as shown in Figure A-22.

The transmitting transducer was excited with a very narrow pulse having a duration of less than 10 μsec. Time-of-flight measurements were made at spatial separations, L, of 10, 30, 40, 50, 60, and 70 cm. Several typical received-signal displays are shown in Figure A-23; Figure A-23a has a time scale of 20 μsec per large division, and Figures A-23b and A-23c a time scale of 50 μsec per large division. The upper trace in each figure is the electrical input pulse to the transmitter, used here as the zero time reference. The lower trace is the signal obtained at the receiving transducer. Analysis of these received signals, based on prior knowledge of the slab thickness, shows that the first indication of a signal in the lower trace is the longitudinal wave which has been reflected from the bottom surface of the slab. It will be noted that at a transducer spacing of 10 cm this reflected signal is obliterated by the Rayleigh wave propagated in the near surface. Inasmuch as the Rayleigh wave velocity is approximately one-half that of the longitudinal wave, increased transducer separation provides time separation of the two signals, as shown in Figures A-23b and A-23c. As the spatial separation is increased beyond the radiation pattern of the transmitting transducer (Fig. A-23c), accurate identification of the reflected pulse becomes impossible, as would be expected. However, assuming that spatial separation between transducers is optimized to provide definite identification of the reflected pulse, as in Figure A-23b, the primary limitation of this technique arises in the precise determination of the start of the received reflected pulse. Unfortunately, even with added signal amplification inherent discontinuities in
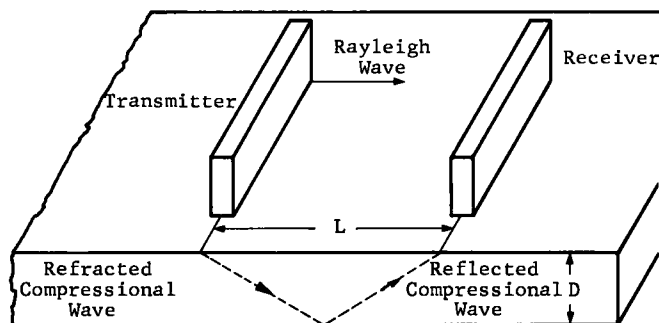
Figure A-22. Transducer arrangement for evaluation of pulse time-of-flight technique.
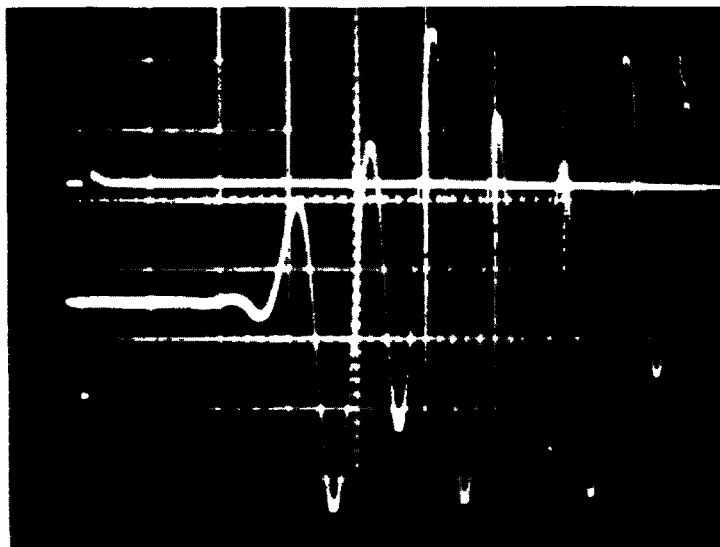
(a) Separation of 10 cm.
The pulse reflected
from the bottom surface
of the slab ($\sim$39 μsec)
is partially obscured by
the surface wave pulse
(41 μsec).
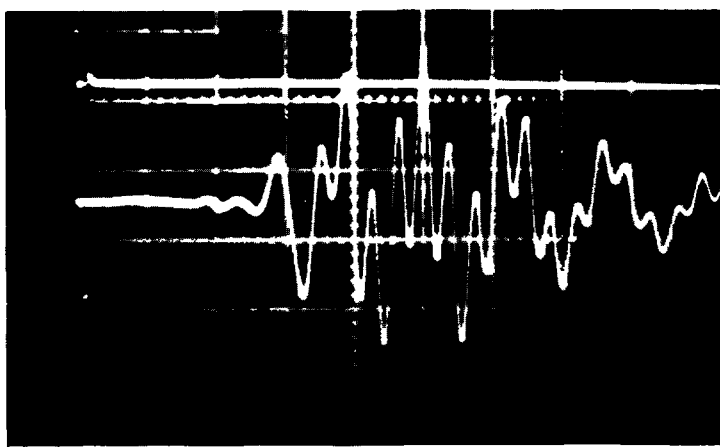
(b) Separation of 30 cm.
The difference in longi-
tudinal and surface wave
velocities allow time
separation of reflected
and surface wave pulses.
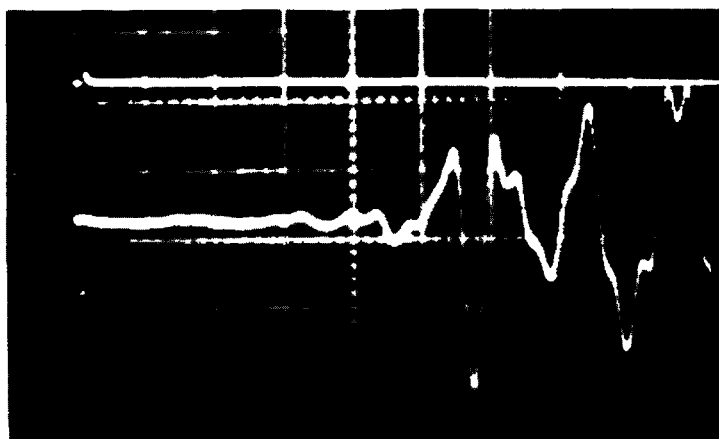
(c) Separation of 60 cm.
The reduced amplitude
of the reflected pulse
($\sim$150 μsec) indicates
the transducer separa-
tion is too great for
the particular radia-
tion pattern of the
transmitter.

Figure A-23. Pulse time of flight for transducer separations.

the concrete will scatter energy toward the receiver along shorter paths than that from the bottom surface, so that some precursors will always be observed prior to receiving the main reflector pulse.

With the simple pulse time-of-flight method described, the two necessary independent measurements were obtained by making two separate measurements with two different separations of the transmitting and receiving trans-

ducers. To obviate the necessity of making the second measurement in this way, a modified time-of-flight technique was developed.

MODIFIED TIME-OF-FLIGHT TECHNIQUE (DUAL-FREQUENCY METHOD)

The modified time-of-flight technique is basically a combination of the standard time-of-flight technique and refraction theory (see earlier section on "Refraction"). In addition, this modified technique incorporates the use of two ultrasonic frequencies. Its major advantages are as follows:

1. Obviates the need for an independent measure of sound velocity normally required for thickness determination using standard time-of-flight techniques.

2. Simplifies identification of the pulse reflected from the bottom surface of the pavement slab through the use of two frequencies.

3. Requires only one placement of transducers per area to be measured.

The basic concept is best understood by considering the system shown in Figure A-24, where transducer elements are coupled to angular lucite wedges, which in turn are coupled to the pavement structure. The lucite wedge is used to introduce the sound wave into the pavement at a given angle of incidence.

When a sound pulse is introduced into the pavement at an incident angle α, both refraction and reflection of the wave occur. Snell's law provides the following relationship between angles of incidence and refraction and velocities:

$$c_1/\sin \alpha = c_2/\sin \beta \qquad (A-74)$$

It will be readily seen that the velocity of sound, c_1, in the wedge material must be selected relative to the velocity, c_2, in concrete to obtain the desired refraction. By definition,

$$c_2 = z/t_2 \qquad (A-75)$$

in which t_2 is the total time of flight in the pavement. From geometrical considerations,

$$h^2 = (z/2)^2 - (x/2)^2 \qquad (A-76)$$

and

$$\sin \beta = x/z \qquad (A-77)$$

in which x is the center-to-center separation of the transducer elements and z is the path of propagation. Thus, substitution of Eqs. A-75 and A-77 in Eq. A-74 gives

$$c_1/\sin \alpha = z^2/(xt_2) \qquad (A-78)$$

and substition of Eq. A-76 in Eq. A-78 gives

$$h^2 = \frac{x}{4}\left(\frac{c_1 t_2}{\sin \alpha} - x\right) \qquad (A-79)$$

Examination of Eq. A-79 shows that only those variables which are easily measured are involved. By use of a fixed-angle wedge, sin α becomes a constant. Similarly, the velocity in the wedge, c_1, need only be measured once and it then becomes a constant. The time of flight in the pavement, t_2, is the difference between the total time of flight (see later discussion for measuring technique) in the system, t_1, and the propagation time in the wedges, t_w; wedge flight time is obtained from c_1, x, and a geometrical constant. Thus it is seen that there are only two variables, the transducer spacing, x, and the pulse travel time, t_2, that need to be measured. The adjustment and measurement of these two variables is discussed in the following.

At this point it should be recalled that for the earlier time-of-flight techniques accurate time measurements and fine tuning for maximum amplitude of a reflected wave were almost precluded due to the presence of spurious signals that arose through mode conversion at the transducer-pavement interface. In fact, the adverse effects of spurious wave propagation are not only relevant to time-of-flight techniques but also appear almost any time that acoustic energy is introduced into a solid, as has already been discussed. Of particular nuisance value in thickness measurements has been the adverse effect of Rayleigh wave interaction with the desired longitudinal wave reflected off the bottom surface of a pavement. The dual-frequency method for measuring transducer spacing and pulse travel time was an attempt to overcome deleterious effects of spurious wave interaction by using a different way of interpreting the output from the receiving transducer.
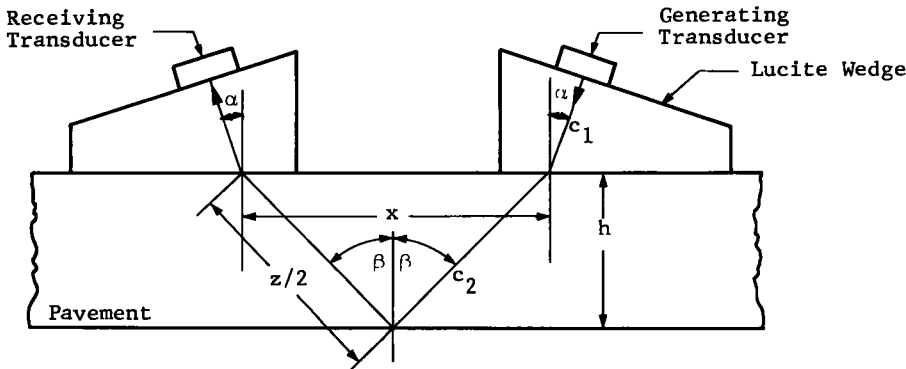
Figure A-24. Combined pulse time-of-flight refraction technique

It has been seen in previous experiments that high-frequency (above 200 kcps) ultrasonic energy is rapidly dissipated in typical pavement structures. However, when pulses of long duration are used in conjunction with slow pulse repetition rates, the low-frequency limit can be extended considerably below that dictated by geometrical considerations. The dual-frequency method takes advantage of these two conditions to provide identification of the various modes of wave propagation present in the pavement.

Figure A-25 shows the transducer and wedge assembly used in the experiments. The technique is best described by first assuming that the transmitting transducer can generate both a high- ($\sim$ 300 kcps) and low-frequency ($\sim$ 60 kcps) signal simultaneously (see earlier section on "Method of Dual-Frequency Excitation"). Both signals undergo mode conversion at the transducer-pavement interface; thus, Rayleigh waves, longitudinal waves parallel to the surface, and longitudinal waves normal to the surface are propagated at both frequencies. However, the high-frequency wave which travels normal to the surface is highly attenuated and thus will not be seen at the receiver. By making the transmitter-receiver spacing, x, small compared to the low-frequency wavelength in the pavement, only a very small fraction of the low-frequency surface wave and longitudinal wave parallel to the surface was seen at the receiver. Consequently, the predominant signals were the high-frequency Rayleigh wave and longitudinal wave propagating parallel to the surface, and the low-frequency longitudinal wave reflected off the bottom surface of the pavement.

A typical received signal is shown in the lower oscilloscope trace of Figure A-26; the upper trace shows the electrical excitation pulse used as the time of flight zero time reference. Figure A-27 is an expanded time scale of Figure A-26. It will be noted that several cycles of the low-frequency Rayleigh wave are present due to a large spacing between transducers. However, the desired effect is quite obvious. The reflected low-frequency signal is of larger amplitude than its Rayleigh wave counterpart because the angle of incidence and transducer spacing were chosen to favor it (see the earlier section on "Refraction" for a detailed discussion of critical angles for various modes of wave propagation).

Through use of this dual-frequency or modified-pulse time-of-flight technique, identification of the reflected signal is greatly enhanced, although at this stage this type of signal presentation under field conditions would not have been acceptable. Further extensive experimental analysis was therefore undertaken in an attempt to improve the system and to further understand the mechanism involved in the dual-frequency effect, as it was not altogether clear why the high-frequency component should disappear so abruptly. A complete frequency analysis was therefore made of the output signal from the receiving transducers with the aid of filters. It was found that the high-frequency component was not necessary as a marker for the signal. In fact, on the oscilloscope pictures the high-frequency component only seemed to disappear abruptly, but in fact was smoothly attenuated. The true indication of the start

of the received signal was a change in amplitude, which is partially masked by complicated interference effects. This can be seen in Figure A-28.

Figures A-29 and A-30 show the type of effect produced by the introduction of a filter into the system. In Figure A-29 a Krohn-Hite model 310-AB active filter was used with a high cutoff frequency at 250 kcps; in Figure A-30 the cutoff frequency was 65 kcps. Analysis of oscilloscope traces obtained in this way showed that the start of the desired signal could be detected only by an amplitude change.

Further improvements were made to the system by cutting the wedge, which was originally made in one piece, completely through the center in order to eliminate direct coupling through the wedge material. The side locating flanges were then used for initial lining-up purposes and later removed because they, too, were sources of potential coupling of unwanted signals. In addition, the optimum spacing of the transducers was found for the thickness of the block being measured. This could be determined quite accurately by observation of the change in amplitude at the point at which the received signal arrived. This necessitated a preknowledge of the thickness of the block to within 2 or 3 in., but in this way the thickness could be measured quite accurately by a skilled person capable of interpreting the oscilloscope signal. A typical example of some measurements made on a portland cement concrete slab is: Actual concrete thickness, 25.5 cm; measured thickness, 24.8 cm.

After the experiments described, it became clear that further improvements in pulse techniques could not be obtained by more sophisticated methods of interpreting the signal. The state-of-the-art had been advanced to the point at which a highly skilled operator could use the modified time-of-flight technique to make quite accurate thickness determinations. Further modifications, however, to enable an unskilled man to operate the device, would require an improvement in the reflected signal/surface wave signal ratio, so that the signal could be handled electronically. The possibilities for doing this were to make transducers which were more highly damped (i.e., low-Q transducers) so that wanted and unwanted signals could be time separated; or to make transducers having a higher diameter/wavelength ratio (the same requirement as for continuous-wave techniques) to reduce the magnitude of the unwanted signal.

DAMPED ELECTROMECHANICAL TRANSDUCERS

It would be possible to ignore the unwanted spurious signals, if it were possible to generate single, isolated pulses of acoustic energy similar to the pulses of electrical energy used to drive the transducers. Unfortunately, however, when a disc of piezoelectric ceramic is energized by an electrical pulse, it continues to ring like a bell long after the pulse has passed. Instead of single acoustic pulses, long wave trains of acoustic energy at the natural frequency of the transducers are produced. Hence, the desired reflected signal from the bottom of the concrete overlaps with the spurious signals, and identification of the
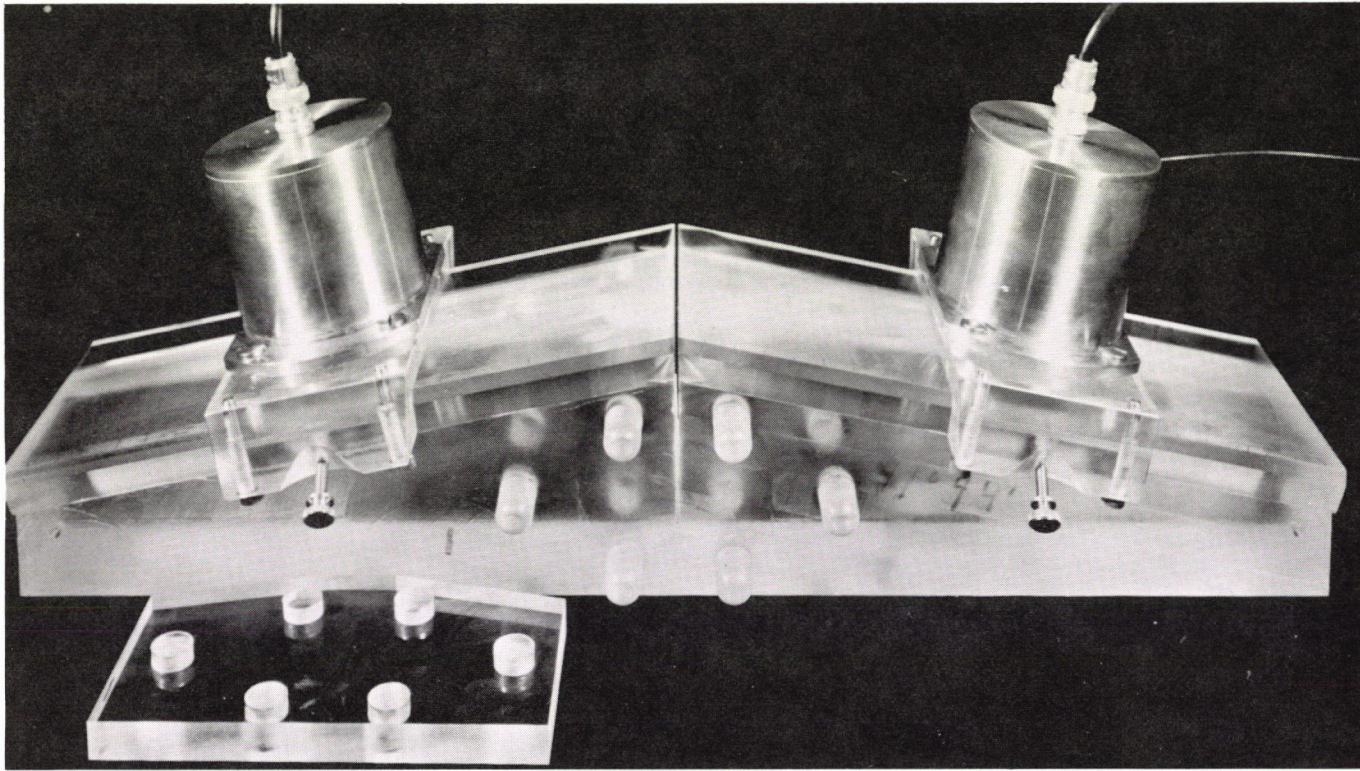
Figure A-25. Transducer and wedge assembly used for the dual-frequency modified time-of-flight technique.

Longitudinal Wave
Parallel to Surface

Rayleigh
Wave

Reflected Longitudinal
Wave Off Bottom
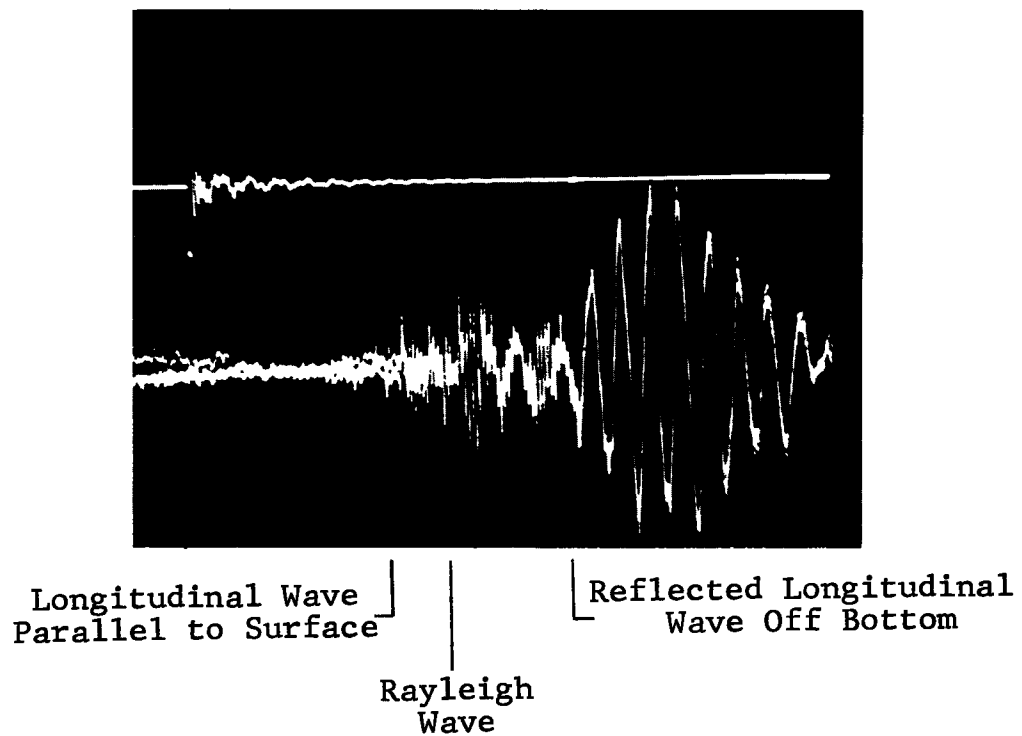
Figure A-26. Typical received signal using dual-frequency modified time-of-flight technique. Signal in upper trace is excitation pulse and zero time reference. Signal in lower trace shows start of various waves propagating in 10-in. thick pavement.
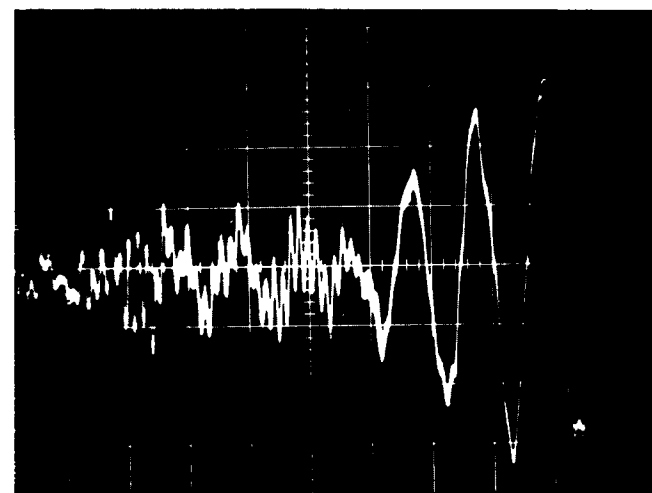
Figure A-27. Received signal of Figure A-26, but with expanded time scale.
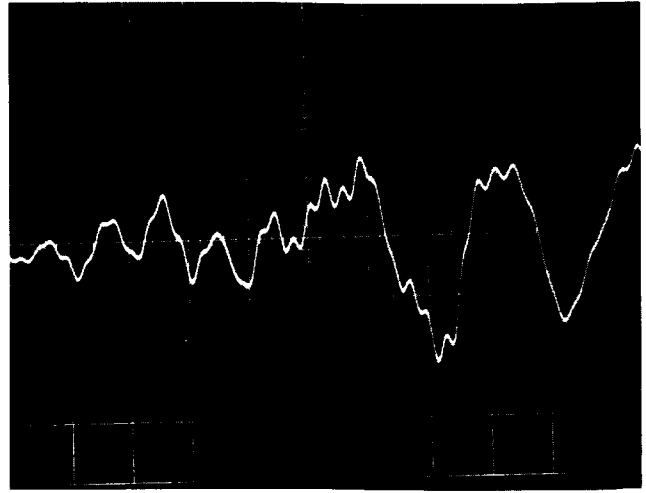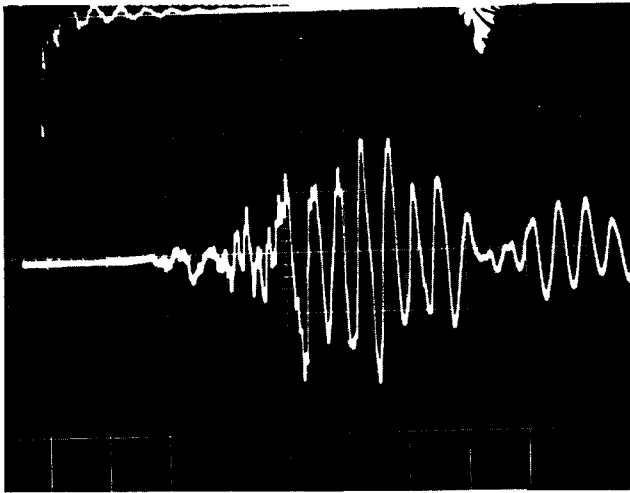
Figure A-28. Oscilloscope trace of dual-frequency signal with no filter in the system. Right trace has time base magnified to show more detail.
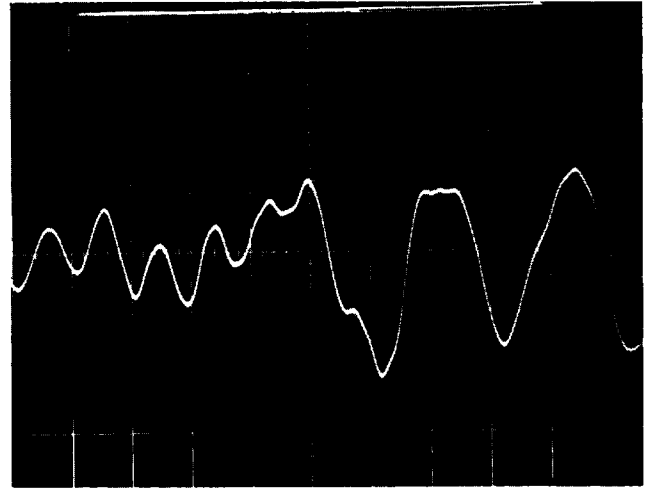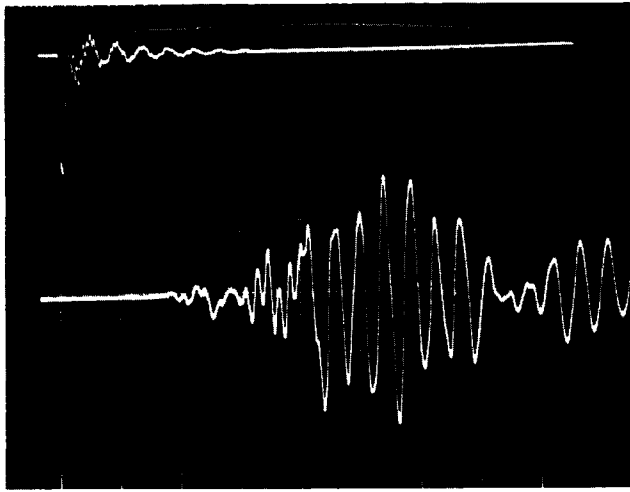
Figure A-29. Oscilloscope trace of dual-frequency signal with filter cutting off frequencies above 250 kcps. Right trace has time base magnified to show more detail.
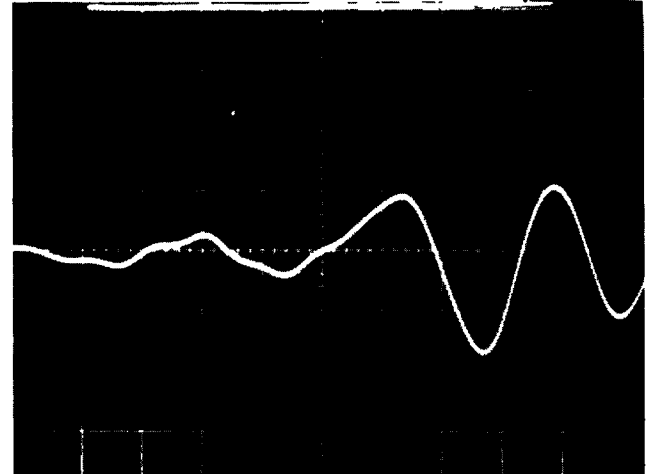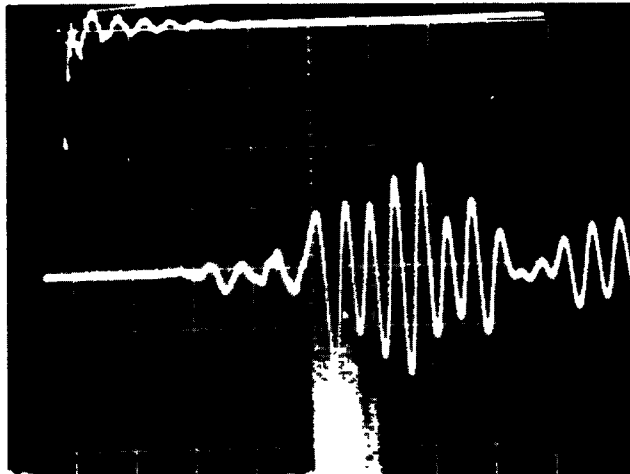
Figure A-30. Oscilloscope trace of dual-frequency signal with filter cutting off frequencies above 65 kcps. Right trace has time base magnified to show more detail.
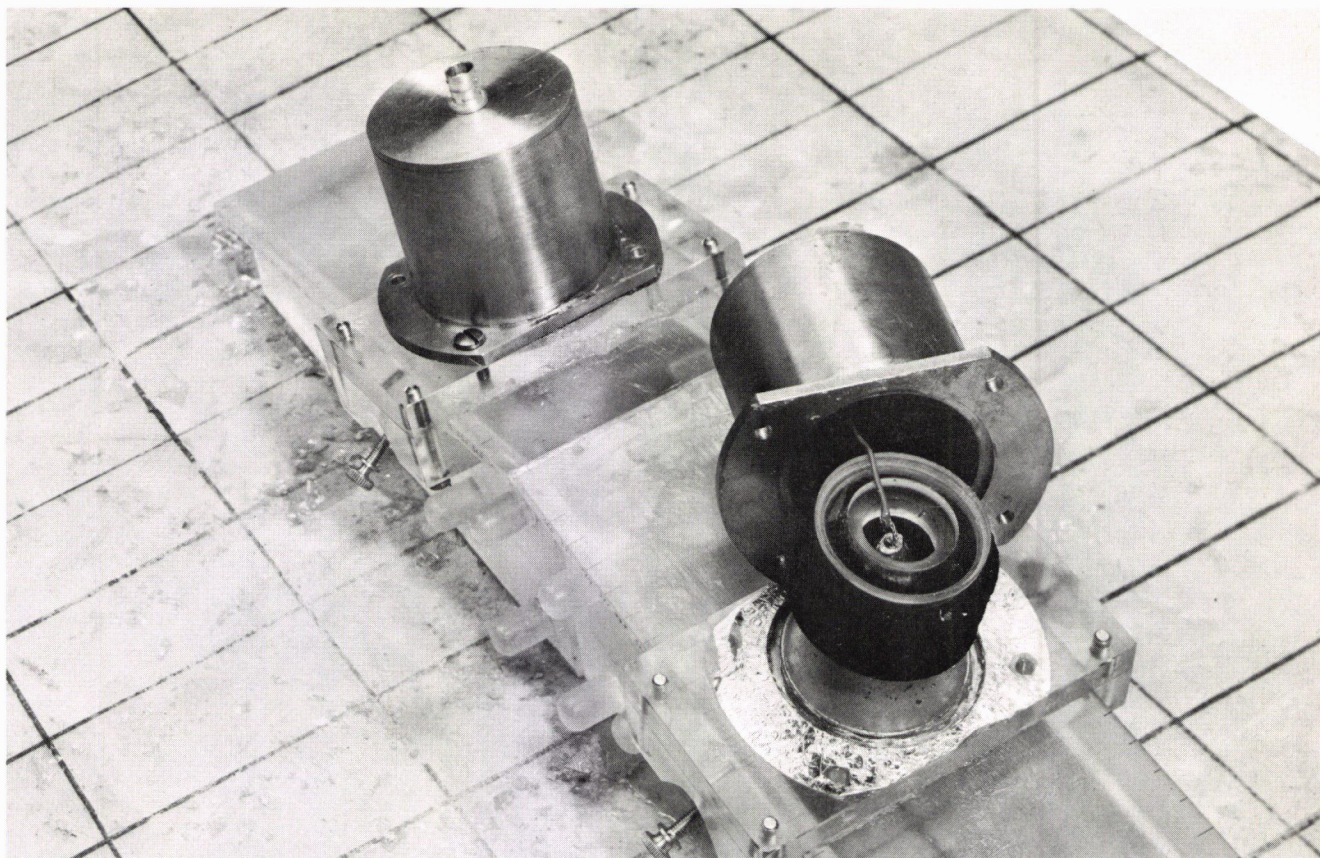
Figure A-31. Transducer housing disassembled, showing the damping arrangement. (Both transducers are mounted on the fixed-angle wedge.)

start of the reflected signal is made difficult. One method of preventing this difficulty is to damp the transducers, either by using a different transducer design or by loading the backface of the transducer. In this way, the mechanical quality factor, Q, of the transducer is reduced and its frequency response is flattened out from a sharp resonance curve. Ideally, to efficiently damp a transducer, it should be arranged for the backface to be radiating into an infinite medium having an acoustic impedance equal to that of the transducer material itself. In practice, what was done was to make a cone of Woods metal alloy, which was bonded onto the backface of a PZT4 disc and mounted inside a transducer housing with a rubber pressure pad (Fig. A-31). For the size of the PZT4 disc used, it was not practical to make a long cylindrical backing, although this may be possible with smaller transducers, thus delaying the reflected signal from the backing cylinder until after the desired signal has reached the receiving transducer. A typical oscilloscope trace seen from the receiving transducer is shown in Figure A-32. As can be seen, it was still difficult to determine the start of the wanted received signal so that the backing material was not as effective as had been hoped for in damping the transducer.

Further attempts were made to construct other types of damped transducer having still lower Q values. Small cylindrical PZT transducers having a long, coiled-wire backing were used with the notion that the time taken for a pulse to be reflected from the end of the wire would be long, compared to the time for the reflected wave to reach
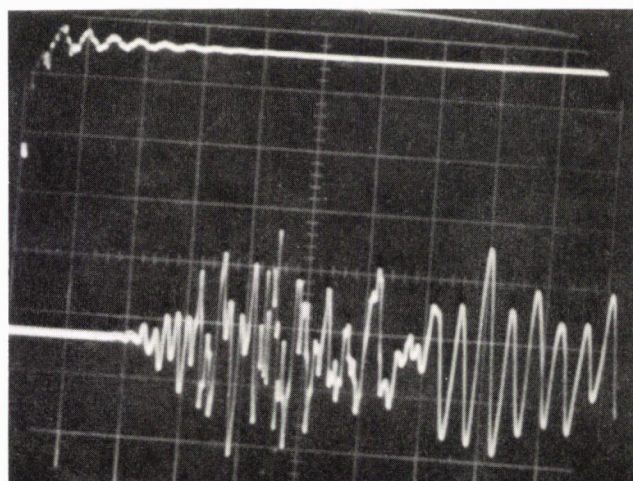
Figure A-32. Oscilloscope trace of signal from damped transducers.

the receiver. However, direct measurements of the Q of these devices with an electrical Q-meter showed that Q was reduced only to a value of 15 to 20. The damped transducers used in the previous experiment had Q's of 20 to 30. In the literature, the lowest Q transducer that could be used for thickness measurement was a magnetostrictive device described by Camp (7), which was designed to operate at 100 kcps with a Q only as low as 10. Inasmuch as a transducer having a Q at least one order of magnitude lower than this would be required for effective time separation, it was concluded that the state-of-the-art of transducer design is not sufficiently advanced in this direction at the present time.

After the development of low-Q transducers had been shown to be impractical, the next logical step was to investigate further the use of transducers having a large dimension/wavelength ratio. Such transducers are not normally constructed from a single piece of ceramic, but rather are made up of a mosaic of smaller pieces. This has the advantage of being less expensive and at the same time reducing unwanted cross modes inside the transducer itself.

MOSAIC TRANSDUCERS (FINAL RECOMMENDATION)

As indicated previously, a promising technique for eliminating the unwanted surface wave is to develop a transducer having a large diameter/wavelength ratio. Elementary diffraction theory shows that the degree of collimation of a sound beam from a transducer depends on the diameter/wavelength ratio. The higher this ratio, the greater will be the degree of collimation and, hence, the greater the suppression of surface waves. This ratio can be made larger either by making the frequency higher or by using transducers having a larger diameter. As has been seen, however, for propagation in concrete there is an upper frequency limit of about 200 kcps. Therefore, to increase the degree of collimation of the beam, it is necessary to work with larger transducers.

To evaluate the effect of the higher degree of collimation on surface wave generation, a transducer was made in the form of a mosaic consisting of a large number of ceramic rods embedded in an epoxy disc. Two transducers (resonant at 100 kcps) were made in this way and mounted on the fixed-angle wedges discussed. It was found that there was a great reduction in the amplitude of the unwanted surface wave. The oscilloscope trace (Fig. A-33) shows a sharp onset for the start of the reflected wave. This onset was sharp enough for electronic handling of the signal using a pulse sing-around system. Using such an arrangement, it was possible to measure the thickness of the concrete test specimens to an accuracy of about 2 percent. This high signal-to-noise ratio, however, could not be reproduced on test blocks varying much in thickness from the specimens used in these experiments without readjustment of the apparatus by a semi-skilled operator. However, because these results were encouraging, it was decided to investigate the properties of transducers having still larger ratios of diameter to wavelength, and hence an even higher degree of collimation and consequent higher degree of suppression of surface waves.

For these subsequent investigations, a transducer which was a simple linear array of rods (see Fig. A-19) was used in a position as shown in Figure A-34. The transducers used in this way thus radiated a beam which was collimated in the plane of the diagram but virtually uncollimated (i.e., behaved as a point source) in directions at right angles to this plane. This meant that surface waves in the direction of interest should have been completely suppressed, although at right angles to this direction there was a strong surface wave contribution to the total energy transmitted. The oscilloscope trace obtained using this arrangement is shown in Figure A-35. From calculations, it was known that the time of flight of the reflected pulse should be about 180 μsec. As can be seen from Figure A-35, there was little or no surface wave signal arriving before the 180-μsec mark, and at about 180 μsec the reflected wave started to arrive. Unfortunately, the risetime of the reflected wave for this one-dimensional array was rather long, and the signal built up only slowly owing to the transducer ringing. This prevented accurate measurement of the time of flight.

Because of the promising results obtained in these experiments, it was decided that a large pair of mosaic transducers would provide a solution to the problem of measuring pavement thickness. A large mosaic transducer-wedge assembly was therefore designed to produce a beam having a semi-angle of 4° in a vertical plane containing the transmitter and the receiver. In this plane the length of the Fresnel zone would be 25 in. In the vertical plane making an angle of 90° with the plane containing the transmitter and the receiver, the corresponding figures for the semi-angle and Fresnel zone length would be 6° and 13 in. To achieve this performance at an operating frequency of 150 kcps, the transducers were rectangular and designed to the following dimensions: Element size, cylinders 0.375 in. long by 0.125 in. in diameter; element spacing, 0.375 in.; overall length along wedge, 10 in.; overall width, 7 in.

The elements were to be made from PZT5 material in order to obtain a damping factor as high as possible. The construction of the transducer in the form of a mosaic of many small elements embedded in an epoxy resin, also has the advantage of reducing cross modes to a minimum and decreasing the Q of the whole array. It is anticipated that the degree of collimation and surface wave suppression that would be attained with these transducers could enable a continuous-wave modified sing-around technique to be used.

In order to obtain further experimental evidence that the construction of these large mosaic transducers would be worthwhile, some further experiments were conducted with existing mosaic transducers. Two 3-in. diameter circular transducers were placed side by side on the fixed-angle wedges and used in parallel as a transmitter. A third smaller transducer was used as the receiver. Once again, a fairly well-defined beam was produced, but in this case it was difficult to evaluate the overall performance of the system owing to a difference between the resonant frequency of the transmitter and the receiver. At this point, all of the experimental results tend to show that a suitable solution to the problems encountered so far would be
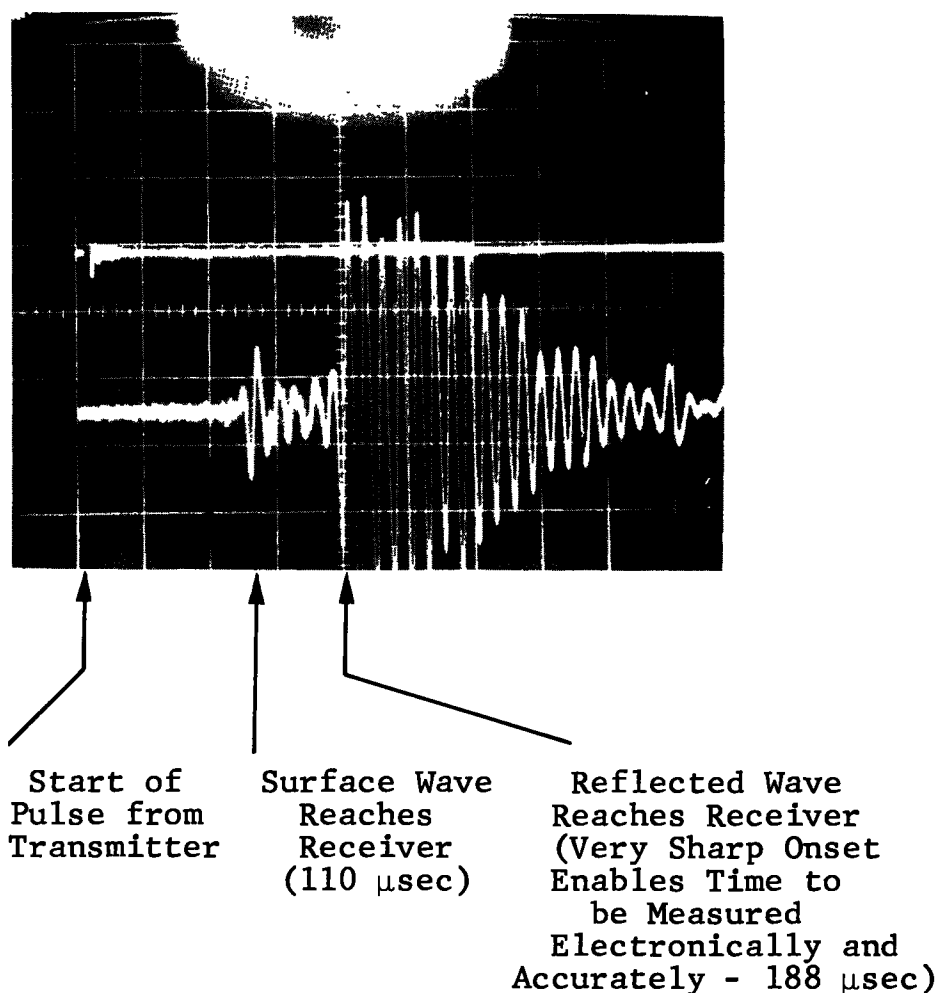
Figure A-33. *Electrical pulse applied to the transmitting transducer (upper trace), and electrical output from the mosaic disc transducer (lower trace), as a function of time. (Time scale is 50 μsec per division.)*

presented by construction of the larger mosaic transducers described.

Although the construction of large mosaic transducers offers a solution to the problem, another promising technique was also investigated. In this technique, time separation of the wanted and unwanted pulse has finally been achieved by using mechanical impact devices instead of conventional electromechanical transducers.

MECHANICAL IMPACT TECHNIQUE (FINAL RECOMMENDATION)

As was demonstrated in the earlier section on "Damped Electromechanical Transducers," it is impossible to get short enough mechanical pulses to enable unwanted surface waves and reflected signals to be time separated using conventional transducers. Because of mechanical ringing in the transducers which could not be damped sufficiently, a mechanical wave train of many times the length of the original pulse was produced when they were excited by the application of a short square pulse of voltage. To avoid
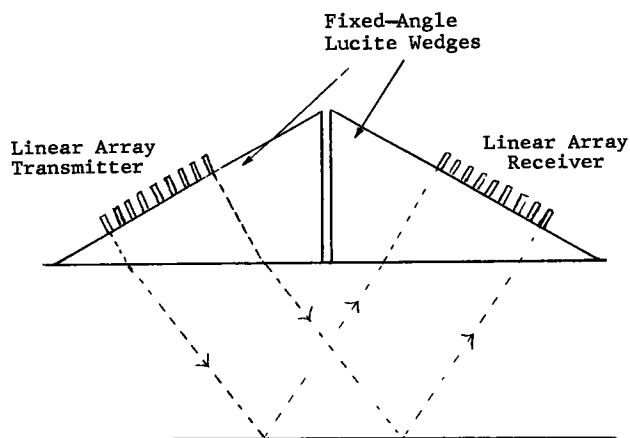
Figure A-34. *Transmitting and receiving linear array transducers. Each array consists of a single line of ferroelectric ceramic elements. The beam is well collimated in the plane of the diagram, but will be poorly collimated in the plane normal to the drawing.*

38
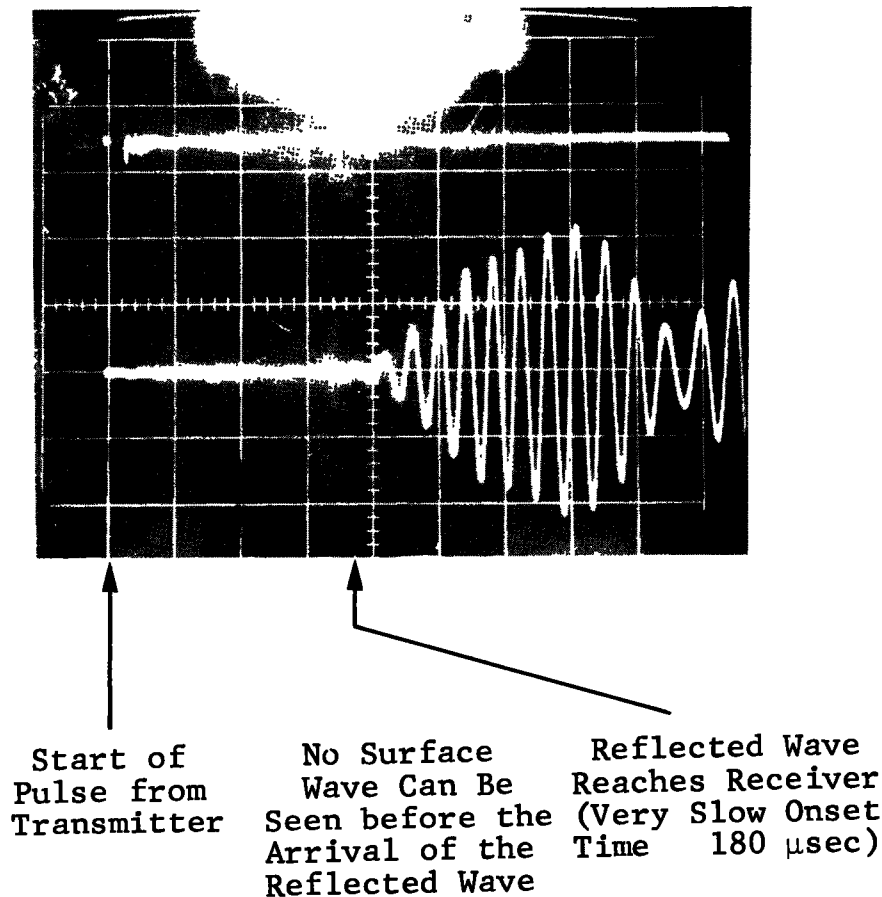
Figure A-35. Electrical pulse applied to the transmitting transducer (upper trace), and electrical output from the line-array-type transducer (lower trace), as a function of time. (Time scale is 50 μsec per division.)

this difficulty, two possibilities using different types of sound sources were considered—(a) a single shock pulse produced by explosives, electrical discharges, an electromagnetic device, or by coupling airborne shocks into the concrete; and (b) mechanical removal of the sound source after a very short interval of time.

Preliminary experiments were conducted to investigate the second possibility, in which small ball bearings and other objects were dropped onto the concrete surface and contact times as short as 10 μsec were obtained. Although a ball bearing has a very high Q and continues to ring after impact with the concrete, the physical contact is broken after it has bounced away from the surface and energy is only radiated into the concrete for the duration of the impact. It was found that to take advantage of these short pulses it was necessary to use a nonresonant type of microphone. As a result, an ultramicrometer, which is essentially a condenser microphone, was used. As can be seen from the output (Fig. A-36), the signal received was just visible above the noise level, but with larger pulses (obtained using shock sources or a high-velocity small projectile bouncing from the concrete surface) the signal level would be quite adequate. The time of flight of the reflected signal in

Figure A-36 enabled the concrete thickness to be determined to within 20 percent, and it was predicted that this error should be capable of being reduced to about 2 percent if higher-amplitude pulses or more sensitive detectors were used.

Further experiments were then performed using very small PZT elements for detectors. The system used for these experiments is shown schematically in Figure A-37. A ball bearing connected by means of a very thin copper wire to an electrical triggering circuit was dropped onto a 0.001-in. thick piece of silver foil secured with vaseline to the concrete surface. The silver foil acted as the second electrode for the triggering circuit and a single sweep of the oscilloscope was started as soon as contact was made between ball and silver foil. Spaced along the concrete surface at known distances from the impact point were three receiving transducers. The output from each of these transducers was amplified and then filtered to remove any spurious unwanted frequencies, before being displayed on the oscilloscope. By using an oscilloscope having a memory storage feature, the time differences between the arrival of the reflected pulse at the first and second transducers, and the second and third transducers, could be measured; and

Time of Ball Bearing Impact | Surface Wave Pulse (Time - 65 μsec) | Reflected Wave Pulse (Time - 120 μsec)
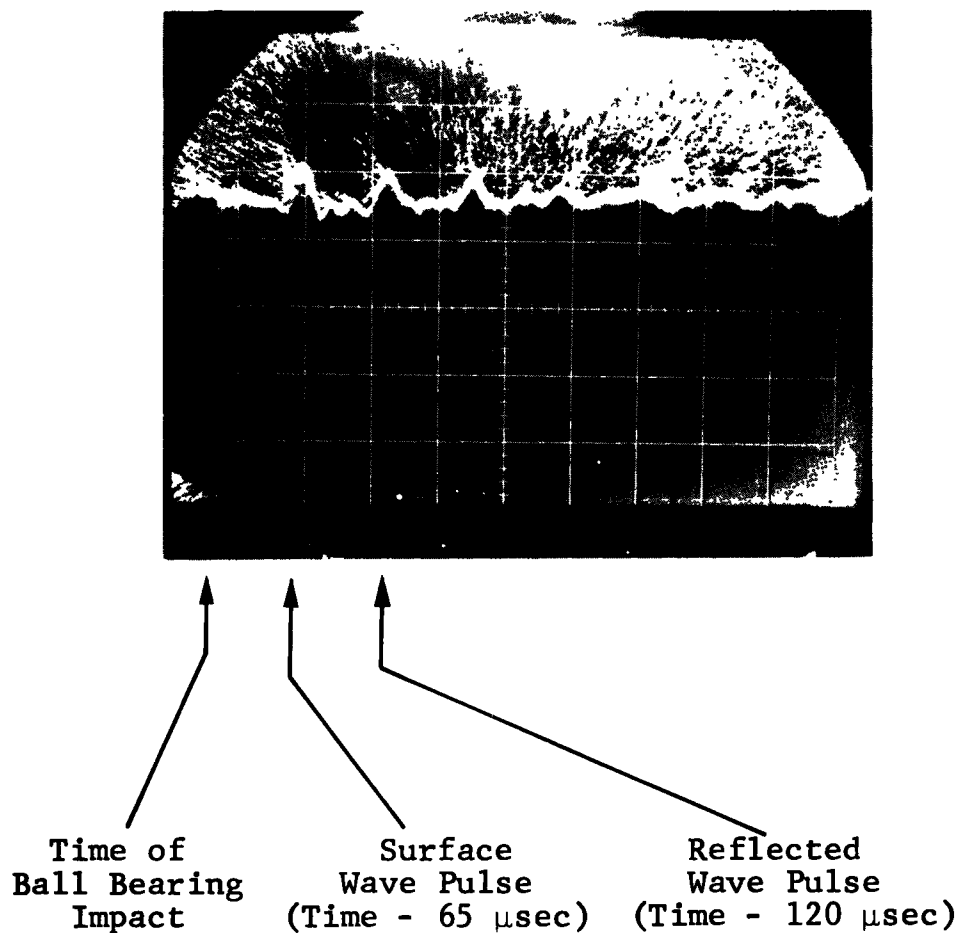
Figure A-36. Trace showing electrical output of a transducer mounted directly on the surface of the concrete. The pulse was produced by dropping a ball bearing onto the concrete a short distance from the receiving transducer. The times of flight in this experiment are shorter because there is no time spent in traveling through coupling blocks. The apparent fogging of the picture is due to the fact that an oscilloscope with a memory storage feature was used, resulting in some background emission. (Time scale is 50 μsec per division.)
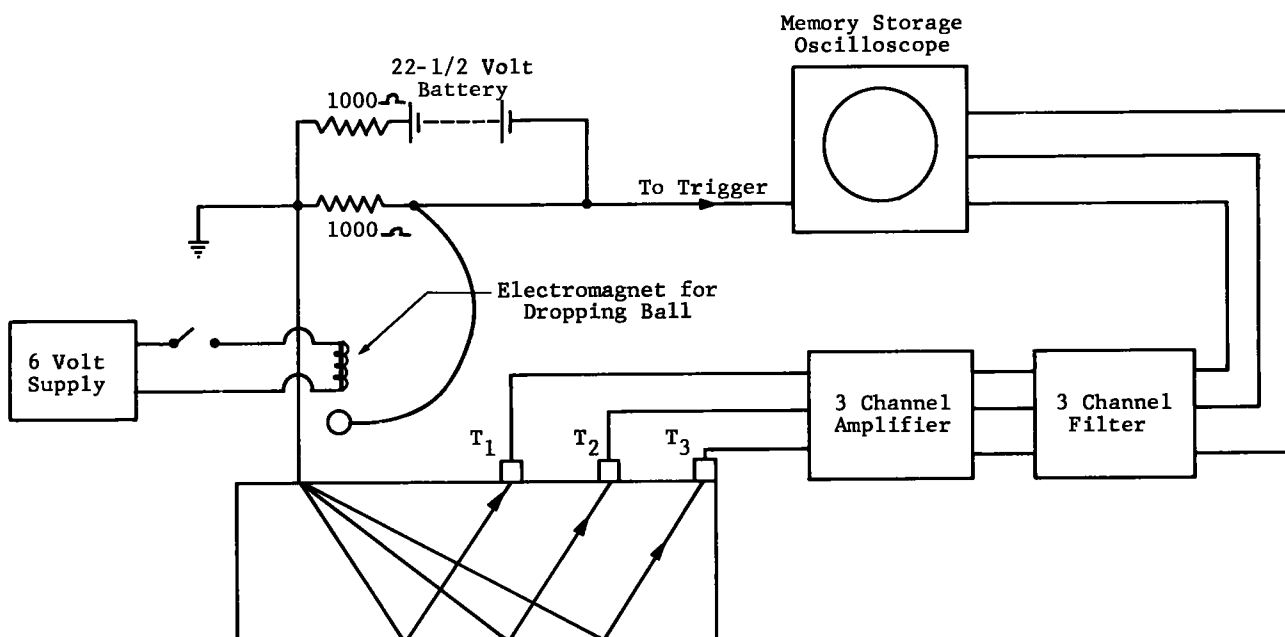
Figure A-37. Block diagram of apparatus used for pulse time separation experiment.

by eliminating the sound velocity from the equations as described in previous reports, the thickness could be calculated. The reflected pulse was the second pulse to arrive at the transducer in each case, being clearly discernible from the first surface wave pulse (see Fig. A-36). However, the thickness of the block obtained in this way was not accurate and showed spurious deviations from one experiment to the next. This was eventually found to be due to a complicated interaction between a signal produced by the ringing of the receiving transducers and the electrical filter-amplifier arrangement.

To circumvent this difficulty, it was necessary to use the condenser microphone again. Then sensitivity of the condenser microphone was very low because essentially a condenser microphone is a low-impedance detector and concrete is a high-impedance medium. There was thus a severe mismatch. For this reason it was necessary to consider other methods for producing very short pulses having a somewhat larger amplitude.

Initially the pulse amplitude was increased simply by increasing the impact velocity of the ball. An air rifle and balls propelled from an explosive-driven tube were used for this purpose. It was found, however, that although the pulse amplitude could be increased in this way, the pulse length also increased to the point at which time separation could no longer be obtained. Measurements were then made of the duration of contact of the missile with the concrete, using the electrical triggering circuit to measure the time. The missiles used varied from long rods to small

ball bearings. A typical curve of contact time against the length of the rod (or diameter of the ball) is shown in Figure A-38. Generally it was found that balls or rods having a rounded end had a longer contact time than rods having a flat end. Smaller balls and rods had a contact time much longer than that predicted theoretically (the theoretical contact time is equal to the time required for an acoustic pulse generated by the impact to be reflected from the top end of the rod, provided this time is much less than the propagation time through the concrete).

It was concluded that this disagreement resulted from the impact being not purely elastic, with a certain amount of plastic deformation of the concrete or the missile tending to increase the contact time. It was to be expected that this plastic deformation would be more prominent for curved surfaces (smaller impact area), smaller missiles, and higher velocities; and indeed, it was found experimentally that generally under these conditions the contact time was greater. In an effort to maintain a short contact time and still obtain higher pulse amplitudes, a long rod having its upper end case hardened was used to couple the impact into the concrete. The rod was made 40 in. long so that reflections to and fro along its length would not arrive in the concrete until much later than the desired pulses. Initial experiments using this arrangement have proved to be very successful and high-amplitude pulses having a duration of only 10 μsec have been produced by striking the top end of the rod with a ball bearing fired from an air gun (see Fig. A-39).
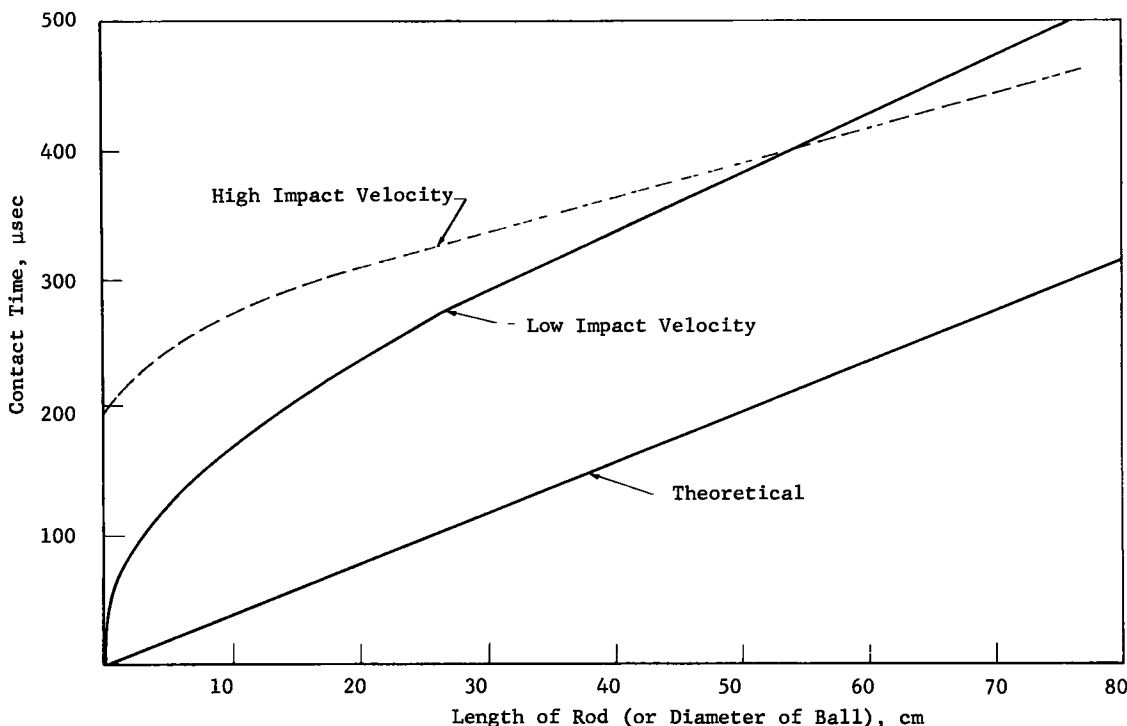
Figure A-38. Experimental curves of impact times against length for rods and balls dropped onto concrete surfaces.
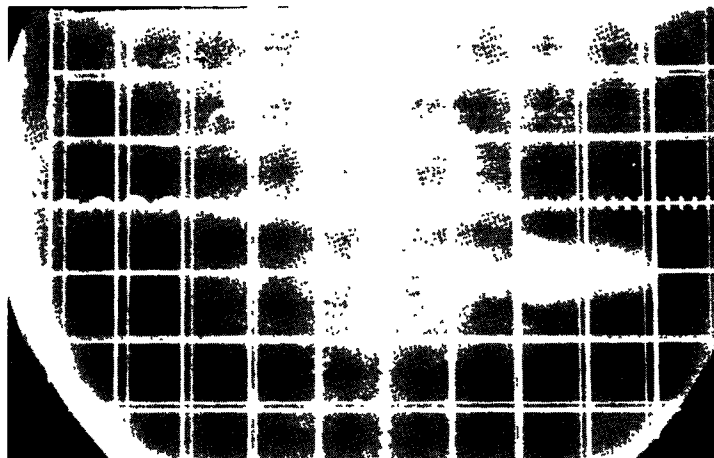
Time (1 div = 10 μsec)
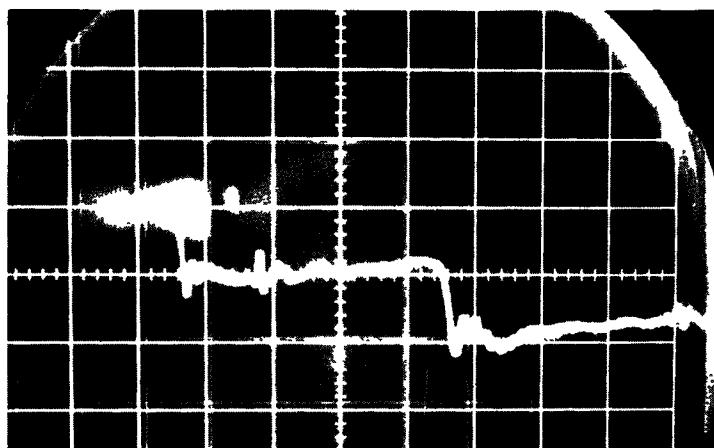
Time (1 div = 100 μsec)

Figure A-39. Oscillogram showing (upper trace) signal received by ultramicrometer at the end of a steel rod for a pulse produced at the other end with a ball fired from an air gun, and (lower trace) arrival of the second reflection nearly 400 μsec later.

In Figure A-39, the pulse appears as a step-function and the width of the step is a measure of the width of the pulse. The reason for this step-function shape is that the condenser microphone actually measures displacement of the rod, which is the integral of the velocity with respect to time. Thus, differentiating the step-function would yield a curve representing a single-velocity pulse. This method of producing short pulses is the most successful of all the various methods tried so far. These include small explosive detonators placed on the concrete, airborne shocks produced by powder charges, and explosively propelled missiles. It was found that detonating types of explosives produced pulses which were too short and hence were rapidly attenuated in the concrete by scattering from the aggregate. The pulse could only be lengthened by increasing the dimensions of the detonating explosive to a

dangerous size. For the airborne shocks, not enough energy could be coupled into the concrete from an explosion of a size reasonable to use on a highway. Although other methods, including an electromagnetic shock source and the underwater spark method of producing short pulses, still remained to be explored experimentally, work was suspended owing to the satisfactory performance of the system using the case-hardened rod and the air gun.

The only remaining difficulty with the pulse method was the choice of a suitable detector. Although the condenser microphone is perfectly suitable for laboratory experiments, some modification may be needed before using it in the field, owing to the fact that usually instruments having the requisite sensitivity are extremely delicate and need precise alignment and setting before being used. It is possible that a modified condenser microphone could be constructed for

a final thickness-measuring device which would be reasonably sturdy and fairly easy to use. Further work was continued, however, in an attempt to find a substitute for the condenser microphone. Types of microphone that were constructed include small ferroelectric elements, carbon granule types (telephone mouthpieces), and a small magnetostrictive detector. In all cases, it was impossible to get a faithful response to the pulse without ringing occurring.

For a final overall evaluation of the method, the ultramicrometer was used and the thickness of a 10-in. slab of portland cement concrete on a 4-in. thick base course was measured to an accuracy of ± 2 percent. A high degree of accuracy was also obtained using an air-backed slab of bituminous concrete, although in this case the bottom surface was so rough that even direct measurements with a ruler were only accurate to ± 5 percent. Attempts to measure the thickness of a layer of bituminous concrete on portland cement concrete were unsuccessful, probably owing to the fact that a sufficiently large acoustic mismatch was not present at the boundary.

APPENDIX B

NUCLEAR TECHNIQUES

ISOTOPES PLACED ON THE SUBSTRATE

Consider a layer of radioisotope distributed uniformly over the base course with an area density of σ gm per cm^2. Let ρ denote the density of the concrete, A the atomic mass of the radioisotope, λ its disintegration constant, N_0 Avogadro's number, k_1 the fraction of disintegrations resulting in emission of a gamma ray of energy E_1, and S the area of a detector placed on the top surface of the concrete. Then the gamma rays entering the detector per second are found by

$$\frac{k_1 \rho \sigma N_0 \lambda S}{2A} e^{-\lambda t} E_2(\mu_1 \rho Z) \qquad \text{(B-1)}$$

in which E_2 is the exponential function (8) defined by

$$E_2(x) = \int_1^\infty (e^{-xy} dy/y^2) \qquad \text{(B-2)}$$

This method also shows the greatest sensitivity when $\mu_1 \rho Z \simeq 2$; i.e., for a high-energy gamma ray.

In this technique one can tell the difference between $Z = 17.5$ cm and $Z = 20$ cm in a medium of density 2.35 with a detecting system whose overall accuracy is 1 percent if

$$E_2(41.1 \mu_1) - E_2(47 \mu_1) > 0.01 E_2(41.1 \mu_1) \qquad \text{(B-3)}$$

This is satisfied by any practical values for μ_1, provided, of course, that $E_2(41.1 \mu_1)$ is not too small to be detectable.

Taking As^{76} as an example and using $k_1 = 0.10$, $E_1 = 1.20$, $\mu_1 = 0.058$, a detector of area 50 cm^2, and an efficiency of 20 percent, one obtains for $Z = 20$ cm,

$$\sigma \times \frac{0.10 \times 6 \times 10^{23} \times 0.73 \times 10^{-5} \times e^{-0.73} \times 0.2 \times 50}{2 \times 76}$$

$E_2(2.73) = 2 \times 10^{11} \sigma$ counts/sec.

Similarly, for $Z = 17.5$ cm one obtains a value about 70 percent higher. Because 20 counts/sec are sufficient to statistically establish this difference of 70 percent in 1 sec, $\sigma = 10^{-13}$ g of arsenic are required per cm^2 of base course area. Figure B-1 shows the dependence of the relative counting rate of 1.2 Mev gamma rays, $E_2(0.136 Z)$, versus the thickness, Z, for As^{76}.

ISOTOPES PLACED ABOVE THE PAVEMENT

Consider a pavement of mass density, ρ_p, and thickness, Z, over a base course of mass density, ρ_s. Let μ_s be the effective mass scattering coefficient of the source radiation and μ_a be the effective mass absorption coefficient of the backscatter radiation. An approximate analytical treatment ignoring the angular and energy dependences of the scattering process can be made, assuming μ_s and μ_a are independent of energy and that the scattered radiation is distributed isotropically.

If a source emitting Q gammas per second is placed on the surface of the pavement, and if this point is taken as the origin of a coordinate system such that the z axis is perpendicular to this surface, the scattered radiation produced per unit volume at points $z < Z$ is

$$R = \frac{Q \rho_p \mu_s}{4\pi(x^2 + y^2 + z^2)} e^{-\mu_s a \rho_p (x^2 + y^2 + z^2)^{\frac{1}{2}}} \qquad \text{(B-4)}$$

and for $z > Z$, ρ_p is replaced by ρ_s in the fraction and by the factor $(\rho_p Z/z - \rho_s Z/z + \rho_s)$ in the exponent. If the detector, of area A, is located at the point $(X, 0, 0,)$, the number of gammas entering the detector per second is

$$\int_0^\infty dz \int_{-\infty}^{+\infty} dx \int_{-\infty}^{+\infty} dy \frac{R A z}{4\pi [(x - X)^2 + y^2 + z^2]^{3/2}}$$
$$\times e^{-\mu a \rho (x^2 + y^2 + z^2)^{\frac{1}{2}}} \qquad \text{(B-5)}$$

in which $\rho = \rho_p$ for $z < Z$ and $\rho = \rho_p Z/z - \rho_s Z/z + \rho_s$ for $z > Z$. This integral is difficult to evaluate, even though
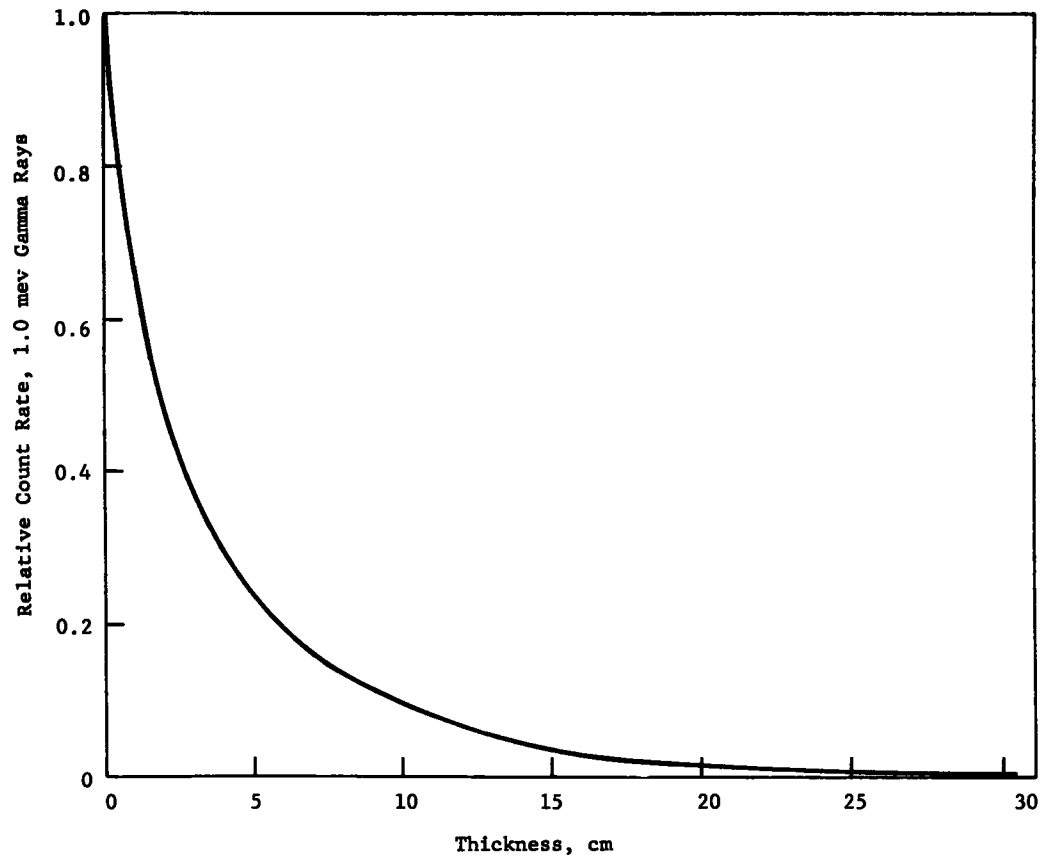
Figure B-1. Relative count rate vs pavement thickness with radioisotope As^{76} spread over subbase.

it is an approximate treatment. The influence of pavement thickness and density on backscattered gammas is best determined by direct experimentation.

ISOTOPES INTIMATELY MIXED WITH PAVEMENT MATERIALS (9)

Consider a radioactive isotope intimately mixed with the cement paste. Let ρ denote the density of the concrete, and f denote the fraction by mass of the radioactive isotope of atomic mass A. Then if λ is the disintegration constant (half-life equals $0.693/\lambda$), the number of disintegrations per unit volume at a time, t, after the mixing is given by

$$\frac{f}{A} \rho N_0 \lambda \exp(-\lambda t) \qquad \text{(B-6)}$$

in which N_0 is Avogadro's number ($6.02 \times 10^{2.3}$ per gram atomic mass). If each disintegration is accompanied by emission of gamma radiation, the gamma rays may be of several energies depending on the decay scheme of the radioactive isotope. If one considers a particular gamma ray energy, E_1, emitted in a fraction, k_1, of the disintegrations, and if the mass absorption coefficient for gammas of this energy is μ_1, the gamma rays per second entering a detector of area, S, placed on the surface of the pavement from a unit volume located at a depth, z, below the

surface point, which is a distance, r, from the center of the detector, is given by

$$\frac{k_1 \rho f N_0 \lambda S z}{4\pi A (r^2 + z^2)^{3/2}} \exp[-\lambda t - \mu_1 \rho (r^2 + z^2)^{\frac{1}{2}}] \qquad \text{(B-7)}$$

Multiplying by the volume element, $r\,dr\,dz\,d\phi$, and integrating over ϕ from 0 to 2π, over r from 0 to ∞, and over z from 0 to Z, one obtains

$$\frac{k_1 f N_0 \lambda S e^{-\lambda t}}{2\mu_1 A} \cdot [0.5 - E_3(\mu_1 \rho Z)] \qquad \text{(B-8)}$$

in which E_1 is the exponential function (10) defined by

$$E_1(x) = \int_1^\infty (e^{-xy} dy/y^3) \qquad \text{(B-9)}$$

This method will show the greatest sensitivity in determining the thickness, Z, when the derivative of Eq. B-9 with respect to Z is a maximum; i.e., for the largest value of

$$- \frac{k_1 \rho f N_0 \lambda S e^{-\lambda t}}{2A} E_1{}'(\mu_1 \rho Z) \qquad \text{(B-10)}$$

This occurs when $\mu_1 \rho Z = 0$; i.e., for zero thickness or zero absorption. Because the thickness is likely to be of the order of 20 cm, the absorption needs to be low. This requirement, in turn, means a relatively penetrating gamma ray; i.e., a high-energy gamma ray.

In order to tell the difference between $Z = 17.5$ cm and $Z = 20$ cm in a medium of density 2.35 gm per cm^3 with a detecting system whose overall precision is 1 percent, a value of μ_1 is needed which makes

$$E_3(41.1\,\mu_1) - E_3(47\,\mu_1) > 0.01\,[\tfrac{1}{2} - E_3(47\,\mu_1)] \quad \text{(B-11)}$$

which implies that μ_1 must be less than about 0.065, so that the gamma energy must be greater than about 1.0 Mev.

Other requirements of this method are: (1) a high value for k_1, and (2) a high value for $\lambda e^{-\lambda t}$. Inasmuch as the time after mixing at which the measurement is likely to be made may be of the order of a few days, or 10^5 sec, λ should be of the order of 10^{-5} sec^{-1}.

A search for the radioisotopes best satisfying these requirements has not been made. Nevertheless, a possible candidate might be As^{76}, which has a half-life of 26.5 hr ($\lambda = 0.73 \times 10^{-5}$ sec^{-1}) and emits gammas of energy 0.55 Mev in about 40 percent of the disintegrations, gammas of energy 0.64 Mev in about 9 percent of the disintegrations, gammas of energy 1.20 Mev in about 10 percent of the disintegrations, gammas of energy 1.40 Mev in about 1 percent of the disintegrations, and gammas of energy 2.05 Mev in about 2 percent of the disintegrations (11). Selecting the 1.20-Mev gamma ray (by using a scintillation detector or other detector which can select

gammas in a narrow energy range), one can put the values $k_1 = 0.10$ and $\mu_1 = 0.058$ cm^2 gm^{-1} (which is a good value for elements from $Z = 10$ to $Z = 40$) (10) into the foregoing equations. Using $\rho = 2.35$ gm per cm^3 for the concrete and $A = 76$ for arsenic, one obtains, for $Z = 20$ cm,

$$\frac{0.10 \times 6 \times 10^{23} \times 0.73 \times 10^{-5} \times e^{-0.73} \times Sf}{2 \times 76 \times 0.58}$$

$$[0.5 - E_3(0.058 \times 2.35 \times 20)] = 1.2 \times 10^{16}\ Sf\ \text{gammas/sec} \quad \text{(B-12)}$$

Similarly, for $Z = 17.5$ cm, one obtains about 1.4 percent fewer gammas per second. Figure B-2 shows the relative counting rate of 1.2-Mev gamma rays, $1.0 - 2E_3(0.136\,Z)$, versus the thickness, Z, in cm, for As^{76}.

If one wants to detect this 1.4 percent difference in 1 sec and if a detector of efficiency 20 percent and area 50 cm^2 is used, and since 5×10^4 counts per second are required to realize 1.4 percent statistical accuracy in 1 sec, a value of 4.2×10^{11} results for f, the number of grams of As^{76} per gram of cement. Although this value seems small, it amounts to 0.1 μcuries per gram of concrete or 0.1 curies per ton of concrete. The problem of obtaining such large amounts of radioactive isotope and mixing it uniformly in the concrete looms very large, although not
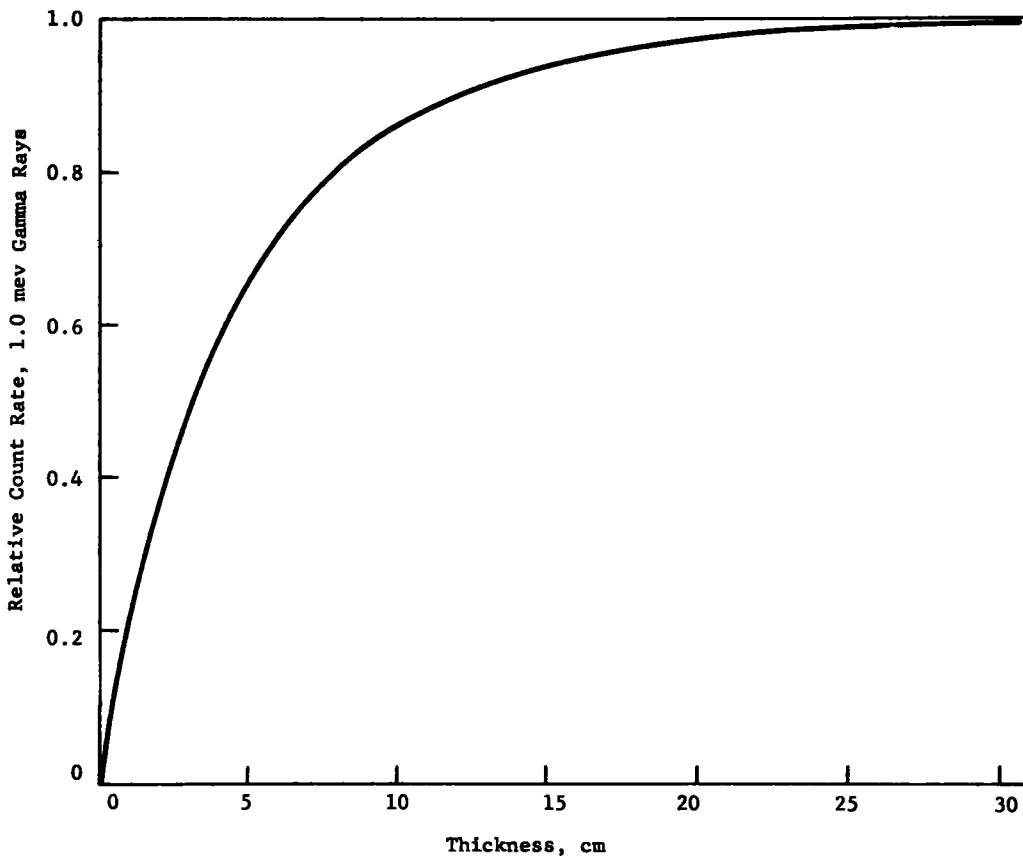
Figure B-2. Relative count rate vs pavement thickness with radioisotope As^{76} mixed in pavement material.

insurmountable. This technique rapidly becomes insensitive at thicknesses larger than 20 cm. For example, a 1 percent difference between the counting rate at 20 cm and that at 17.5 cm becomes only a 0.25 percent difference between the counting rates at 30 cm and at 27.5 cm. To see this difference, the overall system would have to be much more accurate, and the amount of As^{76} would have to be 16 times greater than that required at 17.5 cm. Though these evaluations show that problems exist in the use of this technique for pavement thickness measurements, they do indicate that further considerations should definitely be given to it.

CALCULATION OF GAMMA FLUX

Calculations of the gamma flux are based on the geometry given in Figure B-3. A thermal neutron source of strength S_n (neutrons per sec), assumed to be a point source for simplification of the calculation, is placed at point 0 on the surface of the concrete. At any point in the pavement, the neutron flux density, $\phi_n(r, z)$, coming from the source at the origin, 0, is approximated by using the solution to the neutron diffusion equation for an infinite medium; i.e., (12, p. 167),

$$\phi_n(r, z) = \frac{S_n e^{(-1/L)(r^2 + z^2)^{1/2}}}{4\pi D(r^2 + z^2)^{1/2}} \qquad (B\text{-}13)$$

The diffusion length for thermal neutrons is L; the thermal neutron diffusion constant (sometimes also called the diffusion coefficient) is D. Both L and D are characteristic constants of the material through which the neutrons are diffusing and both have the dimensions of length (cm). For type 04 portland cement concrete: $L = 9$ cm and $D = 0.7$ cm (13, p. 662).

Activated Isotopes with Long Half-Lives in Additive Layer

If the thickness, d, of the additive layer is much less than that of the pavement, z, the neutron flux at any point in this layer will be $\phi_n(r, z)$, and the number of activated atoms per unit area, $N(r)$, at this point immediately after neutron irradiation will be

$$N(r) = \left(\frac{N_0 \rho d}{W}\right) \sigma \tau \phi_n(r, Z) \qquad (B\text{-}14)$$

as long as the time interval, τ, during which the neutron source remains at 0 is short compared to the half-life, $T_{1/2}$, of the activated isotope in the additive layer. If this condition is not met, the assumption that only a negligible number of the atoms activated during the interval τ will have decayed by the end of that interval is not valid. The additive layer is assumed to be composed of a single element with a mass density of ρ(gm cm^3), a gram-atomic weight of W(gm), and a thermal neutron activation cross section of σ(cm^2 per atom); N_0 is Avogadro's number.

Due to the neutron activation, the additive layer has become a circularly symmetrical planar source of gamma radiation of one or more characteristic energies, E_i, depending on the particular element used. The initial gamma source strength, $S_{\gamma i}(r)$ (photon cm^{-2} sec^{-1}), is obtained
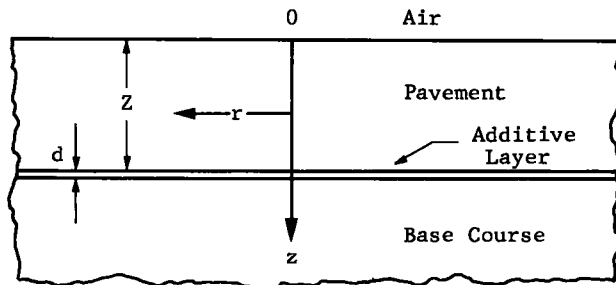
Figure B-3. Assumed pavement configuration for activation of gamma counting from additive layer.

by multiplying the initial number of activated atoms per unit area by the disintegration or decay probability constant,

$$\lambda = \frac{\ln 2}{T_{1/2}} \qquad (B\text{-}15)$$

and the fraction, k_i, of decays emitting a gamma ray of energy E_i, or

$$S_{\gamma i}(r) = k_i \lambda N(r) = k_i \left(\frac{\ln 2}{T_{1/2}}\right)\left(\frac{N_0 \rho d}{W}\right) \sigma \tau \phi_n(r, Z) \qquad (B\text{-}16)$$

Eq. B-16 is the initial, and also the maximum, gamma source strength. The assumption is made that the gamma radiation will be measured at point 0 immediately after the neutron source is removed from this point. The number of activated atoms remaining after the n-source is removed decreases exponentially, so that the gamma source strength at any later time, t, is

$$S_{\gamma i}(r, t) = S_{\gamma i}(r)e^{-\lambda t} \qquad (B\text{-}17)$$

The initial gamma ray flux density at the origin, 0, is given by the expression for flux density on the symmetry axis of an axially symmetric, thin-disc source radiating isotropically (12, p. 219); i.e.,

$$\phi_{\gamma i}(0) = \int_0^R S_{\gamma i}(r) \frac{2\pi r}{r\pi(r^2 + Z^2)} e^{-\mu_i(r^2 + Z^2)^{1/2}} \qquad (B\text{-}18)$$

The upper limit of integration, R, has been taken to be infinity in all the following examples. It could be assigned a finite value with only a slight added complication in the calculation. This was not done in computing these initial estimates, however, because the contribution to the integral decreases rapidly for large r, and for any measurement away from the edge of an actual pavement R will be much greater than Z. In Type 04 portland cement concrete (Table B-1), μ_i is the gamma ray attenuation cross section (in cm^{-1}) for gamma rays of energy E_i. The values of μ_i used in the following examples were obtained by interpolation (13, p. 653, Table 8-10).

The complete expression for the initial gamma flux density at 0 in terms of known quantities may now be written by combining Eqs. B-16, B-17, and B-18; i.e.,

$$\phi_{\gamma i}(0) = \frac{S_n(\ln 2) N_0 k_i \rho d \sigma \tau}{8\pi D T_{1/2} W} \int_0^\infty \frac{r}{(r^2 + Z^2)^{1/2}} e^{-t} dr \qquad (B\text{-}19)$$

TABLE B-1

COMPOSITION OF PORTLAND CEMENT CONCRETES

| ELEMENT | PERCENTAGE BY WEIGHT | |
	TYPE 04 PORTLAND CEMENT CONCRETE [a]	TYPICAL ORDINARY PORTLAND CEMENT CONCRETE [b]
H	0.55	1.0
O	49.60	52.9
Si	31.40	33.7
A	4.55	3.4
Fe	1.23	1.4
Ca	8.25	4.4
Mg	0.26	0.2
C	—	0.1
Na	1.70	1.6
K	1.91	1.3
S	0.13	—
Co	—	Trace

[a] Ref. 13, p 660; density = 2.35 gm/cm³.
[b] Ref 12, p 262: density = 2.3 to 2.4 gm/cm³.

in which

$$x = (\mu_t + 1/L)(r^2 + Z^2)^{\frac{1}{2}} \qquad \text{(B-20)}$$

The integral, however, becomes

$$\int_0^\infty \frac{r}{(r^2 + Z^2)^{3/2}} e^{-x} \, dr$$

$$= (\mu_t + 1/L) \int_{(\mu_t + 1/L)Z}^\infty \frac{e^{-x} \, dx}{x^2}$$

$$= \frac{E_2 [(\mu_t + 1/L)Z]}{Z} \qquad \text{(B-21)}$$

The function $E_2(x)$ has been tabulated (14) for $0 \le x \le 10$ and plotted graphically (13, p. 215) for $0 \le x \le 20$.

This result was used to estimate the gamma flux density from an additive layer of thickness $d = 1$ mil ($= 2.5 \times 10^{-3}$ cm) under a pavement of thickness $Z = 20$ cm, after irradiation by a neutron source of strength $S_n = 10^6$ neutrons/sec for a duration $\tau = 10$ min. The elements considered for the additive material were manganese and

indium, which were chosen (13, Table 8-6) as the elements most likely to produce the highest value of $\phi_{\gamma_t}(0)$. The results are given in Table B-2.

Total Gamma Dose from Activated Isotopes with Short Half-Lives in Additive Layer

In order to consider possible added activated isotopes with half-lives of the order of 1 min, it will be necessary to make some changes in the analysis. As indicated previously, unless the half-life, $T_{1/2}$, of the activated isotope is much longer than the time of neutron irradiation, τ, Eq. B-14, in which $N(r)$ depends directly on τ, is not accurate. Actually, at any time, t, during neutron irradiation, the number of activated atoms per unit area $N(r, t)$ satisfies the differential equation

$$\frac{dN}{dt} = \frac{N_0 \rho d}{W} \sigma \phi_n(r, Z) - \lambda N \qquad \text{(B-22)}$$

in which the first term on the right represents the rate at which activated atoms are added due to the absorption of neutrons, and the second term the rate at which they are removed by gamma decay. As time goes on, the system approaches an equilibrium condition in which dN/dt becomes 0 and $N(r, t)$ remains at a constant value. If it is stipulated that τ be about equal to or greater than $5T_{1/2}$ in the consideration of isotopes with short half-lives, equilibrium will approximately be reached, and the new value of $N(r)$ may be taken as

$$N(r) = \frac{1}{\lambda} \left(\frac{N_0 \rho d}{W} \right) \sigma \phi_n(r, Z) \qquad \text{(B-23)}$$

obtained by setting $dN/dt = 0$ in Eq. B-22.

The gamma source strength for energy E_t per unit area at any time, t, after the neutron irradiation is stopped will again be given by

$$S_{\gamma_t}(r, t) = k_t \lambda N(r) e^{-\lambda t} \qquad \text{(B-24)}$$

However, because of the rapid decay of the activated isotope, it was thought that it would be more reliable to measure the integral of the gamma flux at the origin, rather than to attempt to measure an instantaneous initial value of the rapidly changing gamma flux. If the gamma measurement is continued over a period about equal to

TABLE B-2

POSSIBLE ACTIVATED ISOTOPES WITH RELATIVELY LONG HALF-LIVES FOR USE IN AN ADDITIVE LAYER

ELEMENT	ACTIVATED ISOTOPE	σ (BARNS/ ATOM) [a]	$T_{1/2}$	E_t (MEV)	k_t	μ_t (CM⁻¹)	$\phi_{\gamma_t}(0)$ (PHOTONS/ CM²/SEC)
Mn	Mn⁵⁶	13	2.58 hr	0.845	0.990	0.1617	1.8×10^{-3}
				1.810	0.235	0.1114	1.4×10^{-4}
In	In¹¹⁶ [*]	145	54.20 min	1.270	1.290	0.1330	7.0×10^{-3}
				2.090	0.260	0.1030	2.77×10^{-3}

[a] 1 barn = 10^{-24} cm².
[*] Metastable (excited) state

or greater than $5T_{1/2}$, approximately all of the activated atoms will have decayed, and the total gammas emitted per unit area of the additive layer will be

$$\int_t S_{\gamma i}(r, t)\,dt = k_t N(r) \qquad \text{(B-25)}$$

Applying this to the exponential attenuation law used before for gamma radiation gives the following for the integrated gamma flux at the origin:

$$\int_t \phi_{\gamma i}(0)\,dt = \int_0^\infty k_t N(r) \cdot \frac{2\pi r}{4\pi(r^2 + Z^2)}\, e^{\mu_t(r^2 + Z^2)^{1/2}}\, dr \qquad \text{(B-26)}$$

Substituting in Eq. B-26 the explicit expressions for $N(r)$ and $\phi_n(r, Z)$ gives

$$\int_t \phi_{\gamma i}(0)\,dt = \frac{S_n N_0\, d\, T_{1/2}\, k_t \rho\, \sigma}{8\pi D(\ln 2)\bar{W}}\, \frac{E_2 [(\mu_t + 1/L)\, Z]}{Z} \qquad \text{(B-27)}$$

Again, Table 8-6 of (13) was consulted, this time considering activated isotopes with half-lives shorter than 5 min. Rhodium, dysprosium, and vanadium were chosen as most likely to give high values of $\int_t \phi_{\gamma i}\,dt$. The results obtained for these elements are given in Table B-3. The configuration of Figure B-3 was again used, with $Z = 20$ cm and $d = 1$ mil.

Activation Gamma Radiation from the Pavement Itself

In order to compute an estimate for a particular activated isotope occurring in the pavement itself, the slab must be considered as made up of a series of infinitesimal layers of thickness dz, each of which contributes to the gamma flux or dose per unit area (depending, again, on the relative magnitudes of τ and $T_{1/2}$) according to Eqs. B-19 and B-27. The constant, Z, in those equations must be replaced by the variable, z, over which an integration must be performed to get the total flux per unit area, and ρ will now represent the effective density of the isotope in grams of isotope per cm³ of concrete.

Integrating either Eq. B-19 or Eq. B-27 over z results in a constant term times the integral

$$\int_{Z_1}^{Z_2} \frac{E_2 [(\mu_t + 1/L)z]\, dz}{z} \qquad \text{(B-28)}$$

The lower limit of integration, Z_1, cannot be simply set to zero in this integral, for the integrand has a singularity at $z = 0$, and the integral becomes indeterminate. This indicates that if a realistic estimate of the activation gamma radiation from the pavement is expected, a more realistic geometrical configuration than that of Figure B-3 must be considered. Such a configuration is shown in Figures B-4 and B-5.

In practice, most thermal neutron sources use a material like paraffin to slow down the neutrons to thermal velocities. Thus, in Figure B-4 the origin has been moved to a point 5 cm above the top surface of the pavement, and the intervening space is considered to be filled with the paraffin moderator. The point source of neutrons, now thought of as a small piece of a neutron-emitting radioactive isotope, is placed at 0.

A commonly used detection system for gamma radiation is a scintillation crystal of NaI or CsI, which, upon excitation by gamma radiation, emits visible light, which in turn is detected by a photomultiplier tube. Therefore, suppose that immediately upon removing the neutron source at the end of the interval τ, it is replaced by the gamma-detection system of Figure B-5 with the center of the 10-cm thick scintillation crystal placed at 0, the former position of the neutron source.

Now, because there will be no activation in the region $0 < Z < 5$ cm, the integral (Eq. B-28) will be evaluated between the limits $Z_1 = 5$ cm and $Z_2 = 25$ cm. The resulting value of Eq. B-19 or Eq. B-27 will represent the gamma radiation at the center of the detector crystal. In doing this, there is the implicit assumption that the properties of portland cement concrete and paraffin for neutron diffusion, and those of portland cement concrete and NaI for gamma attenuation, are identical. Actual values of relevant parameters are given in Table B-4. To avoid mathematical complexity, no attempt was made to correct for this inaccuracy.

The required integral (Eq. B-28) cannot be worked analytically in closed form. Therefore, substitution of variables ($x = (\mu_t + 1/L)\, z$) was made, and

TABLE B-3

ACTIVATED ISOTOPES WITH SHORT HALF-LIVES FOR USE IN ADDITIVE LAYER

PARENT ISOTOPE	ISOTOPIC ABUNDANCE (%)	σ (BARNS/ ATOM)[a]	ACTI-VATED ISOTOPE	$T_{1/2}$		E_i (MEV)	k_t	μ_t (CM⁻¹)	$t\int\phi_{\gamma i}(0)dt$ (PHOTONS/ CM²)
Rh¹⁰³	100	140 ± 30	Rh¹⁰⁴	42	sec	0.556	0.02	0.1970	2.34×10^{-2}
		12 ± 2	Rh¹⁰⁴*	4.4	min	0.051	1.00		
Dy¹⁶¹	28.18	510 ± 20	Dy¹⁶⁵	1.25	min	0.108	0.90	0.3850	2.66×10^{-2}
						0.515	0.06	0.2022	8.8×10^{-2}
						0.361	0.04		
V⁵¹	99.80	4.5 ± 0.9	V⁵²	3.76	min	1.440	1.00	0 1239	1.03

[a] 1 barn = 10^{-24} cm².
* Metastable (excited) state of nucleus

48
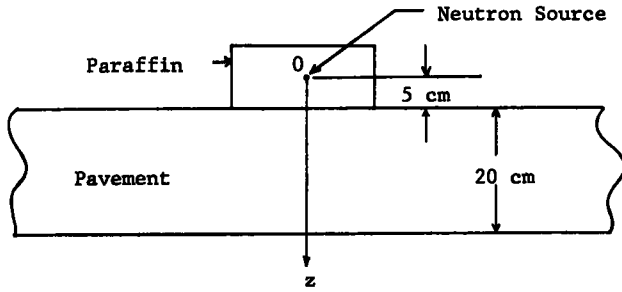
Figure B-4. Neutron activation of concrete.
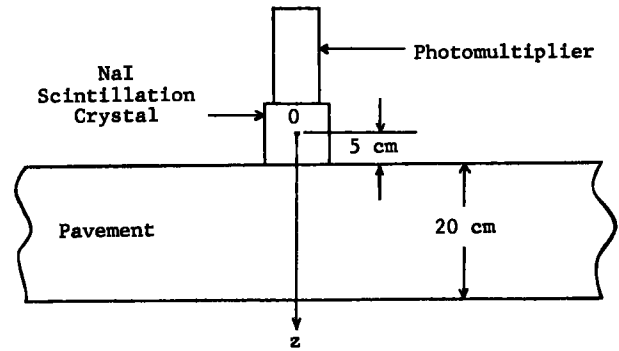
Figure B-5. Gamma radiation detector.

$$\int_{Z_1}^{Z_2} \frac{E_2 [(\mu_t + 1/L)z]}{z} \, dz = \int_{(\mu_t+1/L)Z_1}^{(\mu_t+1/L)Z_2} \frac{E_2(x)}{x} \, dx \quad \text{(B-29)}$$

An accurate graph of $E_2 (x)/x$ versus x was plotted, and the integral evaluated between the appropriate limits for each element in Tables B-5 and B-6 by measuring the area under the curve.

For long half-lives (Table B-5), the gamma flux is given by

$$\phi_{\gamma i}(0) = \frac{S_n(\ln 2) N_0 \, k_t \, \rho \, \sigma \, \tau}{8\pi D \, T_{1/2} \, W} \int_{Z_1}^{Z_2} \frac{E_2 [(\mu_t + 1/L)z]}{z} \, dz$$

(B-30)

For short half-lives (Table B-6), the gamma flux is given by

$$\int_t \phi_{\gamma i}(0) \, dt = \frac{S_n \, N_0 \, T_{1/2} \, k_t \, \rho \, \sigma}{8\pi D (\ln 2) W} \int_{Z_1}^{Z_2} \frac{E_2 [(\mu_t + 1/L)z]}{z} \, dz$$

(B-31)

Calculation of Neutron-Capture Gamma Ray Flux

Using these same methods of calculation, one may estimate the capture gamma ray flux from neutron capture in the nuclei of the additive layer. In terms of the previous notation, the capture gamma source strength for gamma radiation of energy E_t is

$$S_{\gamma i}(r) = k_t \frac{N_0 \rho \, d}{W} \sigma \, \phi_n(r, z) \quad \text{(B-32)}$$

in which σ is now the capture cross section of an atom in the additive layer and k_t is the fraction of neutron captures causing the emission of a capture gamma ray of energy E_t. $\phi_n(r, Z)$ is obtained by the same neutron diffusion equation as before, and the same gamma-attenuation law holds, so that the capture-gamma flux at 0 in Figure B-3, due to the additive layer, is

$$\phi_{\gamma i}(0) = \frac{S_n \, N_0 \, d \, \rho \, k_t \, \sigma}{8\pi D \, W} \frac{E_2 [(\mu_1 + 1/L)Z]}{Z} \quad \text{(B-33)}$$

Because of its large capture cross section ($\sigma = 3,500$ barns), cadmium was considered as a suitable additive material. The capture gamma ray spectrum of cadmium is a complicated one extending over a broad range of gamma ray energies, rather than an emission at one or two discrete energies, as the activation gamma emissions considered were. Thus, all gamma rays of energies greater than 5 Mev were counted, and the value $\mu_t = 0.0674$ cm^{-1} for $E_t = 5$ Mev was used. The result for a 1-mil thickness of Cd, again using $Z = 20$ cm and $S_n = 10^6$ neutrons sec^{-1} is $\phi_\gamma(0) = 1.07$ photon/cm^2/sec.

The competing capture gamma intensity from the pavement itself was estimated by using a formula analogous

TABLE B-4

PROPERTIES OF PORTLAND CEMENT CONCRETE COMPARED TO NaI AND PARAFFIN

	NEUTRON DIFFUSION [a]		GAMMA-RAY ATTENUATION (PER CM) IN CROSS SECTION μ_t FOR $E_t =$							
MATERIAL	CONSTANT, D (CM)	LENGTH, L (CM)	0.1 MEV	0.5 MEV	1.0 MEV	3.0 MEV	5.0 MEV	6.0 MEV	10.0 MEV	REFERENCE
Type 04 portland cement concrete	0.688	8.93	0.397	0.2045	0.1492	0.0853	0.0674	0.0630	0.0538	*13*, pp. 662, 653
NaI (scintillation crystal)	—	—	5.757	0.3304	0.2116	0.1346	0.1272	0.1272	0.1342	*13*, pp. 653
Paraffin ($\sim C_{25}H_{52}$)	0.106	2.14	—	—	—	—	—	—	—	*13*, pp. 112, 115

[a] For thermal neutrons.

TABLE B-5

INITIAL GAMMA FLUX PER UNIT AREA FROM ACTIVATED ISOTOPES
IN PAVEMENT WITH LONG HALF-LIVES

PARENT ISOTOPE	ρ GM ISOTOPE/ CM³ CONCRETE	σ (BARNS/ ATOM)	$T_{\frac{1}{2}}$	E_ι (MEV)	k_ι	μ_ι	$\phi_{\gamma_\iota}(0)$ (PHOTON/ CM²/SEC)
Fe⁵⁸	9×10^{-5}	0.90	45.1 days	1.29	0.43	0.1321	1.02×10^{-7}
				1.10	0.57	0.1428	1.23×10^{-7}
Si³⁰	0.023	0.11	2.65 hr	1.26	7×10^{-1}	0.1327	4.11×10^{-6}
Ca⁴⁶	6.4×10^{-6}	0.25	4.90 days	1.31	0.71	0.1304	7.90×10^{-8}
Na²³	0.040	0.53	15.10 hr	2.76	1.00	0.0901	1.73×10^{-2}
				1.38	1.00	0.1271	1.17×10^{-2}
K⁴¹	3.1×10^{-3}	1.15	12.40 hr	1.58	0.18	0.1188	2.64×10^{-1}

TABLE B-6

TOTAL GAMMA DOSE PER UNIT AREA FROM ACTIVATED ISOTOPES
IN PAVEMENT WITH SHORT HALF-LIVES

PARENT ISOTOPE	ρ (GM ISOTOPE/ CM³ CONCRETE	σ (BARNS/ ATOM)	$T_{\frac{1}{2}}$ (MIN)	E_ι (MEV)	k_ι	μ_ι	$\int\phi_{\gamma_\iota}(0)\,dt$ (PHOTONS/ CM²)
S³⁶	4.8×10^{-1}	0.140	5.04	3.120	0.900	0.0839	139.500
Al²⁷	0.107	0.210	2.30	1.780	1.000	0.1088	2.06×10^4
Ca⁴⁸	3.6×10^{-4}	1.100	8.80	3.100	0.898	0.0842	1.04×10^3
				4.050	0.100	0.0741	128.000
Mg²⁶	6.8×10^{-1}	0.026	9.45	1.015	0.290	0.1490	13.500
				0.834	0.700	0.1641	27.000
				0.181	0.010	0.3050	0.114

to that used in the activation analysis based on Figures B-4 and B-5; namely,

$$\phi_{\gamma_\iota}(0) = \frac{S_n N_0 \rho k_i \sigma}{8\pi D\,W} \int_{z_1 = 5\,cm}^{z_2 = 25\,cm} E_2\,\frac{[\mu_\iota + 1/L)z]}{z} \quad \text{(B-34)}$$

Evaluating Eq. B-34 for each element in the pavement and summing gives a total of 19.5 photons/cm²/sec for all energies greater than 5 Mev.

QUANTITIES REQUIRED FOR A CONTINUOUS LAYER OF RADIOACTIVE MATERIAL

Let B = activity per unit area, $d\sigma$ = an element of area in the radioactive layer, and ξ = the distance from $d\sigma$ to some point on the surface. Then the surface flux from $d\sigma$ is

$$f = \frac{B\,d\sigma}{4\pi\xi^2}\,e^{-\mu\xi}\cos\phi \quad \text{(B-35)}$$

Using the following substitutions (Fig. B-6),

$$\cos\phi = x/\xi \quad \text{(B-36)}$$

$$d\sigma = 2\pi\,\eta\,d\eta$$
$$x^2 + \eta^2 = \xi^2,\ \eta\,d\eta = \xi\,d\xi, \quad \text{(B-37)}$$

Eq. B-35 can be written as

$$f = \frac{B}{2}\,\frac{x\,d\xi}{\xi^2}\,e^{-\mu\xi}\ \text{counts/cm²/sec} \quad \text{(B-38)}$$
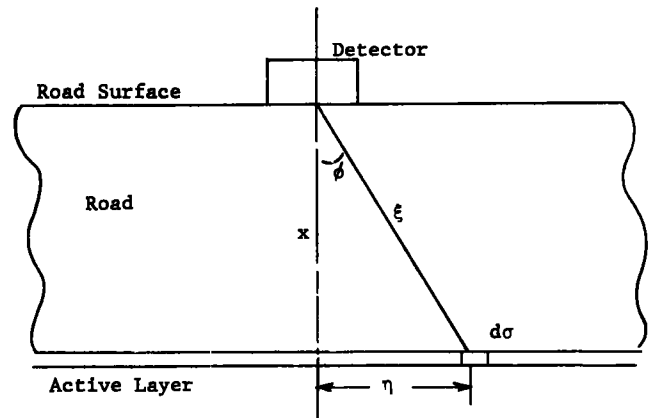
Figure B-6. Diagram for computation of the gamma ray flux at the road surface due to the presence of a layer of radioactive material underneath the road.

The total flux at the road surface is given by

$$F = \int f\, d\sigma = \frac{B\,x}{2} \int_x^\infty \frac{e^{-\mu\xi}}{\xi^2}\, d\xi$$

$$= \frac{B}{2}\, E_2(\mu x) \text{ counts/cm}^2/\text{sec} \qquad (B\text{-}39)$$

in which $E_2(\mu x)$ is a tabulated function defined by

$$E_2(a) = \int_1^\infty \frac{e^{-at}}{t^2}\, dt \qquad (B\text{-}40)$$

For 1-Mev gamma rays, $\mu = 0.1492$ cm^{-1} and the road is about 20 cm thick. Assuming a counting rate of 10^3 per min in a counter of area 45.5 cm^2, and substituting into Eq. B-39, gives $B = 1.5 \times 10^{-8}$ curies/cm^2 after converting disintegrations per sec to curies. Assuming a 30-ft road width, the total quantity of radioactive material required is approximately 2 curies per mile.

A MEASUREMENT TECHNIQUE SENSITIVE TO THICKNESS BUT INDEPENDENT OF DENSITY AND COMPOSITION

Assuming a small radioactive source beneath the pavement, consider the ratio of the counting rate at the surface of the pavement to the counting rate at a distance, d, above the surface. The counting rate at the surface is given by

$$R_s = AD\,\frac{e^{-\mu x}}{4\pi x^2} \qquad (B\text{-}41)$$

in which A = counter area, D = source strength, μ = linear absorption coefficient, and x = pavement thickness. The counting rate at distance, d, above the surface is given by

$$R_d = AD\,\frac{e^{-\mu x}}{4\pi (x + d)^2} \qquad (B\text{-}42)$$

as there is negligible attenuation in the air. The ratio of the two rates is

$$\frac{R_s}{R_d} = \frac{(x + d)^2}{x^2} = \left(1 + \frac{d}{x}\right)^2 \qquad (B\text{-}43)$$

Thus, when the detector is raised to a height $d = x$, $R_s/R_d = 4$. The road thickness is therefore equal to the height of the detector, which reduces the counting by a factor of four from its value at the surface. The dependence on the material through μ completely drops out. In practice, one must allow for the fact that the effective center of detection will not coincide with the road surface, even when the detector is sitting on the road. This correction is readily included, however, and will not alter the simplicity of the technique.

The sensitivity of this technique can be determined by looking at the change in the count ratio, R_s/R_d, caused by a change in pavement thickness. For simplicity, let $R_s/R_d = F$. Then the change in F is given by

$$\delta F = \frac{\partial F}{\partial x} \delta x = \left[\frac{\partial}{\partial x}\,(1 + d/x)^2\right] \delta x$$

$$= 2(1 + d/x)(-d/x^2)\,\delta x \qquad (B\text{-}44)$$

The fractional change in F is given by

$$\frac{\delta F}{F} = \frac{-2d}{x^2}\,\frac{1}{1 + d/x}\,\delta x = -\frac{2d}{x+d}\,\frac{\delta x}{x} \qquad (B\text{-}45)$$

When $d \cong x$,

$$\frac{\delta F}{F} = -\frac{\delta x}{x} \qquad (B\text{-}46)$$

so that the percent change in the count ratio is the same as the percent change in pavement thickness. For example, a 0.125-in. change in nominal 10-in. pavement is 1.2 percent. This thickness variation would cause a 1.2 percent change in the count ratio. This could be detected with counting periods on the order of a few minutes.

ACTIVITY REQUIRED IN A PELLET SOURCE UNDER CONCRETE

Assume a point source (pellet) under a 20-cm road with a counter directly above the pellet. As the counter has a radius of only 3.81 cm (1.5 in.), the approximate counting rate is

$$R \cong AD\,\frac{e^{-\mu x}}{4\pi x^2} \qquad (B\text{-}47)$$

in which R is the counting rate, A is the counter area, D is the source strength, μ is the coefficient of linear attenuation, and x is the road thickness. Assuming $R = 10^3$ counts/sec, $A = 45.5$ cm^2, $\mu = 0.1492$ cm^{-1}, and $x = 20$ cm, $D = 0.98$ μcurie.

SENSITIVITY OF AN ATTENUATION MEASUREMENT TO CHANGES IN THICKNESS AND IN LINEAR ATTENUATION COEFFICIENT

To calculate the effect of a change, δx, in road depth on the counting rate, it is required to know $\partial R/\partial x\,\delta x = \delta R$, where R is the counting rate; that is,

$$\delta R = \frac{\partial R}{\partial x}\,\delta x = \frac{\partial}{\partial x}\left[AD\,\frac{e^{-\mu x}}{4\pi x^2}\right]\delta x$$

$$= AD\left[\frac{-\mu e^{-\mu x}}{4\pi x^2} - \frac{2e^{-\mu x}}{4\pi x^3}\right]\delta x$$

$$= R\left[-\mu - \frac{2}{x}\right]\delta x \qquad (B\text{-}48)$$

Therefore, the percent change in R is given by

$$\frac{\delta R}{R}\,(100) = -\left(\mu + \frac{2}{x}\right)\delta x(100)$$

For $x = 20$ cm, $\mu = 0.15$ cm^{-1}, and $\delta x = 0.3$ cm ($= 0.125$ in.), $\delta R/R \times 100 = 7.5$ percent. A 0.125-in. change in the road depth therefore produces a 7.5 percent change in counting rate.

To calculate the effect of μ on the counting rate, it is necessary to know $\delta R = \partial R/\partial\mu\,\delta\mu$. Using the same form for R as in Eq. B-48,

$$\delta R = \frac{\partial}{\partial\mu}\left[AD\,\frac{e^{-\mu x}}{4\pi x^2}\right]\delta\mu = -xR\,\delta\mu \qquad (B\text{-}50)$$

The percent change in R is therefore given by

$$\frac{\delta R}{R}\,(100) = -x\,\delta\mu(100) \qquad (B\text{-}51)$$

Assuming $\delta\mu = 0.015$ (10 percent of μ) and $x = 20$ cm, $\delta R/R \times 100 = 30$ percent. Therefore, a 10 percent change in μ will result in a 30 percent change in the counting rate. As this approximation is linear in $\delta\mu$, a 1 percent change in μ will result in a 3 percent change in the counting rate.

ATTENUATION METHODS

Approximate calculations have been made of the sensitivity to thickness using a source of radiation beneath the pavement. This method shows the greatest sensitivity for relatively high-energy gamma rays (say 1 Mev) and shows promise for thickness up to about 25 cm (10 in.) Using As^{76} as a typical example of a radiation source, this technique can determine a thickness change from 17.5 cm to 20 cm in a medium with a density of 2.35 gm/cm³ in 1 sec using 0.2 μcuries/cm² of As^{76} as the source. For longer time intervals, the same measurement can be made with proportionately less activity per unit of area. A curve of the relative count rate versus pavement thickness is shown in Figure B-1. Details of the calculations are contained in an earlier section of this appendix.

The radiation source can be produced in several ways. If the activity is produced by spreading a radioisotope, the total activity soon reaches the level where handling problems are significant. The amount of time between the preparation of the material and the measurement of thickness is also limited (see later section on "Distributed Source Methods"). Neither of these problems exists, of course, if the radiation is produced in-situ by neutron activation or by neutron capture.

When a neutron is absorbed by a nucleus, it emits radiation (generally a gamma ray). The process usually results in a change of the atomic mass and/or the atomic number of the nucleus. This changed nucleus may be stable or unstable. In the latter case, artificial radioactivity has been produced by "neutron activation." The unstable nucleus may then emit gamma rays at a rate governed by the half-life of the artificial radioisotope. Hence, there are two possible techniques utilizing irradiation by neutrons from a neutron source and the detection of resulting gammas. In the first technique, "neutron capture gammas" are detected during the neutron irradiation; in the second, "neutron activation gammas" are detected after the irradiation. In both cases the gamma rays have an energy which is characteristic of the excited state of the nucleus that emits the rays, so that the detector should be capable of rejecting gammas not having energies in a selected interval. In general, the capture gammas are of a higher energy, and therefore of greater penetrating power, than the activation gammas. Because the sensitivity depends greatly on the penetration of the gammas, the capture gamma method may offer greater sensitivity than the activation gamma method.

To further evaluate these methods for producing a radiation source beneath the pavement, the nuclear characteristics of portland cement and bituminous concretes, for neutron and gamma radiation, must be specified. This is necessary to determine the intensity of radiation from competing reactions and to calculate the radiation attenuation.

One can also consider the production of gamma rays in the base course itself. This technique would involve a measurement of the transmission of the neutrons through the pavement to the base course and the transmission of the gammas back from the base course through the pavement to the detector. It may be necessary to make measurements just before and after the pavement is laid to determine the thickness from these transmission effects involving activation of the base course.

USE OF BACKSCATTERED RADIATION

When compared with the transmission technique, the backscattering technique has the disadvantage that the radiation must penetrate the pavement twice. However, there are several important advantages in the use of backscattering. Special work is not required during the actual construction; for example, the uniform spreading of the radioisotope over the base course. In addition, no special materials remain in or under the pavement. After the thickness measurement has been completed, the residual radioactivity is insignificant.

These advantages are counteracted by the fact that the base course, as well as the concrete, will backscatter the radiation. The character of the backscattered radiation from the base course in most cases is not predictably different from that from the concrete.

The choice of radiation to be used for backscattering is quite limited. Charged particles (protons, deuterons, alphas, electrons, and positrons) do not have sufficient ranges to be of any use. Many potential techniques described in the literature were excluded because of this limitation (15). This leaves only gamma rays and neutrons for consideration.

Neutron Backscattering

The neutron moderation technique is used extensively in making moisture determinations in soil and in detecting the amount of hydrogenous material present in the case of oil well logging (16, 17). This technique is based on the fact that a particle loses much more speed colliding with a particle of the same mass than with a particle of much larger mass. Because hydrogen nuclei have nearly the same mass as neutrons, they are much more effective in slowing neutrons down that are nuclei of other materials. The technique employs a source of fast neutrons and a detector sensitive preferentially to slow neutrons. Due to the wide variations in water content of both pavement and base course, this method is probably not directly applicable to portland cement concrete pavement thickness measurements. However, it does show promise for the determination of the thickness of bituminous concrete pavements of known constant hydrogen content laid on a nonhydrogenous dry base course. For example, tests of the application of moisture measuring equipment to the determination of hydrogen content of bituminous concrete pavements have shown that the results depend on the thickness of the

pavement, unless that thickness is 4 in. or greater (18). This dependence may be extended to greater thicknesses by some alteration in the technique, such as increasing the distance from source to detectors.

If the neutron backscattering method is altered by using a source of thermal neutrons instead of fast neutrons, the number of neutrons backscattered into the slow-neutron detector is no longer primarily dependent on hydrogen content. Instead, the problem becomes one of neutron diffusion, for which solutions are well known though quite complicated. Alternately, one could use a source of fast neutrons with a detector of fast neutrons. In either case, the number of neutrons entering the detector depends on the scattering and absorption cross sections of the various nuclides in both pavement and base course and on the number of the various nuclides per unit volume (19, 20). Because these cross sections are not well-behaved functions of atomic number, and because of the variability in the elemental compositions of pavement and base course, it is difficult to predict whether a difference exists in the effective cross sections of pavement and base course. If there is no difference, the neutron diffusion depends only on the number of nuclei per unit volume (i.e., on ρ/A, where ρ is the density of the material and A is the atomic mass).

It is felt that no further investigation of this technique, relative to portland cement concrete, should be made until more precise information is available concerning the ranges and variations in the elemental compositions of the various base courses and pavements. However, this technique still bears consideration relative to bituminous pavements, as noted.

Gamma Ray Backscattering

The gamma ray backscattering technique is used extensively in oil well logging and many other applications to measure the local density of materials whenever the thickness of the material is large compared to the average penetration distance of the gammas (21, 22). It is quite a successful technique, and a 1 percent change in density can easily be measured (5 percent change in counting rate). Thickness may also be measured (17, 23, 24) if there is a significant difference in density between the concrete and the base course, and the thickness is not large compared to the average penetration distance. However, in a practical situation the base course in most cases will look like an additional thickness of pavement when measured using a backscattered gamma technique, because the amount of gamma radiation that is backscattered is dependent primarily on total electron density (both bound and free) in the medium. This in turn depends on the product of density times Z/A, the ratio of the atomic number to the atomic mass. Because this ratio is nearly constant (varying from 2.0 for helium to 2.5 for gold), only a difference in density will result in a difference in the backscattering. Thus, the only situations in which the gamma backscattering technique may show promise for pavement thickness measurements are those for which the base course has a constant known density appreciably different from the density of the concrete. For example,

tests of equipment constructed for the measurement of soils spread over a thick steel plate showed a dependence on the depth of the soil for thicknesses less than 5 in. (18).

An analytic treatment of the backscatter process is given in the earlier section on "Isotopes Placed Above the Pavement." The equation is quite difficult to evaluate, and because it is based on only an approximate treatment it would be more appropriate to determine the dependence of the backscattered gammas on pavement thickness and on densities of pavement and base course by direct experimentation. A decision as to the desirability of future investigations of this technique can be made only after obtaining more information concerning the ranges and variations in the densities of the various base courses and the various pavements. One can imagine a procedure (in cases where the density differences are sufficient) wherein the density of the base course is measured before the pavement is laid, and then the density of the pavement (using low-energy gammas) and its thickness (using high-energy gammas) are measured after the pavement is laid.

An alternative technique which might be considered is the production of a large density difference between pavement and base course by covering the base course with a large thickness of lead or other dense material. Although this would make the thickness measurement easier, it is too impractical to be seriously considered.

DISTRIBUTED SOURCE METHODS

The determination of thickness by measuring the radiation from sources distributed throughout the paving mixture has been examined in the earlier section on "Isotopes Intimately Mixed with Pavement Materials." Calculations of the sensitivity have been made for As^{76} distributed in the mixture. For this isotope, a change in thickness from 17.2 cm to 20 cm can be detected in 1 sec using 0.1 μc of As^{76} per gram of concrete. For longer intervals, proportionately less activity per gram is required. For a source distributed throughout all the concrete, this amounts to 0.1 curies per ton of concrete. The problem of obtaining such large amounts of radioactivity and mixing it uniformly in the concrete is formidable. An additional consideration is that the material must remain permanently imbedded in the road, although its radioactivity will decay with a characteristic half-life. Although all possible isotopes have not been considered in detail, the amount of radioactive material present in the pavement will almost certainly constitute an unacceptable health hazard.

Large quantities of radioisotopes are not involved if the radiation is generated by neutron capture or is generated by neutron activation. First, only the inert material need be activated where a thickness measurement is required. In addition, because the measurement can be made immediately after activation, materials that yield short half-life isotopes can be selected. A distributed source, however, is not as sensitive to thickness as a source placed beneath the pavement. For example, the sensitivity rapidly decreases for thicknesses larger than 20 cm when using a distributed As^{76} source.

This method (19) may be particularly suitable in the case of bituminous pavement over a base course contain-

ing negligible carbon by detecting one of the carbon capture gamma rays with energies of 3.68 or 4.95 Mev (*11*). A partial theoretical analysis can be made with additional information on the characteristics of the medium, but an experimental evaluation is necessary to correctly determine the complex effects of multiple scattering and radiation diffusion. A curve of relative response versus pavement thickness is shown in Figure B-2.

At this stage the work performed on the evaluation of nuclear methods had reached the point at which further information on the nuclear properties of concrete was required. An investigation into the nuclear properties of concrete was one of the objectives as originally mentioned in the work statement. This work is discussed in the following section.

NUCLEAR PROPERTIES OF CONCRETE

The nuclear properties of portland cement concrete have been studied in connection with its use as a shielding material for both neutron and gamma radiation around nuclear reactors and other intense radiation sources. The type of portland cement concrete used in the calculations as representative of those used in highway pavements is listed as Type 04 (*13*, p. 659). Its elemental composition is given in Table B-1.

This particular concrete was chosen because it had the most tabulated data for both neutron and gamma transmission. It is compared to other ordinary portland cement concretes (*13*), and another typical portland cement concrete from a different reference is listed for comparison in Table B-1. The word "ordinary" is used to described these concretes to distinguish them from special-purpose heavy portland cement concretes sometimes used in shielding application (e.g., concretes using iron ore, etc., as the aggregate in place of gravel).

ACTIVATION GAMMAS FROM THIN ADDITIVE LAYER

The simplified geometrical configuration shown in Figure B-3 was used in the calculation of the gamma radiation returning to the surface of the pavement after being induced in the thin additive layer by neutrons. The results are based on an assumed neutron source strength of 10^6 thermal neutrons per sec. The additive layer was assumed to be 1 mil (2.54 × 10⁻³ cm) thick under an 8-in. (20 cm) thick portland cement concrete slab. The calculations are described in the earlier section on "Calculation of Gamma Flux."

The first set of results describes the gamma radiation from additive layers which form long half-life gamma emitters when activated by neutrons. Manganese and indium were selected as materials of this type most likely to give high gamma fluxes. For this set a neutron irradiation period of 10 min was assumed.

Table B-2 gives the results, which may be interpreted as follows. Selecting the entry with the largest gamma flux (1.27 Mev gamma energy from indium), one asks how long a gamma counting period would be required to obtain about 1,000 counts. This number of counts is chosen because it gives a statistical accuracy of about

3 percent (100 counts gives an accuracy of 10 percent, and 10,000 counts an accuracy of 1 percent). A gamma detector having a surface area of about 125 cm² (5 in. in diameter) will thus require about 20 min to count 1,000 of these 1.27-Mev gammas from an indium layer. Adding this time to the neutron irradiation time of 10 min means that under the conditions assumed (neutron source of 10^6 per sec and 1-mil thickness of additive layer), the total time required for a thickness measurement with about 3 percent accuracy is about one-half hour.

This time can be appreciably reduced only by increasing the neutron source strength or by increasing the thickness of the additive layer. Increasing either of these by a factor of 100 can reduce the total measurement time to 3 min (1 min irradiation and 2 min counting). Increasing the source strength to 10^8 neutrons per sec probably would require giving up the concept of a portable instrument. Still further, one could consider a heavily shielded trailer with remote-controlled operation; in such a case, a neutron source strength of 10^{10} neutrons per sec may be feasible. In this latter case the thickness of the additive layer of indium could be reduced to a thin (0.01 mil) film. A section of pavement 1 mile long and 30 ft wide would require about 60 lb of indium for a 0.01-mil thickness, or about 3 tons for a 1-mil thickness. The economic feasibility will depend on the supply and demand, as well as the chemical form in which it may be convenient to add the layer. These factors are not evaluated here.

A second set of results describes the gamma radiation from additive layers which form short half-life gamma emitters. Rhodium, dysprosium, and vanadium were chosen as materials of the type most likely to give high gamma fluxes. For this set of results, the neutron irradiation period is assumed to be long compared to the half-life. Likewise, the counting period is assumed to be long compared to the half-life. During this counting period the gamma flux decreases from a maximum at the end of the irradiation period to nearly zero; therefore, the time integral of the flux is measured. Table B-3 gives the results based on Eq. B-17. As before, a neutron source strength of 10^6 neutrons per sec was assumed. Also, the thickness of the additive layer was again taken to be 1 mil.

Table B-3 indicates that vanadium gives by far the highest integrated flux per unit area. However, it also has the longest half-life and consequently the longest counting period. In the calculation for rhodium, only the activation directly to the ground state of Rh^{104} was considered. Because of the relative values of the cross sections, the inclusion of the effect of the decay of the metastable state would have less than a 10 percent effect on the final result for 0.556 Mev.

This second set of results may be compared to the first set after noting that they are different in their dependence on the irradiation and counting times, and that no increase in these times can give an increased number of counts. A 5-in. diameter detector can give only 125 counts from the additive vanadium layer unless either the neutron source strength or the layer thickness is increased. To get a statistical counting accuracy of about 3 percent, an

increase in neutron source strength by about a factor of 100 (to 10^8 neutrons per sec) is required. Because the density of vanadium is near that of indium, a few tons would also be required for a mile of pavement 30 ft wide if the vanadium layer thickness is 1 mil. Thus, it is desirable to decrease this thickness. If the thickness is decreased to 0.01 mil, the neutron source strength must be correspondingly increased to 10^{10} neutrons per sec.

ACTIVATION GAMMAS FROM THE PAVEMENT

Elements already present in portland cement concrete may also be activated by the neutrons. This gamma radiation will come from sources distributed through the volume of the pavement and must be estimated in order to determine whether the radiation due to the material in the additive layer can be distinguished from this spurious radiation. Formulas for making these estimates are derived in the earlier section on "Calculation of Gamma Flux."

The results for Type 04 portland cement concrete using a neutron source strength of $S_n = 10^6$ neutrons per sec are given in Tables B-5 and B-6. In Table B-5, as before, the irradiation period is 10 min; in Table B-6 it is again assumed that both the irradiation and detection periods are long compared to the half-life. Eq. B-21 was used for Table B-5 and Eq. B-22 for Table B-6.

These results do not look encouraging when compared to the results presented in Tables B-2 and B-3. The contribution from the aluminum content in the pavement material is especially large and would almost certainly make detection of gammas from both vanadium and indium extremely difficult. The emision from the activated aluminum decays much faster than that from the activated indium, but even with a 10-min irradiation period one would have to wait about one-half hour for the aluminum emission to decay sufficiently for its counting rate to decrease to the point where it is only about ten times as great as the counting rate of the indium gammas (this assumes a 1-mil thickness of indium). At about this level a large NaI crystal spectrometer may begin to distinguish the indium gamma ray peak at 1.27 Mev against the Compton tail from the larger (by a factor of 10) aluminum peak at 1.78 Mev. The background due to Ca^{18} is not initially as high as the aluminum background, but it decays more slowly and hence may be as great a problem as the aluminum.

The most disappointing feature of these results is the fact that if one tries to decrease the additive layer thickness below 1 mil and to compensate for the decrease by increasing the source strength to maintain the value of the gamma flux from the layer, the background gamma flux due to activated material in the pavement increases in proportion to the increase in source strength. There are two possibilities which may work to counteract this fact. One is the possibility of utilizing an additive layer which is not continuous but is arranged in some pattern that looks random to the pavement contractors but is known to the thickness monitor operators. The second possibility is that the calculations of the background have overemphasized the contributions from the portion of pavement next to the detector. The calculations have assumed that the neutrons coming from the point source were already thermalized, whereas in practice the neutrons emitted from the source are fast and slow down to thermal in the pavement. Thus, too large a value has been assumed for the thermal neutron flux near the point at which first the source and then the detector is placed. Moreover, even if this overestimate is not of a large order of magnitude, the ratio of the gammas from the additive layer to those from the background may be greatly improved by locating the detector at some point other than that occupied by the source. These effects will have to be investigated experimentally, because they greatly complicate the calculations and tend to make the computed results uncertain.

One potentially bright feature of these results is the fact that if paving situations exist in which there is relatively little aluminum present in the base course material, the aluminum in the pavement itself may be used to make a thickness measurement without the necessity of using any additive material.

CAPTURE GAMMAS FROM ADDITIVE LAYER AND FROM PAVEMENT

In addition to the consideration of activation techniques, the possibility of using neutron-capture gamma radiation from a thin additive layer was also examined analytically. In this process the gamma ray photon is emitted instantaneously upon the capture of a neutron by a nucleus. For this purpose (see earlier section on "Calculation of Gamma Flux") cadmium was chosen as the material for the additive layer, because it is most likely to give a high gamma flux. As before, a 1-mil thickness was taken for the additive layer. Again the results show that the background due to capture gamma rays from the material in the pavement is greater by a factor of 20 than the capture gamma rays from the additive layer, making the measurement of the latter gamma rays difficult. In this case one cannot improve the situation by waiting, because the capture gammas must be measured while the neutron irradiation is taking place. The other possibilities of improvement for activation gammas apply also to the capture gammas.

The work performed at this point had fulfilled the following objectives of the nuclear investigation as outlined in the work statement: (1) a survey of the nuclear properties of portland cement concrete, (2) the experimental evaluation of the capture gamma and activation gamma technique, (3) the investigation of neutron scattering techniques for bituminous pavement, and (4) the consideration of any other nuclear technique which appeared promising during the progress of the work. Some promising techniques were revealed, but technical difficulties still had to be solved. At this point, however, a new nuclear technique not previously considered was discovered. This technique involved placement of radioactive pellets on top of the base course prior to laying the pavement. Examination of this technique showed it to be promising indeed, and it is this method that is the final recommendation.

NEW THICKNESS-MEASURING TECHNIQUE USING RADIOACTIVE PELLETS (FINAL RECOMMENDATION)

One general technique which has been considered for thickness measurements is to either place or produce a radioactive material under the pavement and measure the activity at the surface. Although a technique such as spreading a continuous layer of radioactive material was discarded earlier because of the large quantities of radioisotopes required (approximately 2 curies per mile, as calculated in the earlier section on "Quantities Required for a Continuous Layer of Radioactive Material"), a variation of this technique using discrete sources has been examined recently. The use of radioactive pellets, rather than a continuous active layer, reduces the amount of radioactive material required by a factor of 400 and eliminates many of the previous objections to laying a radioactive material. Pellets can be used in several ways, but in conjunction with a measuring technique described in the following they provide a technique for thickness measurement which is simple and completely independent of pavement composition and density.

In any technique utilizing radioactive pellets, the investigator must first sweep out areas of the road until a meter or other indicator shows that his detector is over a pellet. This should present no problem, and once this is done the preferred technique, which does not depend on the paving material or the presence of reinforcing rods, is as follows. The counter is placed on the road surface directly over the pellet and the counting rate is measured. Then the detector is raised until the counting rate decreases by a factor of four. The distance the detector is raised is equal to the road thickness (derivation in earlier section on "A Measurement Technique Sensitive to Thickness but Independent of Density and Composition"). A 1 percent change in road depth would produce a 1 percent change in detector height. This could be observed with counting periods of the order of a few minutes. The measurement would be independent of the water content of the concrete, location of reinforcing rods, or any other characteristics of the material. The only calculation would be to divide the counting rate at the road surface by four. The measurement could be made with a ruler.

This description is slightly oversimplified, because it assumes a point detector. However, even introducing a finite detector will not destroy the simplicity of the technique. The only effect would be to change the factor of four slightly, or one can keep the factor of four (or any factor for that matter) and use a specially calibrated ruler. Of course one could use a calibration curve and measure the count rate at a fixed height, but the simplicity of making the depth measurement with a ruler has an undeniable appeal.

This technique appears to be the most direct method for measuring the road thickness. It could easily be applied to bituminous roads of all thicknesses if the appropriate size counter is used. Radioactive pellets can also be mixed with identical-looking dummy pellets and spread over the entire roadbed to avoid placement in specific locations. This technique also has advantages in terms of the amount of activity required, health hazards, and cost of active material.

If a counting rate of 10^4 per min in the energy region of interest is required, each pellet will have to contain k_i μcuries of activity, where k_i is the fraction of the activity which produces events in the energy region of interest (see earlier section on "Activity Required in a Pellet Source Under Concrete"). If $k_i = 1$ (as in Co^{60}), 1 μc per pellet is the desired activity. If a discrete source were placed in every linear foot of road (1 μc each), 5.3×10^3 μc would be required in each mile. The average flux on the road surface would be 0.001 counts/cm^2/sec. The maximum flux corresponds (for 1-MeV gammas) to a radiation dose rate of 7.6×10^{-7} roentgen per hr, which is 800 times smaller than the allowed exposure rate for the population at large. Hence, there is no danger whatsoever from the road surface. One might also compare the 1-μc pellet activity with the activity in a luminescent watch, which may be as high as 100 μc of Pm^{147}.

The pellets could consist of aspirin-tablet-size capsules or pellets, which are sprinkled on the roadbed. The active material can be imbedded in glass, if desired, to prevent any possible migration. This would be inexpensive. If it is desired to be able to measure the road thickness over a period of 10 or 20 years, Co^{60} would be a possible choice, because both of its gamma rays have high energy (1.2 and 1.3 Mev) and it has a half-life of 5.26 years. The price of Co^{60} from Oak Ridge is $2 per mc (for less than 1,000 mc per order) so that using the pellets, the Co^{60} required for a mile of highway would cost $10.60. Even with fabrication costs, the pellet technique would cost less than $100 per mile. If the road thickness is going to be measured within a month or so after the concrete is poured, Rb^{86} (half-life 18.68 days) could be used. The rubidium costs $0.30 per mc, so pellets for a mile of highway would cost $1.80. Other isotopes with varying half-lives are available from numerous supply houses. Oak Ridge National Laboratory, for example, lists isotopes with half-lives ranging from 14.1 hr (Gallium-72) to 16 years (Europium-154), any of which could be used if desired.

Two other methods of using radioactive pellets appear to be possible, although they are not as attractive as the technique described here.

One technique would use a single measurement of the radiation intensity at the road surface from a pellet source beneath the pavement. The counting rate in the high-energy region of the spectrum provides an accurate measurement of the product of thickness times density. Assuming that the density is known or is measured, the thickness can be accurately determined. The depth sensitivity is good, because a ⅛-in. change in the depth of the concrete would produce a 7.5 percent change in the counting rate (see earlier section on "Sensitivity of an Attenuation Measurement to Changes in Thickness and in the Linear Attenuation Coefficient"). This change would be detectable in less than 1 min of counting with the assumed counting rate of 10^4 per min. On the other hand, if μ, the coefficient of linear absorption, changes by 1 percent, the counting rate changes by 3 percent. This implies that μ, which is dependent on density, will have to be

known within 1 or 2 percent. From a sample of concrete taken during placement, μ can be determined or the density can be measured nondestructively with a gamma backscatter gage. If this method is used, the pellets should be placed between the reinforcing rods so that the rods do not obscure the measurement.

Another method using the pellets is to use the ratio of the counting rate in the highest energy peak of the given spectrum to the total counting rate as a depth measure. This ratio decreases with depth, because the deeper the pellet the more gamma rays are scattered into lower energy channels. The general advantage of this method is that it does not depend on the source strength. However, this technique is basically sensitive to the thickness-density product also and would require accurate density information, as with the simple attenuation technique.

It is apparent that the best method (in terms of simplicity, cost, activity, and convenience) for measuring the thickness would be to measure the activity at the road surface from a pellet placed beneath the pavement, raise the detector until the counting rate drops by a fixed factor, and simply read the detector height, which equals road thickness, directly on a ruler. The price of the active material need be no more than about $100 per mile, the average direct radiation flux at the road surface would be 1/300,000 of the acceptable value, the method is direct reading (no graphs, charts, or interpolations needed), and the instrumentation is conventional, simple, and readily available. In addition, this method can be used for any type of pavement that has been previously prepared with the active pellets. Thus, of all nuclear techniques available the radioactive pellet method is by far the best and is highly recommended.

In conclusion, a few additional comments are made on the cost and storage aspects of the proposed nuclear technique using radioactive pellets. Cost estimates are given for two different types of sources and radiation from a stockpile of pellets is compared with standards for allowable radiation exposure.

Limitations on radiation exposure are normally expressed in terms of the exposure per quarter year. However, it is usually more convenient to reduce this to an average exposure per week or per hour for practical use. For gamma radiation, the maximum permissible whole body (trunk) dose is close to 100 mr per week. For the extremities (hands, forearm, feet, ankles) a higher value of 1,500 mr per week is acceptable. Assuming a continuous exposure for a 40-hr week, these values reduce to 2.5 and 37 mr per hr, respectively.

For comparison, a few common dose rates are as follows: cosmic radiation and natural body activity produce an exposure of 0.04 mr per hr, the average chest X-ray gives a dose of 200 mr, a watch with 0.1 μc of Ra^{226} on the dial gives about 0.1 mr per hr at 1 in. distance, and typical nuclear density gages produce about 10 to 30 mr per hr at the surface of the shielding.

For radioactive pellets with, say, 1 μc of Co^{60} in each pellet, the radiation would be about 0.8 mr per hr per 500 pellets at 1 yard. The volume of these pellets would be less than 1 cu in. Placed inside a portable lead-lined container about 4 in. in diameter and 6 in. high, the radiation would be reduced by a factor of 10 to 0.08 mr per hr at 1 yard and to 25 mr per hr at the surface of the shield. Such a container could be carried 8 hr a day, 5 days a week without exceeding the accepted radiation limits. Even with the top off the can, the radiation would only be 50 mr per hr at 4.5 in. so that pellets could be picked out one by one with tweezers if desired. An automatic dispensing device would be simpler, of course. Stored in such cans, the pellets can be readily stocked and moved. If pellets are placed in the road with an average separation of 10 ft, about 1½ cans of 500 pellets each would be enough for a strip of concrete 15 ft wide and a mile long. A stockpile sufficient for a strip 15 ft wide and 10 miles long would produce less than 1 mr per hr at 1 yard. This would not produce an overexposure to radiation, even assuming a continuous exposure for a 40-hr week, every week of the year.

To minimize the radiation exposure, it is not recommended that any sources be carried in a pocket. If sources are accidentally carried in a pocket, however, the most likely sources of radiation exposure are the beta radiation dose to the adjacent skin and the gamma dose to the gonads. If deemed necessary, the beta radiation can be eliminated in the fabrication technique by absorbing all beta particles within the pellet itself. This is possible because the beta particles from Co^{60} travel at most about 0.03125 in., even in a low-density material such as plastic. The gamma radiation at 4 to 5 in. from a single 1-μc Co^{60} source is 0.1 mr per hr. Ten pellets in a pocket would thus produce a gonadal dose of only 1 mr per hr, which is not an excessive level. A larger number of pellets could lead to overexposure, but this would generally require a long exposure of hours or days.

The primary cost of pellets made from radioactive material will be in the fabrication, inasmuch as the cost of isotopes is generally quite low. For radioactive Co^{60}, the cost is about $2 per millicurie, which is enough for 1,000 pellets. For a sandwich-type disc source with the radioactivity between layers of plastic, one manufacturer indicated a maximum cost of $2 per source in lots of 10,000. Another manufacturer estimated a cost of $0.90 for a similar sandwich-type source. These costs appear unnecessarily high when compared with the cost of sources produced by activating cobalt metal pellets or cobalt glass pellets. Thousands of pellets can be irradiated simultaneously in a nuclear reactor at a very low cost. This technique eliminates much of the labor cost for fabrication.

Assuming $10 per pound for cobalt, this amounts to only $0.001 per pellet. A generous allowance for irradiation costs would be $100 per 1,000 pellets or $0.10 per pellet. Adding another $100 per 1,000 pellets for handling and other costs would still give only $0.20 per pellet as the total cost. This is an order of magnitude below the cost of fabricating the pellets individually. Both the irradiation and handling costs could probably be cut in half from these values, giving a cost of about $0.10 per pellet. If sources are separated by an average distance of 10 ft, a strip of concrete 15 ft wide and 1 mile long requires 800 sources costing about $80.

APPENDIX C

ELECTRICAL TECHNIQUES

SELF- AND MUTUAL INDUCTANCE

A sinusoidal current of magnitude I_1 flowing in a coil will produce a sinusoidal magnetic flux, which generates an opposing voltage having a magnitude given by

$$E_1 = \omega L_1 I_1 \qquad (C-1)$$

in which ω is the angular frequency of the sinusoidal current. (In this report the imaginary operator, $j\omega$, has been reduced to simply ω.) Although not strictly true, the magnitudes of voltage and current calculated are correct for low-resistance circuits.

The relation between the voltage, E_1, and current, I_1, is determined by L_1, self-inductance of the coil. If current, I_2, is caused to flow in a second coil placed near and parallel to the first coil, it will also induce a voltage in the first coil, because some of the flux produced by I_2 links the turns of wire of the first coil. This current-voltage relationship is defined by

$$E_1 = \omega M_{12} I_2 \qquad (C-2)$$

in which M_{12} is the mutual inductance between the first coil and magnetic circuit of I_2. This relationship is bilateral ($M_{12} = M_{21}$), so the voltage and current relationships in two coils coupled by mutual inductance are given by

$$E_1 = \omega L_1 I_1 + \omega M_{12} I_2 \qquad (C-3)$$

$$E_2 = \omega M_{12} I_1 + \omega L_2 I_2 \qquad (C-4)$$

In general, the mutual inductance between two coils on a common axis (a) decreases as the coils are separated, and (b) increases with increasing turns on each coil.

Eddy Currents and Mutual Inductance

The inductance of a coil can be reduced by bringing a conducting surface near the coil. It can be shown that the effect of the conducting plate on the coil is the same as the effect of a second coil, identical to the first, carrying a current equal and opposite to the coil current and located on the coil axis at a distance $2d$ from the original coil. This coil is said to be an image of the first.

The voltage induced in the first coil is seen to have two components. The first of these is due to the self-inductance of the coil in space, and the second is due to the mutual inductance between the coil and its image. Hence,

$$E_1 = E_{11} + E_{12} = \omega L_1 I_1 + \omega M_{12} I_2 \qquad (C-5)$$

But I_2, the image coil current, is the negative of I_1, so that

$$E_1 = \omega L_1 I_1 - \omega M_{12} I_1 = \omega I_1 (L_1 - M_{12}) \qquad (C-6)$$

Thus, the induced voltage is seen to be the sum of two components, one a constant and the other a function of coil-to-plate spacing. Therefore, the inductance of the coil can be used to measure coil-to-plate distance, d, if the relationship between M_{12} and d is known.

TWO TYPES OF EDDY-CURRENT GAUGING INSTRUMENTS

One way to measure distance between a coil and a plate would be to prepare a calibration curve presenting d as a function of "free-space" induction, L_0. This has the disadvantage of requiring two extremely accurate measurements of inductance in order to accurately determine the small difference between "free-space" and "near-plate" inductance. A better way is to use a comparison technique as follows.

Two identical coils are used. One, the "measure" coil, is placed near the unknown plate; and the second, the "reference" coil, is placed near a second "reference" plate. A bridge circuit is connected as in Figure C-1, and the distance between the reference coil and reference plate is adjusted so as to make the output voltage, E_0, as small as possible. When $L_1 = L_2$, E_0 will be zero, which is true only when $d_R = d_M$. Thus the distance, d_R, is a duplicate of d_M, and if the reference coil is mounted on a calibrated distance scale, d_M can be read directly. The accuracy of the measurements is limited by the degree to which the coils can be made equal, and the sensitivity is determined mainly by the smallest voltage difference, E_0, which can be distinguished. With careful coil construction and sensitive voltmeter, these two limitations can be easily overcome.

An improvement on this technique uses a somewhat simpler technique of voltage comparison rather than inductance comparison. Consider the case where the measure and reference coils both have two windings on a common coil form. The two coils are made as similar as possible. Each behaves as a transformer, and they are connected as in Figure C-1. With no metal plate near either coil, it is seen that

$$E_2 = I_1 M_{12} \qquad (C-7)$$

and

$$E_5 = I_4 M_{45} \qquad (C-8)$$

The secondary windings are connected so as to add in series opposition, so that

$$E_0 = E_2 - E_5 \qquad (C-9)$$

and the primary windings are in series aiding, so that $I_1 = I_4$. Therefore, substituting Eqs. C-7 and C-8 in Eq. C-9,

$$E_0 = I_1 (M_{12} - M_{45}) \qquad (C-10)$$

Thus, if the two coils are identical, $M_{12} = M_{45}$ and the output voltage, $E_0 = 0$.

Suppose that a conducting plate is placed at some distance, d_M, from the measure coil. Now, coil L_1 will have an "image" at $2d_M$, and the voltage induced in coil L_2 will have an additional component due to the mutual inductance between coil L and the image coil L_3. This mutual induc-
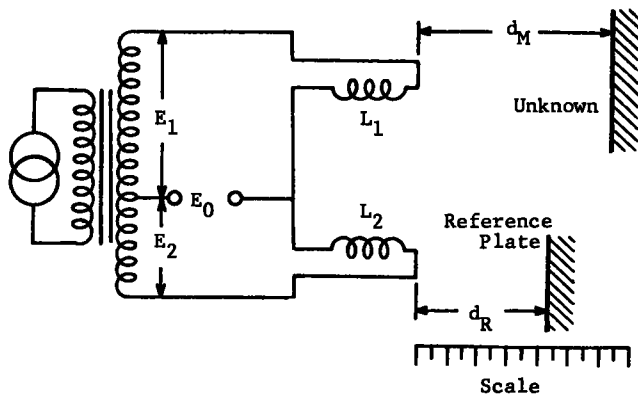
Figure C-1. Bridge circuit for inductance comparison measurements.

tance is denoted by M_{23}, so the current in the image coil will induce in coil L_2 a second voltage, which combines with that induced by the primary current, or

$$E_2 = I_1 M_{12} + I_3 M_{23} \qquad (C-11)$$

But, because coil L_3 is the image of coil L_1, $I_3 = -I_1$, and

$$E_2 = I_1 (M_{12} - M_{23}) \qquad (C-12)$$

Suppose, also, that a reference plate is placed at a distance, d_R, from coil L_3. By the same reasoning,

$$E_5 = I_4 (M_{45} - M_{56}) \qquad (C-13)$$

and

$$E_0 = I_1 (M_{12} - M_{23}) - I_4 (M_{45} - M_{56}) \qquad (C-14)$$

Due to the series connection of the windings L_1 and L_4, $I_4 = I_1$ and

$$E_0 = I_1 [(M_{12} - M_{45}) - (M_{23} - M_{56})] \qquad (C-15)$$

But $M_{12} = M_{45}$, so

$$E_0 = I_1 (M_{23} - M_{56}) \qquad (C-16)$$

If the distance, d_R, is adjusted so that $E_0 = 0$, $M_{23} = M_{56}$ But since both M_{23} and M_{56} vary with d_M and d_R in exactly the same way, due to the identical coil construction, it follows that $d_M = d_R$.

In the case of pavement thickness measurements, d_M is the distance through the pavement to a conducting surface beneath the pavement. It cannot be measured directly, but if two identical sets of coils are used in the manner described, with a reference surface and a coil mounted on a calibrated frame above the pavement, and with the measure coil placed flat on the pavement surface, d_M can be read directly from the calibrated frame.

THE CONDUCTING SURFACE

As stated previously, use of an eddy current technique is predicated upon the placement of a conducting surface between pavement and the base material. Although the theory requires an infinitely large, infinitely thick, infinitely conducting metal layer, laboratory tests have shown the following:

1. The material effectiveness decreases with increasing distance from the coil. For the purpose of pavement thickness measurement, if the metal foil extends two coil diameters beyond the projected area of the test coil, it is as if it were infinite in extent.

2. Losses due to the use of cooper or aluminum, rather than a perfectly conducting medium, are negligible.

3. At 100 kilocycles, increasing foil thickness beyond 0.0015 in. does not increase effectiveness. The lower limit on thickness has not yet been established, but may lie well below 0.0015 in. Aluminized Mylar, with metal film thin enough to be transparent, was *not* effective.

It is difficult to estimate the cost of a plastic film with suitable metallic coating, because the cost is a function of the supply and demand. However, the economies due to accurate pavement thickness may greatly outweigh the additional cost. Fifty square feet of aluminum 0.0015 in. thick will weigh approximately 1 lb.

EFFECTS OF REINFORCING STEEL UPON EDDY CURRENT MEASUREMENTS

Highway pavements generally incorporate a steel reinforcing mesh, laid approximately at mid-depth. This mesh is available in various sizes, classified according to the size of the rectangular mesh and the diameter of the wire. Use of this steel reinforcing affects eddy current measurements by means of the circulating currents induced in the mesh, rather than by changing the magnetic qualities of the concrete. A mesh appears, therefore, as a series of interconnected one-turn coils, and these coils are magnetically coupled to the measuring coil.

The difficulty in estimating the effect of steel mesh on eddy current measurements lies in the relatively high resistivity of steel compared to copper (approximately ten times as great). Due to higher resistivity, the impinging magnetic field is less effective in inducing circulating currents than would be the case with copper or aluminum mesh. This was verified experimentally (Fig. C-2) in two tests. In one, circular loops of copper wire were placed near the test inductor, and the decrease in inductance was noted. Then loops of steel wire of equal diameter were substituted, and the decrease in inductance was found to be less than with copper. Similarly, a resistance was inserted in series with the copper loop, and the effect was also lessened.

The program scope did not permit tests with actual welded steel mesh. It should be noted that inasmuch as the depth of penetration of the field into the conductor is small, galvanized steel with a low-resistivity zinc plating is not equivalent to plain steel mesh. Measurements were made on several models built of solid copper wire. The effectiveness of mesh of two sizes on test coil self-inductance is shown in Figure C-3, which confirms that the larger mesh is less effective than the smaller. However, because the meshes were made of copper, definite conclusions cannot be drawn as to the total effect of steel mesh on the thickness measurements.

Further investigations of eddy current pavement-thickness measurements must include a comprehensive experi-
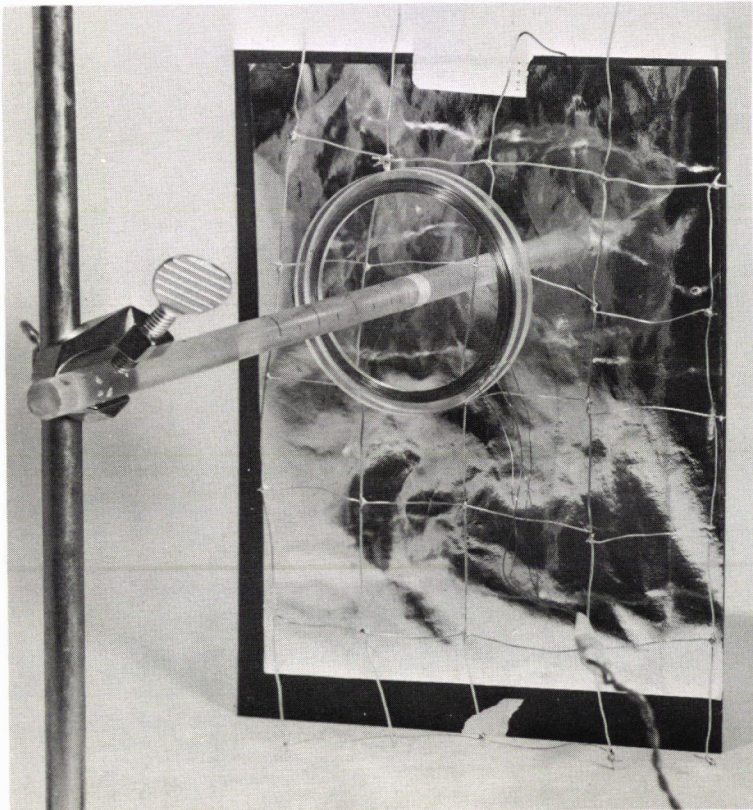
Figure C-2. Simulated reinforcement mesh placed between measuring coil and plate to evaluate interference effects.
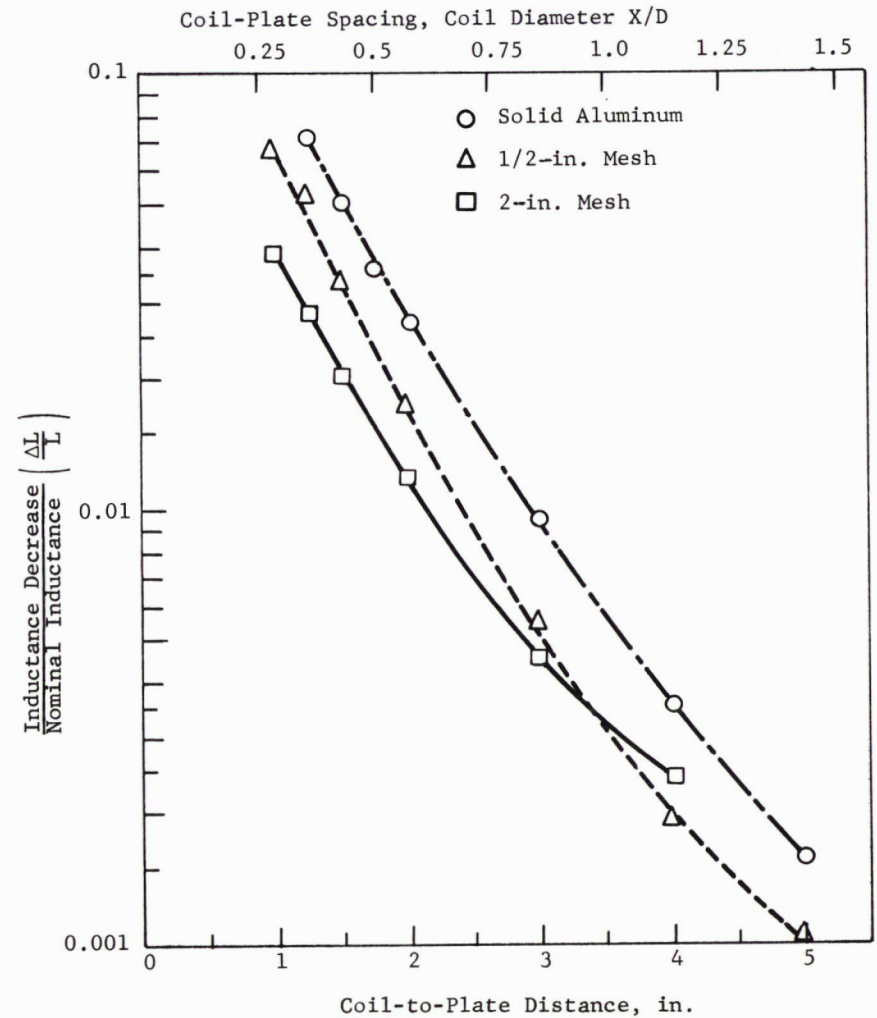

Figure C-3. Relative coil inductance decrease in a coil near square copper and aluminum wire meshes.

mental program to evaluate the effects of actual steel mesh, with welded joints, on the measurement. In an actual pavement situation, the size and gauge of mesh used will be known, as will its approximate depth. If the effect is reasonably small, compensation for the presence of mesh may be possible by inserting a similar section in the reference setup.

SENSITIVITY AND RESOLUTION REQUIREMENTS OF INSTRUMENTATION

The sensititvity requirements were established through experiments carried out in the laboratory. By means of a sensitive inductance comparator, the decrease in inductance of a simple coil was measured as a function of its distance from a metal plate (Fig. C-4). Because the decrease in inductance is due to an increase in mutual inductance between the primary coil of Figure C-5 and its image coil, and because the windings of the coil are tightly coupled, the percentage change in inductance is equal to the percentage change in voltage across the coil. In addition, measurements made on one coil are applicable to other coils of the same shape, as long as the coil-plate distance is expressed in units of coil-diameters, rather than absolute units.

Inspection of the curve (Fig. C-6) of $\Delta L/L$ versus x/D, the coil-plate spacing in coil diameters, shows that the relation is semilogarithmic over a range of x/D from about 0.5 to 1.25. (x is the coil diameter and D the coil-to-plate spacing.) This suggests the relation

$$\frac{\Delta L}{L} = K_1 e^{-K_2(x/D)} \qquad (C-17)$$

Evaluating the constants K_1 and K_2 gives

$$\frac{\Delta L}{L} = 0.22 \, e^{-3.6 \, (x/D)} \qquad (C-18)$$

Figure C-5. Bridge circuit for voltage comparison.

Differentiating Eq. C-18 gives

$$d\left(\frac{\Delta L}{L}\right) = -3.6 \, (0.22 \, e^{-3.6 \, (x/D)}) \, d\left(\frac{x}{D}\right) \qquad (C-19)$$

Hence, for small increments of x/D Eq. C-19 is equivalent to the output voltage, E_0, referred to the coil voltage, or

$$\frac{E_0}{E} = -3.6 \, (0.22 \, e^{-3.6 \, (x/D)}) \, \frac{\Delta x}{D} \qquad (C-20)$$

The results of applying Eq. C-20 to a 1 percent resolution of a 10-in. pavement thickness measurement using various coil diameters are given in Table C-1.

Using an example, this means that to resolve a 0.1-in. change in pavement thickness, using a 10-in. coil on a 10-in. pavement, the null detector must have a resolution of approximately 0.0002, or 0.2 millivolts per volt of coil voltage. With good electronic equipment, this is not at all difficult to do.

Calculation will determine practical values of coil voltage, current, and inductance. A 10-in. diameter coil with only 20 turns of No. 22 wire has an inductance of 224 μhenries, and an impedance of 70 ohms at 50 kilocycles. This means that a coil voltage of 1 v will be obtained for a primary current of 14 milliamperes (0.014 amp). This is a practical value of current, because the current capacity of No. 22 wire is nearly 1 amp.

The foregoing, then, establishes that an adequate resolution of thickness of a 10-in. thick pavement can be obtained with a coil of reasonable dimensions, with moderate to low current and voltage levels, using only moderately sensitive null-detecting equipment.

PRACTICAL FIELD APPLICATION

The eddy current technique can be readily adapted either for "spot" thickness measurements, or for making a continuous profile of thickness along the highway. In either case, the equipment tends to be lightweight and readily transportable.

For spot measurements, the measuring coil is placed flat on the pavement surface and connected by a cable of shielded wires to the electronic null-indicator. A reference coil of identical construction is mounted on a suitable marked frame nearby. This frame is arranged so that the coil can be positioned on a calibrated rod mounted perpendicular to a flat metal plate. The reference coil is similarly

TABLE C-1

RESULTS OF 0.1-IN. CHANGE IN PAVEMENT THICKNESS MEASUREMENT OF 10-IN. PAVEMENT USING VARIOUS COIL DIAMETERS

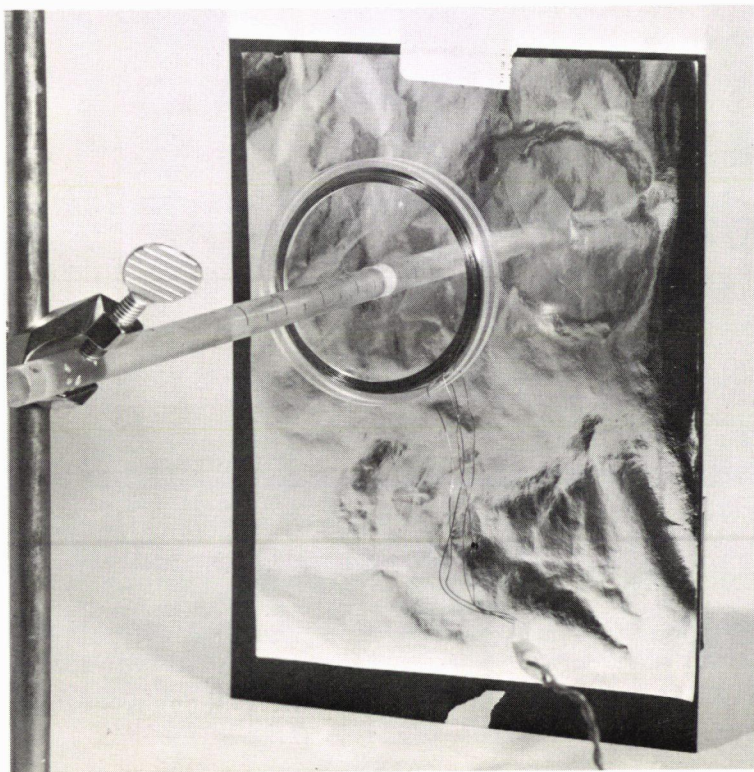| COIL DIAMETER (IN.)	$\dfrac{\Delta x}{D}$	$\dfrac{M}{L}$	$\dfrac{E_0}{E}$
20	0.0050	0.0363	0.001300
15	0.0067	0.0198	0.000720
10	0.0100	0.0060	0.000215
8	0.0125	0.0026	0.000092

Figure C-4. Measuring coil and graduated mount for measuring changes in self-induction as a function of coil-plate spacing.
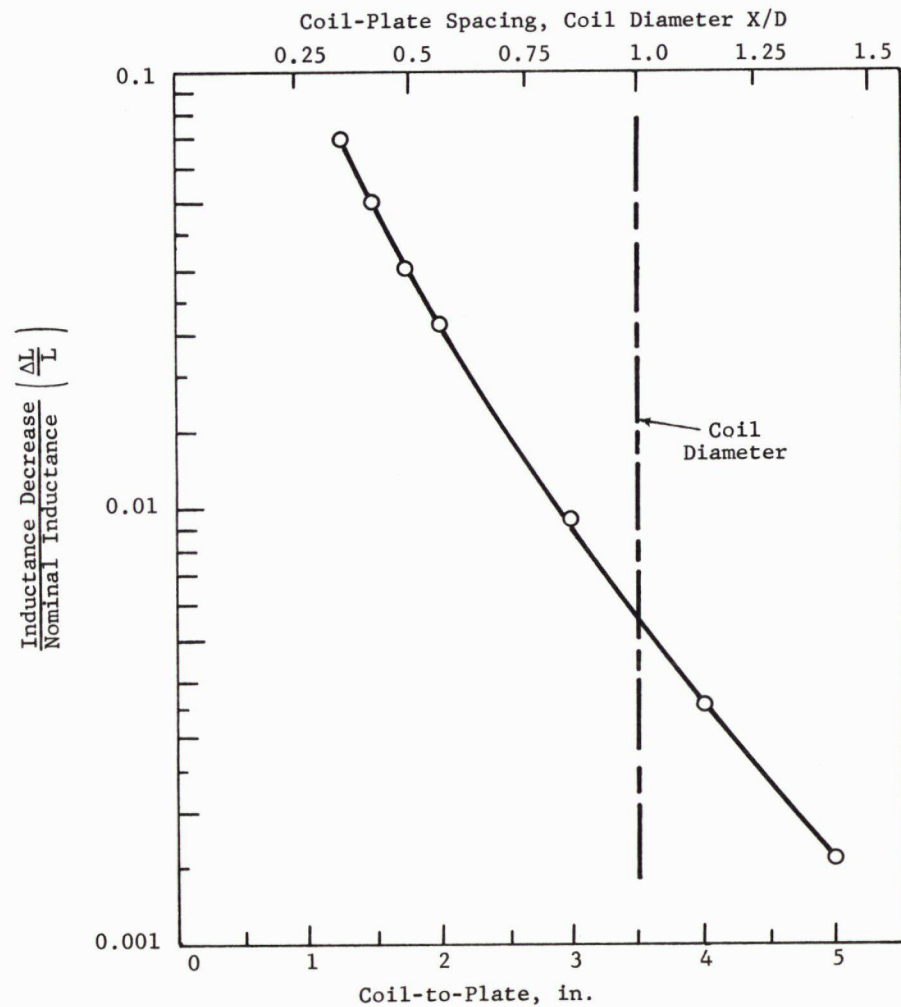

Figure C-6. Relative coil inductance decrease in a coil near a conducting surface.

connected to the null indicator, and the operator adjusts the position of the reference coil so as to obtain a null on the indicator. The pavement depth is then read directly from the mounting rod. The advantage of this method is that no great skill is required of the operator, nor is any interpretation of the measurement necessary.

Continuous measurements would require that the measuring coil be suspended over the pavement at a constant height above the surface, mounted on a wheeled trailer, suitably shock mounted so as to minimize effects of minor surface irregularities. The trailer would be drawn by a truck, in which would be installed the reference coil in its supporting framework. In this case, however, the reference coil would be fixed with respect to the reference plate, at a distance equal to the sum of the measuring coil elevation and the nominal pavement thickness. The electronic equipment would produce an output signal proportional to the error in pavement thickness (departure from nominal). This signal would be recorded on a strip-chart recorder, with the motion of the recording paper synchronized with an external odometer. The chart would thus provide a continuous profile of pavement thickness.

Although the equipment is somewhat more complex than that for the spot method, the system does have the capability for averaging the thickness over a time period of several seconds, and would thus be more likely to detect trends in pavement thickness.

RADIO-FREQUENCY TECHNIQUES

Thickness-measuring methods have been described which depended on the generation of eddy currents produced by low-energy, low-frequency (10 to 100 kcps) magnetic fields. The radio-frequency (RF) techniques discussed in the following subsections depend, in principle, on the same physical phenomenon, but involve the use of much higher-frequency (0.3 to 40 gigacycles per sec) electromagnetic waves. The use of high frequencies, which have very short wavelengths, allows the energy to be propagated in a well-defined manner. It will be noted that many of the parameters considered are similar to those discussed previously; however, these parameters must now be evaluated in terms of RF wave propagation.

The principal properties of a medium that govern the propagation, absorption, and reflection of an RF wave are its electrical conductivity and dielectric constant. In the case of concrete pavement thickness measurements, the use of RF techniques depends on the degree of change in these properties at (1) the air-pavement interface and (2) the pavement-road base interface. Therefore, a knowledge of the manner in which these electrical properties vary as a function of pavement composition, water content, geometry, etc., is essential. Specifically, the various electrical and physical properties of concrete and similar materials which govern the use of RF methods must be considered.

Electrical Properties of Pavement Structures

Little information exists in the literature relative to the electrical properties of concrete pavements at radio frequencies. Based on the present state-of-the-art, including past experience of IITRI personnel, approximations and extrapolation of property values and curves obtained on materials similar to concrete can be made. Although experimental determination of the electrical properties of portland cement and bituminous concrete is beyond the scope of the present project, these approximations indicate the range of values to be expected in addition to some of the problems that might be encountered.

REFLECTION COEFFICIENT

The reflection coefficient of a material is a function of its relative dielectric constant and electrical conductivity. If the reflection coefficient is known, signal characteristics can be calculated and measurable parameters can be determined.

Hammond and Robson (25) have measured both the DC and AC volume resistivity as a function of curing time, and the electrical capacitance as a function of curing time and frequency for three types of concrete. The DC resistivity values are shown in Figure C-7 for concrete consisting of four parts (by weight) of gravel to two parts of silica sand to one part of either normal portland cement, rapid-hardening portland cement, or high-alumina cement, mixed with 0.49 parts (by weight) of water. The curves for the two types of portland cement coincide, hence the time dependence of their volume resistivity is the same. The volume resistivity is simply related to the conductivity by

$$g \text{ (mho/meter)} = 10^{-1} r \qquad \text{(C-21)}$$

in which r is volume resistivity in megohm-centimeters. Thus, the resistivity of portland cement concrete approaches 0.3 megohm-cm, or a conductivity of 0.33×10^{-3} mho/m, whereas alumina cement concrete approaches a conductivity one-tenth as great, or 0.33×10^{-1} mho/m. Figure C-7 clearly shows the rising resistivity (decreasing conductivity) with curing time. Most of the change is undoubtedly due to the changing moisture content of the concrete. Measurements (AC) were also made by Hammond and Robson up to 25 kcps. Their measurements showed a slight drop in resistivity (increase in conductivity) with increasing frequency.

The measurement of capacitance—and therefore of relative dielectric constant—shows a large change with fre-

TABLE C-2

DIELECTRIC CONSTANT OF PORTLAND CEMENT CONCRETE

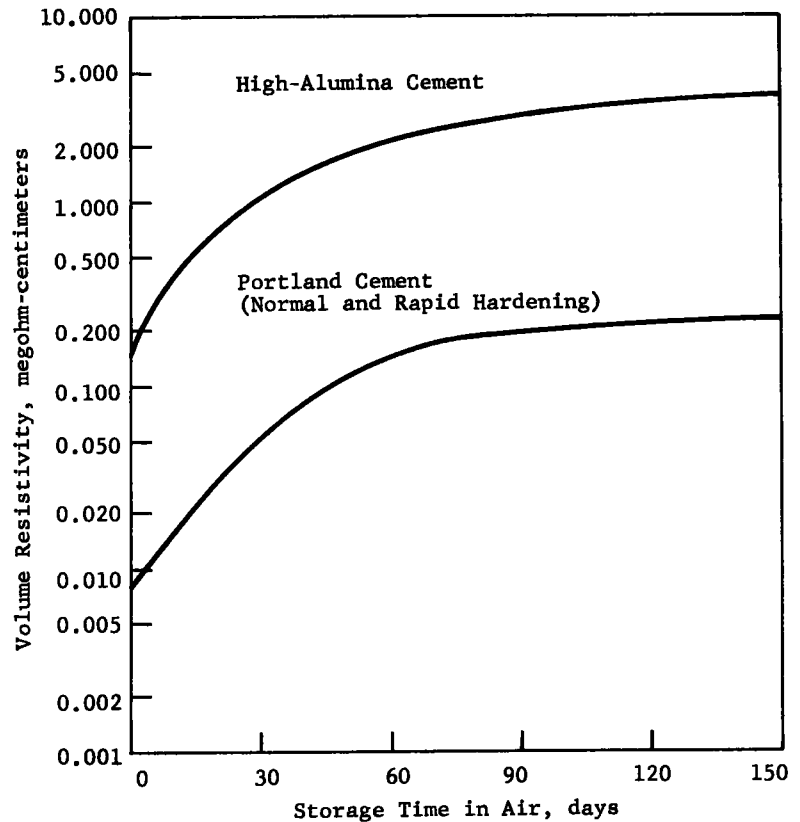| SAMPLE NO.	TIME (DAYS)	DIELECTRIC CONSTANT, ϵ,	
		50 CPS	25 KCPS
1	7	22,000	200
	42	5,600	110
	113	3,300	110
2	126	10,000	19
3	9	98,000	560

Figure C-7. Volume resistivity of three types of concrete as a function of time (from Ref. 25).

quency from 50 cps to 25 kcps (Table C-2). The relative dielectric constant, ϵ_r, is obtained from the measured capacity, C, of a parallel-plate capacitor (25) by

$$\epsilon_r = d\,C/0.225A \qquad (C-22)$$

in which d is the thickness of dielectric, in in.; A is the area of each capacitor plate, in sq in.; and C is the capacity, in picofarads.

The decrease in dielectric constant with increasing frequency is monotonic in almost all dielectric materials. Therefore, the values at the higher frequencies (0.3 gcps and above) considered for RF thickness measurements can be expected to be much lower than those at 10 to 100 kcps. An indication of what these values are is given by measurements made by Balachandran (26) at 3.0 gcps on pure cement. The dielectric constant of dry cement at this frequency is 2.1 and the loss tangent is 0.035. Thus, the conductivity is $g = 2\pi f\,\epsilon_r\,\epsilon_0 \tan\delta = 0.0123$ mhos/m, in which f is the frequency, in cycles per sec; ϵ_0 is the dielectric constant of free space ($= 10^{-9}/36\pi$ farads/m); and δ is the loss angle. Concrete will, of course, have values different from those obtained on pure cement; however, the values will probably be of the same order of magnitude. The change of dielectric constant and loss tangent as a function of curing time is shown in Figure C-8.

INSERTION LOSS OF CONCRETE AT RADIO FREQUENCIES

In a measurement of insertion loss of concrete (that is, of the ratio of signal absorbed or reflected to that transmitted), Cuming (27) found the insertion loss of concrete to be 2.5 db per in. at 8.6 gcps, and negligible at 3.0 gcps. This means that a wave transmitted through a 10-in. thick slab of concrete and reflected back again is attenuated 50 db if it is at a frequency of 8.6 gcps. At a frequency of 3.0 gcps there no doubt would also be some measurable attenuation over a total path length of 20 in.

The validity of the data presented for concrete and cement is borne out by comparison with measurements of various types of soil and water made at different frequencies. Table C-3 gives values of relative dielectric constant and loss tangent.

Another set of values is given for frequencies between 300 mcps and 3 gcps (Table C-4).

Although no firm conclusions can be drawn from such incomplete data, the numbers clearly show the variation of dielectric constant and conductivity with frequency, time, and type of material. The data for distilled, fresh, and sea water certainly indicate that the major factor influencing the change in dielectric constant and conductivity with time (Figs. C-7 and C-8) is the changing moisture content of the concrete.
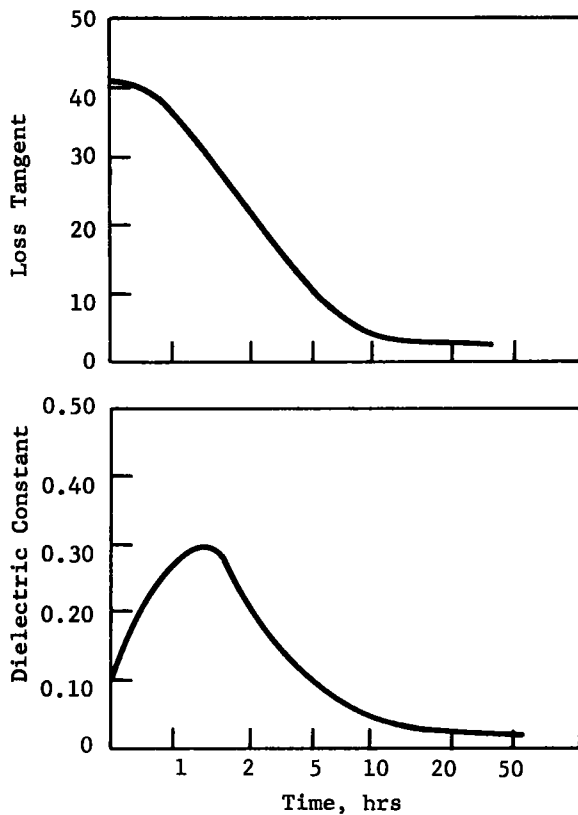
Figure C-8. Change of dielectric constant and loss tangent of portland cement concrete with curing time (from Ref. 26).

TABLE C-3

DIELECTRIC CONSTANTS AND LOSS TANGENTS OF SOIL AND WATER [a]

MATERIAL	DIELECTRIC CONSTANT AT			LOSS TANGENT AT		
	10^6 CPS	10^8 CPS	3×10^9 CPS	10^6 CPS	10^8 CPS	3×10^9 CPS
Soil, sandy dry	2.59	2.55	2.55	0.017	—	0.0062
Soil, loamy dry	2.53	2.48	2.44	0.018	—	0.0011
Water, distilled	78.20	78.00	76.70	0.040	0.005	0.1570

[a] From Ref. (28).

TABLE C-4

DIELECTRIC CONSTANTS AND CONDUCTIVITIES OF SOIL AND WATER BETWEEN 300 MCPS AND 3 GCPS [a]

MATERIAL	DIELECTRIC CONSTANT	CONDUCTIVITY (MHO/M)
Desert land	3	0.0111
Average land	15	0.0278
Fresh water	81	0.0050
Sea water	81	4.6400

[a] From Ref. (29).

Other Factors Influencing RF Thickness Measurements

One of the factors to be aware of in devising RF thickness-measuring techniques for concrete pavements is the measurement fluctuations that will be caused by differences in mixture proportions, and in size and type of gravel and sand used. These kinds of fluctuations will either have to be controlled or taken into account by properly normalizing or calibrating the measurements.

Because both the dielectric constant and the conductivity (and hence absorption) of portland cement concrete change with its moisture content, and because this factor is dependent on weather conditions, water content of the mix and roadbed, setting time, and other relevant factors, it seems likely that an accurate measurement of thickness by RF methods will have to incorporate a calibration technique that takes the moisture content of the concrete into account. Such a technique is certainly feasible to implement electrically if the moisture content is known, though it adds to the complexity of the instrumentation required. It should be pointed out that variability of electrical properties due to moisture content will be greatly reduced in the case of bituminous concrete pavements.

EFFECT OF REINFORCING STEEL

Another factor which might produce a problem in the RF thickness measurement is the presence of reinforcing steel mesh. Steel mesh would reflect much of the RF energy entering the concrete slab, thus greatly increasing the problems caused by spurious signals mentioned in connection with reflections from the surface. The difficulty is even greater because variations in the reinforcing mesh may cause greater variations in the measurements than the thickness variations to be detected. The reason for this is that the size of the loops formed by intersecting rods and the contact resistance at the intersections vary considerably from place to place. At any given point of intersection, the resistance between two rods can be any value between negligible and infinite. Rust and corrosion at the point of contact may also make the junction non-linear. The result of all these variables will be to cause significant changes in the measurements over even one section of a steel-reinforced concrete highway, independent of any thickness variations that may exist. Just how serious these difficulties are should be determined in future studies. It may be possible, for instance, to alleviate this problem by selecting a frequency or group of frequencies whose wavelength is small compared to the mesh diameter.

Direct RF Measurement of Pavement Thickness

A direct RF measurement of pavement thickness is dependent on the accurate determination of the pavement-base course interface. (Direct measurement is used here to describe any RF technique by which thickness is determined from a single measurement made at a given location, as opposed to comparative techniques discussed here.) Two factors must be considered in the development of this technique. One is the difference in dielectric constant between the pavement and base course; the other is the relative amounts of signal absorbed by the pavement material and reflected from its top surface.

Because the main constituents of the pavement, especially in the case of portland cement concrete, may also be the major ingredients of the base course, there may be little difference in their respective electrical properties. This is particularly true where a portland cement concrete pavement is placed on a cement-stabilized soil base. Without a well-defined interface (i.e., significant change in electrical properties), a direct RF measurement of thickness is not possible. However, this difficulty can be overcome by providing a discrete change in the electrical properties through the use of metal foils, metallized plastic films, or other forms of vapor barrier material. The sheet could be continuous or perforated without affecting its reflectivity significantly, providing the diameter of the perforations were small compared to the wavelength of the RF signal used. A certain amount of tearing of the sheet could even be tolerated, so long as the sheet remains in one piece without large gaps.

Another factor that must be considered is the relative absorption and reflection (from the top surface) of the pavement. The signal reflected from the top surface is, in a sense, a spurious or interfering signal which tends to mask the desired signal reflected from the pavement-base course interface. Of course, the greater the absorption in the pavement, the smaller the desired signal becomes. It is possible to circumvent this problem by designing the antenna impedance so that it is matched to the concrete. In other words, the antenna parameters can be chosen so that the reflection coefficient for the signal is zero for an infinitely long concrete slab. Reflection at the pavement-base course interface will then set up a standing wave in the antenna feed line whose magnitude is a direct measure of the distance of this interface from the antenna.

There are a number of difficulties evident in the direct techniques. In need of further investigation are the dielectric constants of both portland cement concrete and bituminous concrete and their variability as a function of external factors. Other factors to be resolved are differences in concrete from batch to batch, the degree of RF discontinuity between the concrete and base course, the desirability of a metallized reflecting layer beneath the concrete, and the effect of steel reinforcement within concrete. The problems of direct RF measurements will no doubt be greatest for reinforced concrete, so that a somewhat different approach may prove more fruitful in this case.

Comparison-Type RF Thickness Measurements

Another method for making RF measurements involves a comparison technique whereby two measurements—one of the concrete pavement surface and one of a reference surface level with the roadbed—are made. A simultaneous comparison of reflections received from these two surfaces can give an accurate measure of the distance between the two reflecting surfaces and, hence, the pavement thickness. This technique, which utilizes the reflection of RF energy from a dielectric or the interface between two dielectrics is similar to a method discussed by Cohn and Ebstein (*30*). Their method used microwave signals (10 and 30 gcps) reflected from a plane surface to measure the distance of the radiating element (a waveguide or dielectric antenna) from a plane surface. The potential accuracy of this method, using wood as the reflecting surface, is better than 0.001 in. at a frequency of 10 gcps. The dielectric constant of wood is lower than that implied (by the data given here) for concrete at these frequencies, which indicates that somewhat better results may be expected from concrete. Figure C-9 shows one of the quantities, magnitude of the reflection coefficient, which is easily measured using waveguide circuit components, to determine waveguide antenna to plane (wood) surface distances.

In general, the accuracy obtainable with such techniques is a function of the frequency of the signal, with accuracy decreasing as frequency decreases. Therefore, the frequency should be such that the wavelength is comparable to or smaller than the distance to be measured. On the other hand, if the wavelength is much smaller than the distance in question, an ambiguity in measurement could result, because two distances differing by an integral number of wavelengths will give the same indication; the quantities being detected are amplitude and phase of a standing wave or reflection coefficient. Hence, the frequency should be of the order of the pavement thicknesses expected. A pavement thickness of 10 in. would correspond to one wavelength at a frequency of 1.2 gcps. At frequencies in this range, the energy can be formed into beams with cross-sectional areas of 1 sq ft or more, which is desirable to average out small-scale variations, which are not of primary interest. This frequency range should be taken as a starting point only, inasmuch as further investigations and experimental results may dictate either higher or lower frequencies. Circuit components in this frequency range (*L*-band) and higher are commercially available and would pose no special equipment problem. Signals in this frequency range and higher are generally transmitted through waveguides, which lend themselves readily to the types of measurements required here.

The comparative technique lends itself well to measurements of pavement thickness both during construction and after curing. Figure C-10 shows a possible arrangement of the horn antennas so that one illuminates the newly laid pavement while the second illuminates the unpaved roadbed. The method is attractive because the surface reflections obtained are large compared to potential interfering signals, due to the wet condition of both the
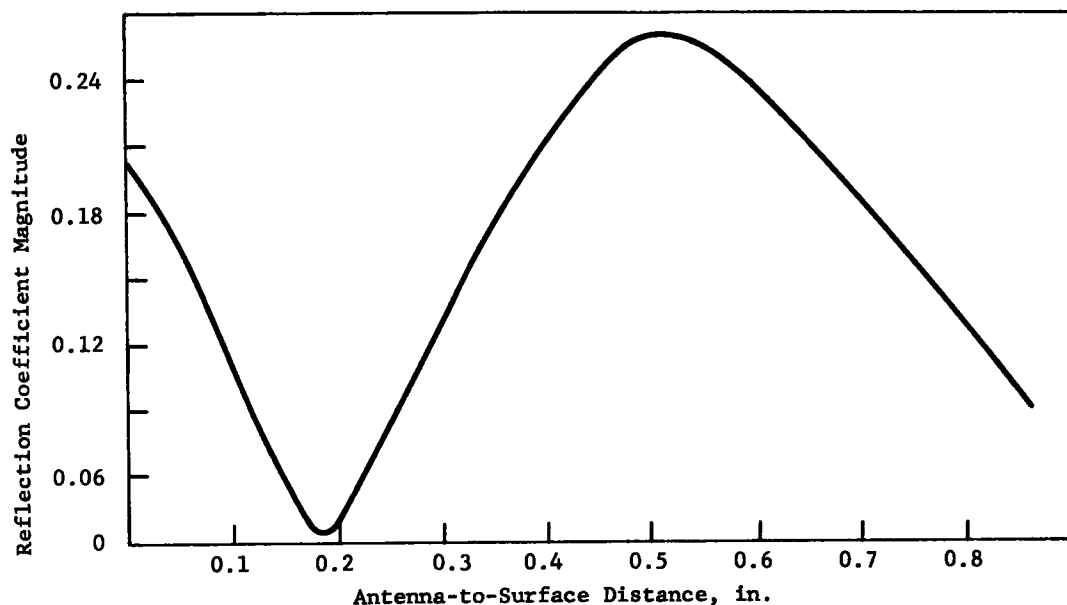
Figure C-9. Reflection coefficient magnitude vs distance from reflecting surface at a frequency of 10 gcps (from Ref. 30).

concrete and the roadbed. Another feature of this technique is that it could give an operator an indication of when the concrete being poured was thick enough. Thus, a continuous measure would be available to insure proper pavement thickness at essentially every point.

In the case of completed pavements, comparative measurements might be obtained by using the road base at the edge or shoulder of the pavement as a reference plane instead of the roadbed just ahead of newly poured concrete. This method is, of course, dependent on whether the shoulder can be taken as a suitable reference plane. This technique also could give essentially complete measurements over the entire concrete surface. In addition, the comparison technique, because it utilizes surface reflection, is more promising for steel-reinforced concrete than is the direct measurement technique.

FURTHER INVESTIGATIONS OF ELECTRICAL TECHNIQUES

At this stage investigations of electrical techniques had shown that reliable thickness measurements could be

Figure C-10. Antenna configuration for radio frequency comparison thickness measurement.

made only if a metal foil could first be placed under the pavement. Even then, thickness measurements could only be made in the absence of any reinforcing steel mesh with existing methods. Further experiments were then planned to evaluate the effect of tears and discontinuities caused to the metal foil when the concrete is initially laid and to test further methods for obviating the difficulties associated with the reinforcing mesh.

These further investigations showed that foil discontinuities do not introduce appreciable error in pavement thickness measurements. The error introduced through the presence of reinforcing steel rods and/or mesh was not so easily overcome. It was found that the effect of reinforcing members could be significantly reduced through the specific placement of two coils and by the proper combination of their inductances.

Several measurement techniques were developed and evaluated on full-scale laboratory models of a length of pavement. An independent- (or single-) coil technique, suitable for spot measurements was shown to have an accuracy of better than 0.5 in. for a 10-in. thick pavement. This parallel-coil technique provided somewhat higher accuracy, but it could not be used for spot measurements because the resultant thickness indication depended on "averaging" over a length of pavement.

The dimensions of the foil and coils to be used were optimized for the different measuring techniques. In general, for a specific foil-to-coil distance the larger the coil, the more sensitive the measurement. The independent-coil technique required two concentric coils of different diameters; for example, 18 and 24 in. The parallel-coil technique required two separated coils of the same diameter; for example, 24 in. coils separated 48 in. on centers. For this latter technique, foil strips of the same width as the
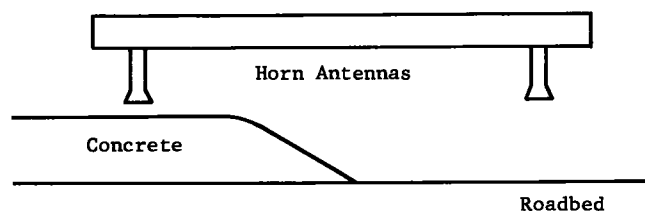
coil separation are laid across the highway. The coils are mounted in a longitudinal line and moved down a normal traffic lane of the pavement.

Considerations of cost, availability, and conductivity indicate that aluminum foil be used rather than copper, steel, or any other metal foil. Experiments have shown that 0.001-in. (1 mil) foil is the thinnest that can be used without appreciable loss of sensitivity. The cost of the foil and its placement for the averaging technique should be about $450 per lane-mile. The technique can be used on any pavement structure which is transparent to electromagnetic waves; i.e., bituminous and portland cement concretes in both their aged and plastic states.

Scaling of Dimensions

To facilitate matters, some of the experiments were performed with coils much smaller than those which will be used for actual thickness measurements. However, the data can easily be applied to larger coils by normalizing the variables, because the coil and foil variables are expressed as a function of the relevant coil or foil parameter; i.e., as new normalized parameters.

The most important variables are the inductance change (caused by the presence of foil), ΔL, and the foil-to-coil distance, X_F. To normalize these variables, the inductance change is divided by the inductance (in the absence of foil), or $\Delta L / L \infty$; and the foil-to-coil distance is divided by the coil diameter, or X_F / D. Other linear dimensions can also be normalized with the diameter, D. For instance, normalized variables were used to find the inductance change of a large coil at a given X_F from the known X_F versus ΔL relationship of a smaller coil.

Finite Foil Approximation of an Infinite Sheet

For the inductance change of a coil to be a measure of the foil-to-coil distance, the inductance change should be only a function of the distance. When the electrical parameters of the foil are constant, the inductance change will be only a function of the foil-to-coil distance if the metal foil is so large that it has the same effect on the coil as an infinite foil sheet. Otherwise, edge effects are present and the inductance change is a function of the size of the foil sheet and the lateral position of the coil. For one of the measurement procedures, the coil was moving. It is necessary that when the coil is directly over a foil section movements of a few inches should not cause inductance changes except as they are a function of the foil-to-coil distance.

The experiment reported in this subsection was performed to determine the foil sheet dimensions that would approximate an infinite sheet for a centered coil. Constant inductance for lateral coil movements would require proportionally larger foil sheets.

A 3.5-in. diameter coil was placed one diameter from 1-mil aluminum foil squares of variable size. Figure C-11 gives the change in inductance caused by the different sizes of foil squares. A 16- by 16-in. square causes the same change in inductance as an infinite sheet and

thus yields a square edge to coil diameter ratio, l/D, of 4.5. Comparison of these results with other experiments indicates that the size of the foil sheet needed to approximate an infinite sheet is proportional to X_F and must subtend some relatively constant solid angle viewed from the center of the coil. For example, when $D = 2X_F$, $l/D = 2$ is required.

A General Radio type 1605A impedance comparator was used to measure the inductance change for all the experiments. Although the GR comparator measures impedance rather than inductance, instrument readings were considered to be inductance because the coil impedance has an extremely small resistive component. The measurement coil was connected to one set of terminals; a standard impedance, which included a trimmer capacitor, was connected to the other. The inductance of the measurement coil in the absence of any foil was usually matched to the standard impedance by varying the trimmer capacitor. The change in inductance, $\Delta L / \Delta \infty$, when the coil was placed near the foil, was read directly on the comparator.

Foil Discontinuities

Tears, holes, and other discontinuities in the metal foil can cause errors in the thickness measurements. When the foil is placed on the ground, there is the possibility of it being torn by workers' feet or by sharp-edged metal braces. The foil can be reinforced by attaching a paper backing to it, although tears can still occur. Experiments were performed with simulated foil discontinuities to determine the error that they can cause.

The experimental setup is shown in Figure C-12. A 3.5-in. diameter coil was placed one diameter from the foil. The experiment was performed first with the tear at the center of the coil and then at the edge of the coil. The size of the tear was varied and the inductance change recorded (Fig. C-13). A tear of a given size located at the edge of the coil caused a larger impedance change than one located on the coil axis. A 5-in. tear at the edge caused an error equivalent to a 0.625-in. thickness variation. Tears can also be normalized with the coil diameter. Normalized data indicate that a tear at the edge and one coil diameter from a 10-in. coil must be 15 in. long to cause a measurement error of about 2 percent (0.1875 in.). Similarly, a 5-in. tear would yield a measurement error of less than 1 percent. Thus, it appears that any reasonably small tear will only cause a tolerable measurement error.

The "tear tests" were performed under the assumption that the torn foil remains in the plane of the foil sheet. This is reasonable, because the pavement material will press any nonplane foil onto the pavement base. It does, however, raise the question of how large a piece of foil can be missing without affecting the thickness measurement.

Tests were conducted in which circles of varying diameter were missing from the foil, as shown in Figure C-14. This experiment used a 3.5-in. diameter coil located 3.5 in. from the foil. The missing circle of foil was located at different radial distances, l, from the center of the coil. The inductance change from that of an infinite plane was
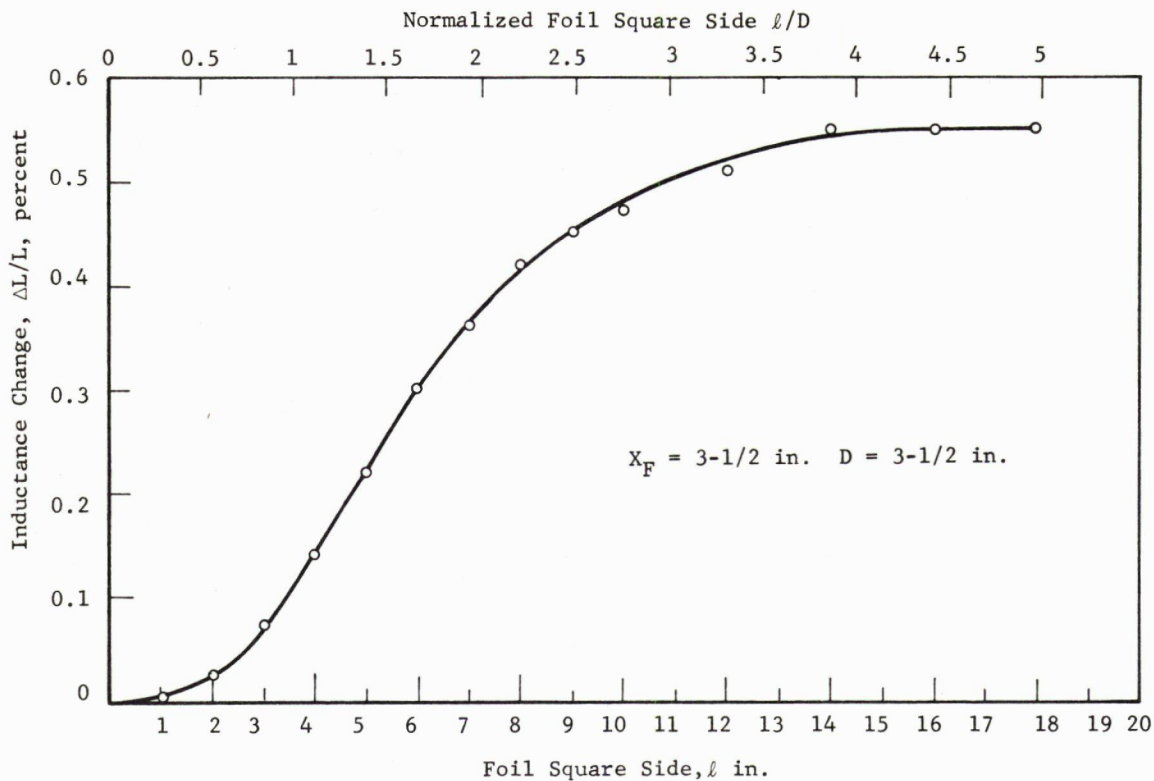
Normalized Foil Square Side ℓ/D

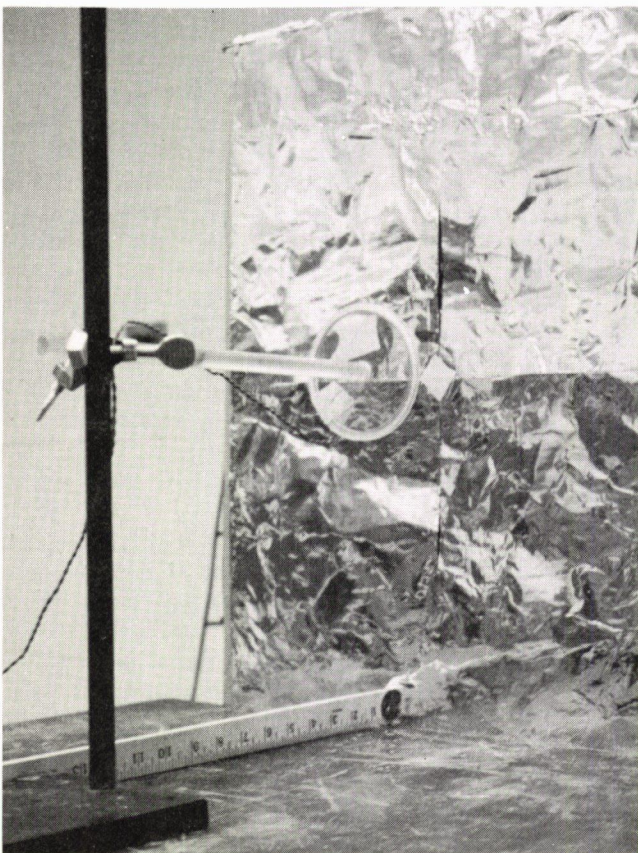*Figure C-11. Finite approximation of an infinite foil sheet.*

Figure C-12. Measurement setup for simulated foil tear effects.

recorded. The largest change occurred with the center of the circle opposite the edge of the coil. Normalizing these data indicates that a 10-in. coil would give a maximum error of 0.1875 in. for a 6-in. missing foil circle.

The final test in this series involved replacing an infinite sheet of foil by two overlapping sheets, as in Figure C-15. An 18-in. by 24-in. sheet was placed 3.5 in. from a 3.5-in. diameter coil and the inductance noted. The single sheet was then replaced by two sheets that overlapped opposite the center of the coil, but were insulated from each other at the overlap. The inductance change was not large enough to cause a significant measurement error. Thus, in general, these tests indicate that a tear or other anomaly in the foil will not cause appreciable errors in thickness measurements.

Independent-Coil Technique

The independent-coil technique is especially suitable for spot measurements. It depends on the nonlinear relationship between the inductance change and the metal distance to remove the effect of the mesh. Foil is placed under the pavement where the measurements are to be made, and the inductance changes that occur when each of two coils is placed at the same spot are a measure of the pavement thickness. The theory of this technique is explained in the following.

As a sheet of foil approaches a coil, the inductance decreases nonlinearly with the coil-to-foil distance, X_F. A normalized curve of the inductance change as a func-
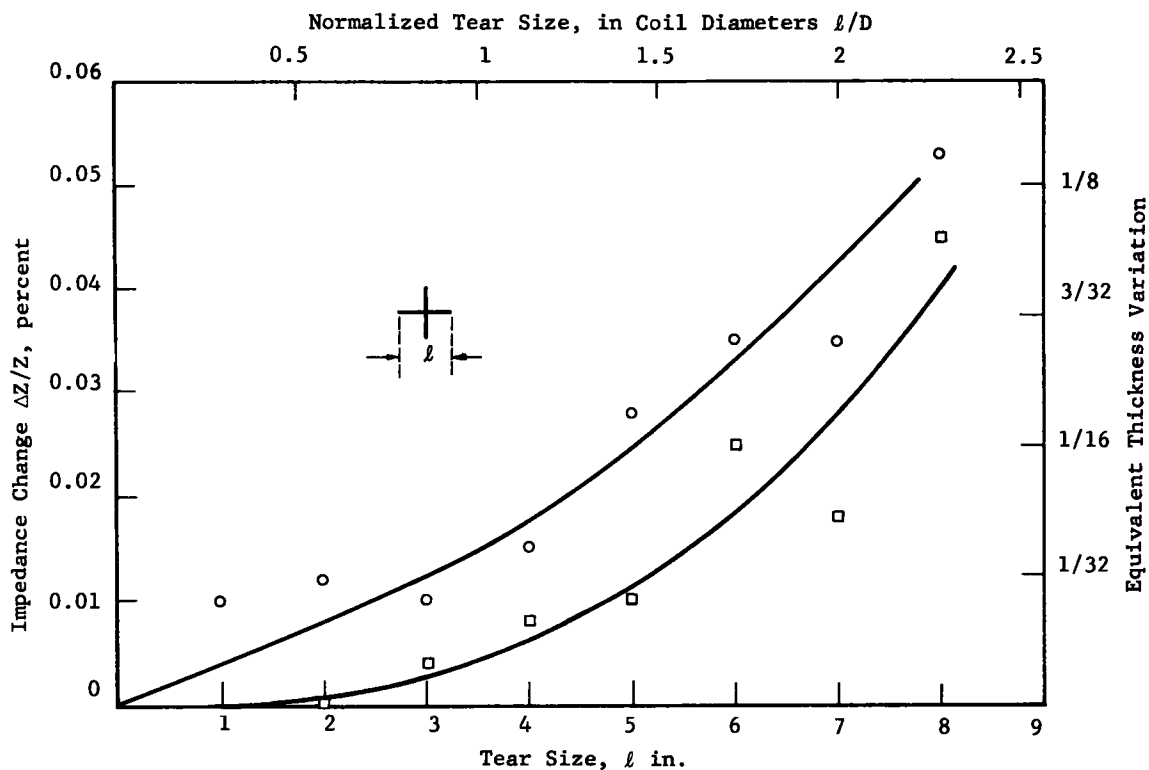
Figure C-13. Simulation of a tear.

tion of X_F is given in Figure C-16. The inductance is also a function of the coil diameter, D. Another variable is introduced when steel reinforcement mesh is placed between the coil and the foil, as in Figure C-17. This is the coil-to-mesh distance, X_M. The variables can be expressed in the functional form

$$\frac{\Delta L}{L} = f\left(\frac{X_F}{D}, \frac{X_M}{D}\right) \qquad (C-23)$$

or as the set of curves in Figure C-18. (In this discussion the coil position with respect to the grid of the mesh is considered as constant. The actual inductance variations that lateral coil movements cause are discussed in the paragraphs on experimental results.)

Inasmuch as variations of either X_F or X_M will cause a change in $\Delta L/L$, the source of inductance variation in only one coil cannot be detected. With two coils of different diameters, D_1 and D_2, the source of variation can
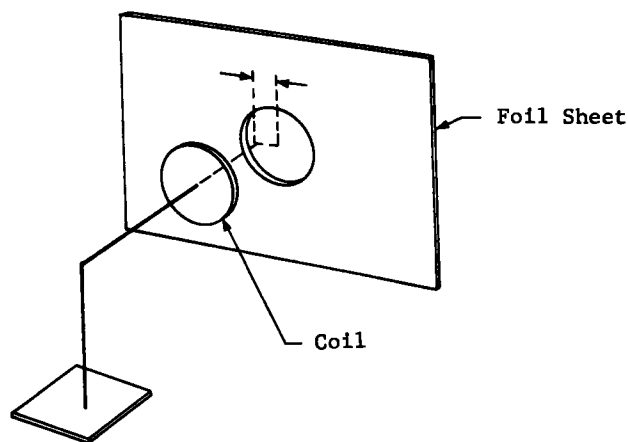
Figure C-14. Missing circle of foil.
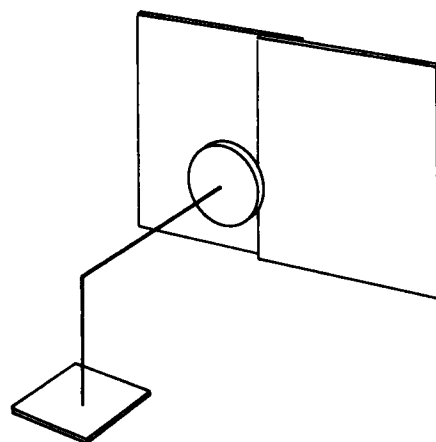
Figure C-15. Foil overlap.
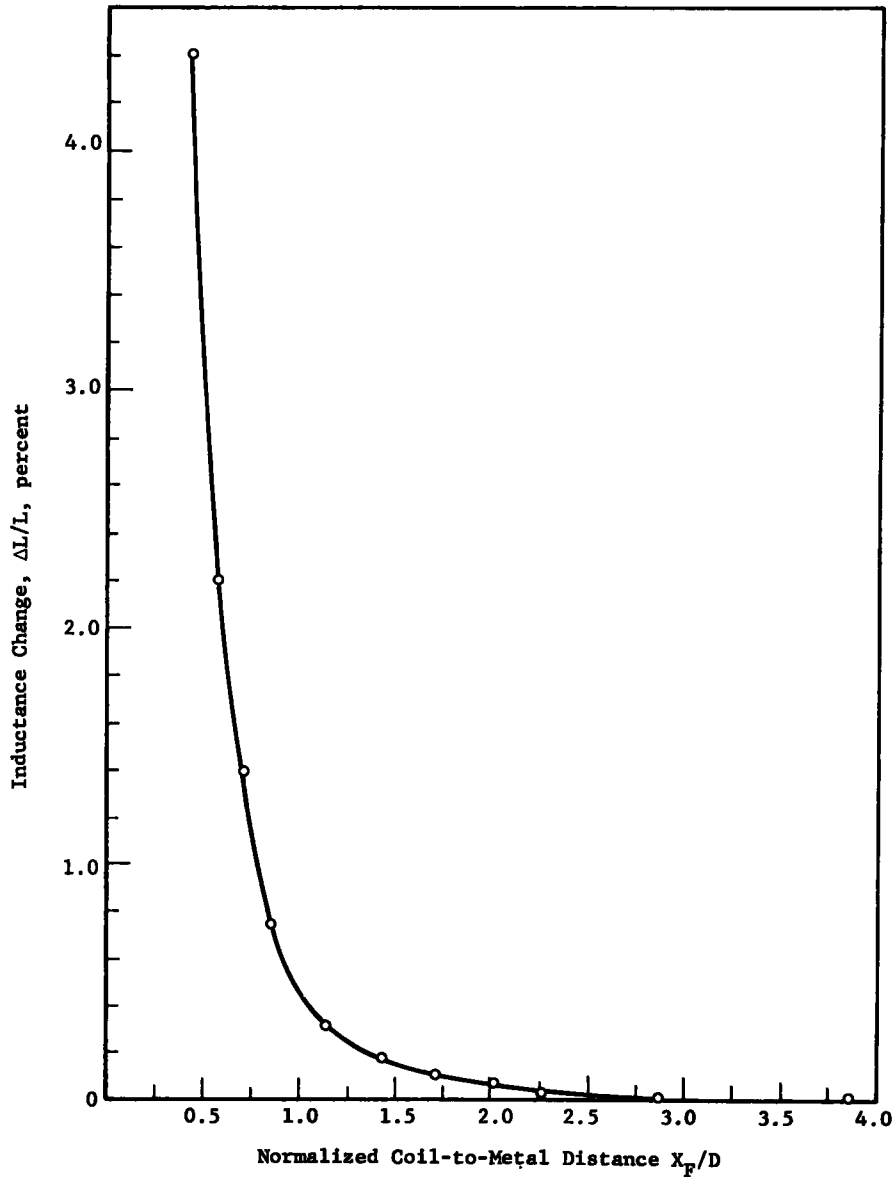
Figure C-16. Inductance change in the presence of a metal sheet.

be isolated, because the coils have different inductance changes, $\Delta L_1/L_1$ and $\Delta L_2/L_2$, and produce independent sets of curves like those in Figures C-18 and C-19. For any value of $X_F = X_{FS}$ and $X_M = X_{MS}$, the coils will have inductance changes $(\Delta L_1/L_1)_S$ and $(\Delta L_2/L_2)_S$. These values are indicated in Figures C-18, C-19, and C-20. By combining the data of Figures C-19 and C-20, $\Delta L_1/L_1$ and $\Delta L_2/L_2$ can be plotted with X_M and X_F as parameters, as shown by Figure C-21, in which the more vertical family of curves is for constant values of X_F, while the other is for constant values of X_M.

Figure C-21 shows why two coils are necessary. For any one inductance change, such as $\Delta L/L = (\Delta L_1/L_1)_S$, there are an infinite number of values of X_F and X_M. However, if one value of change is taken from each of two coils of different diameters, a point is determined in the plane; for example, X_{FS} and X_{MS}. Thus, each pair of values X_F and X_M is uniquely determined by a pair of values $\Delta L_1/L_1$ and $\Delta L_2/L_2$.

In terms of functional relations, two coils give two independent equations involving two unknowns, X_F and X_M. Proper combination of the two equations will remove X_M as a variable and give an expression for X_F in the form

$$X_F = f\left(\frac{\Delta L_1}{L_1}, \frac{\Delta L_2}{L_2}\right) \qquad (C-24)$$

Thus, by measuring the inductance change of two coils, is should be possible to determine X_F. (In actual use this measurement technique would not involve calculations, but might necessitate the use of tables or graphs.)
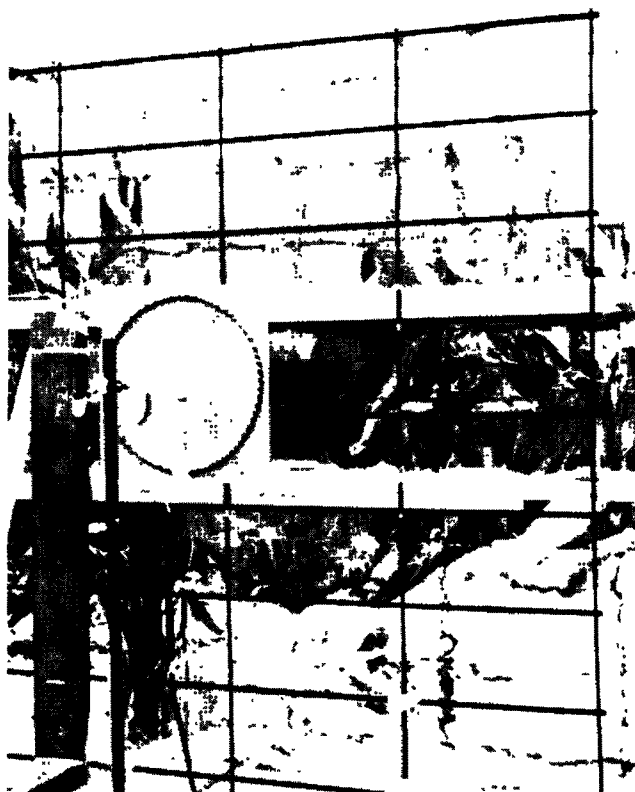
Figure C-17. Test setup for independent-coil technique experiments.

Foil Distance in Coil Diameters, X_F/D

Figure C-18. Inductance change in the presence of foil and mesh.

Experiments were conducted to test this theory. The experimental arrangement is shown in Figure C-17. Data taken for a 10-in. and an 18-in. diameter coil are plotted in Figure C-22 similar to Figure C-21. The inductance changes were measured at $X_F = 10$ and $X_M = 5$. The
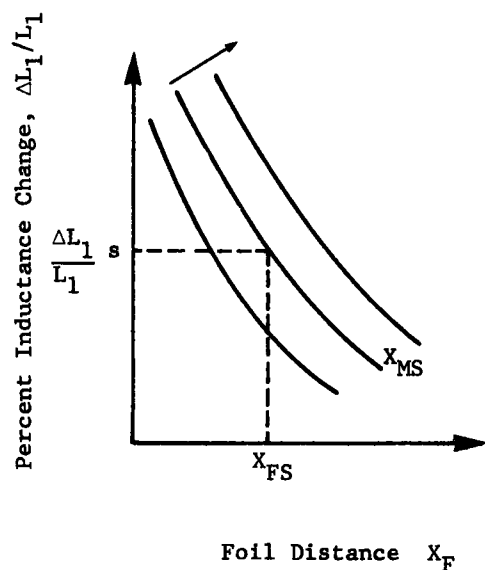
more vertical gradients are for the constant foil depth, X_F, and the others are for the constant mesh depth, X_M. Variations of X_F of 0.5 in. were detectable. There were also inductance variations for lateral variations in the coil placement with respect to the mesh grid; i.e., the mesh had a variable effect that depended on the lateral position of the coil with respect to the mesh grid. For the 10-in. coil the inductance variations were 0.3 percent in the horizontal (longitudinal) direction and 0.02 percent in the vertical (transverse) direction. The larger horizontal inductance variation correlated with the larger horizontal wire spacing.

The accuracy with which X_F can be determined, assum-

Foil Distance X_F

Figure C-19. Inductance change for coil 1.

Foil Distance, X_F
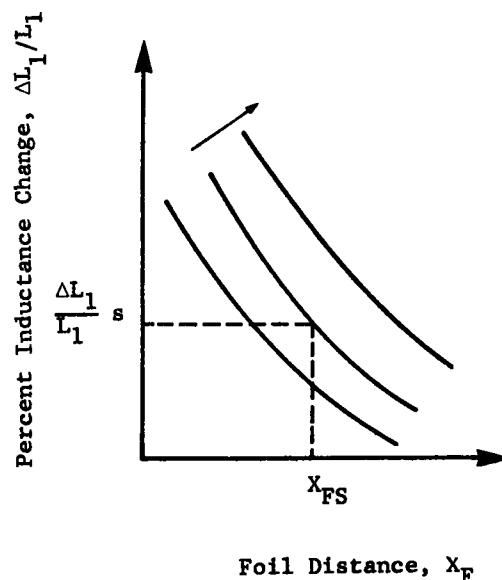
Figure C-20. Inductance change for coil 2.

72
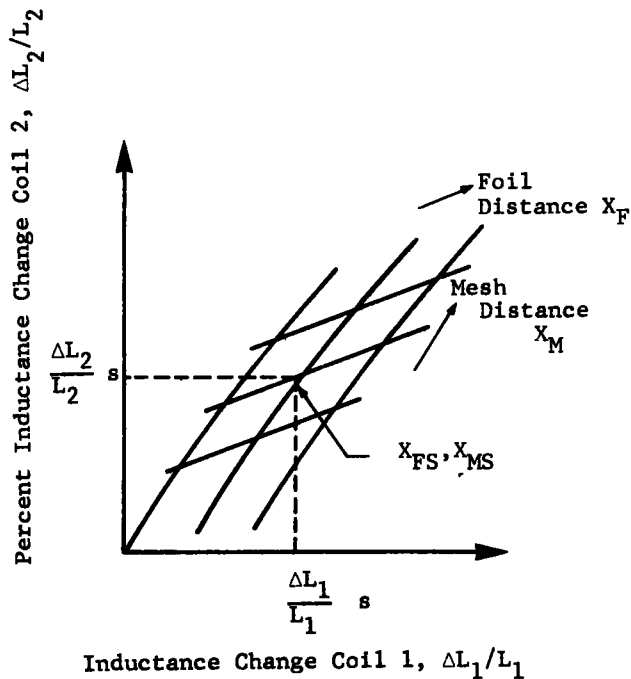
Figure C-21. Parallel-coil technique determination of X_F.

Figure C-22. Parallel-coil technique data.

ing that the coil position with respect to the mesh grid is known, is limited by the accuracy of the inductance change measurements. If a 0.01 percent inductance change can be detected (the limit of the GR comparator), variations of X_F of 0.5 in. should be detectable.

Magnetic Cancellation Technique

An attempt was made to reduce the effect of the mesh on a coil inductance by using the ferromagnetic properties of the steel mesh, which might be expected to increase coil inductance. Opposing this increase is the eddy current effect, which decreases coil inductance. The eddy currents can be increased (inductance decreased) by increasing the coil excitation frequency. Both the eddy current and the ferromagnetic effects are reduced as the mesh is moved away from the coil. In many cases involving ferromagnetic materials the inductance change varies as a function of the coil-to-metal distance, X, similar to Figure C-23, where X_A is a function of the coil excitation frequency and the coil-to-metal distance. At this point the inductance is the same as when the ferromagnetic material is not present, because the two effects have canceled each other. For $x < X_A$ the ferromagnetic effects are dominant, but for $x > X_A$ the eddy current effects are dominant.

Experiments were performed to discover whether X_A exists for the mesh. Frequencies in the range of 1 to 500 kc were tested; 10- and 18-in. diameter coils did not exhibit dominant magnetic effects for any frequency or for any distance from the mesh. However, a 3.5-in. diameter coil had an X_1 of 0.5 in. or smaller in the

frequency range of 50 to 100 kc. The axes of the coils were always located at the intersection of the mesh wires. The absence of significant magnetic effects is probably due to the small thickness of steel in the direction of the coil axis.

Parallel-Coil Technique

The parallel-coil technique can determine the average thickness for a length of pavement, but it cannot be used
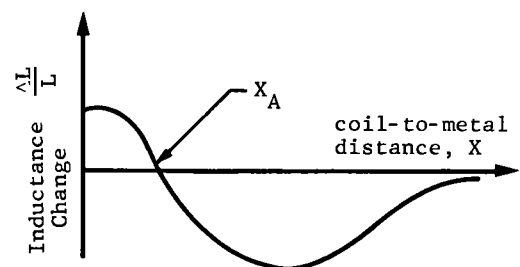

Figure C-23. Inductance change as a function of coil-to-metal separation.

for spot measurements. Similar to the independent-coil technique, it uses two coils, but of the same diameter. The coils are moved steadily along the pavement. The significant data are the percent of inductance difference of the two coils,

$$\% \Delta L = \frac{L_1 - L_2}{L_1} \times 100 \qquad (C-25)$$

The coils are arranged one behind the other along the length of the highway, as in Figure C-24. If there is no foil under the pavement, and because both coils are always over the mesh, the inductance difference will always be zero. This, however, ignores mesh irregularities. In the actual situation, foil strips placed under the pavement across the width of the highway are the cause of the inductance differences. If one coil is over the mesh and a large foil plane, while the other coil is only over mesh, the percent ΔL will be a function of the foil depth; i.e., the pavement thickness. If the coils are moved along the highway, the percent ΔL will vary in a cyclic fashion, as in Figure C-25, with the peaks occurring whenever one coil is over an "infinite" sheet.

Pavement thickness, then, is a function of the peak-to-peak value of the percent ΔL. Because of irregularities in the mesh and foil, it is necessary to average the peak-to-peak values for about 10 foil cycles. The result is a value which is a measure of the average thickness of a length of pavement. The percent ΔL is also a function of inter-related coil and foil parameters. The relationships between the parameters of the foil, mesh, and coils are used to determine the dimensions of the coils and foil which must be used for the percent inductance difference to indicate the actual pavement thickness.

The width of the foil strips must be within certain limits. The maximum width of the aluminum foil is that which is commercially available, 63 in. The minimum width of the foil is at least twice the diameter of the coils, so that it appears to a coil as an infinite sheet for longitudinal movements of a few inches. If there are no mesh or foil irregularities, the percent ΔL is a constant maximum for those few inches of movement, as shown in Figure C-25. Because the irregularities are present, the percent ΔL is irregular, and the specification of the maximum can be difficult. Inasmuch as ideally the maximum percent ΔL is a constant over a short distance, this value can be approximated by smoothing the irregularities. To provide a symmetrical inductance difference signal with respect to the zero percent ΔL line, the space between the foil strips is the same width as the foil strips.

Foil thickness is another variable that affects the inductance change of the coils. All the experiments in this study were performed, for convenience, with ordinary household aluminum foil, which is 1 mil thick. Samples of other foil thicknesses were obtained and their inductance change was compared with that of 1-mil foil. The different thicknesses of foil were placed 1 in. (approximately 0.667
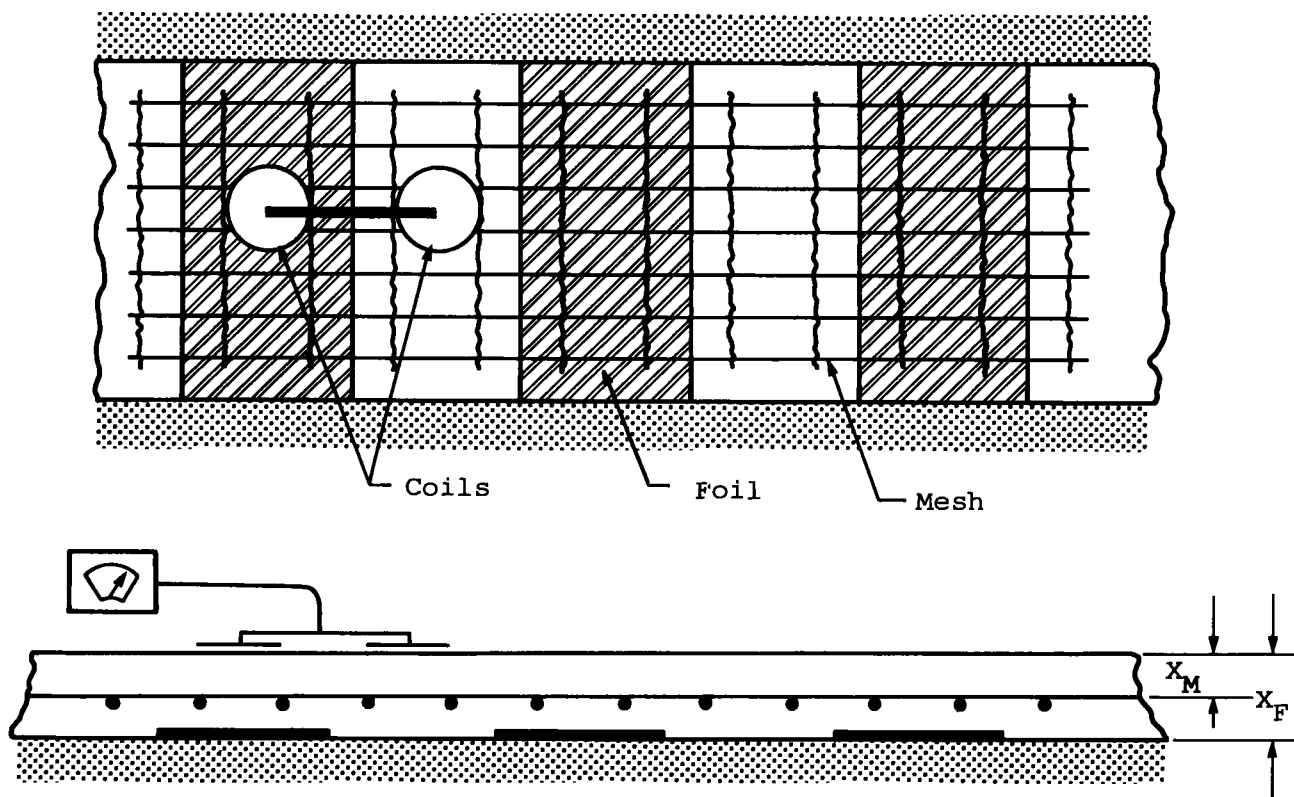

Coils   Foil   Mesh

Figure C-24. Placement of foil under pavement.

of a diameter) from a 1.625-in. diameter coil. Percent of inductance change for each foil thickness is given in Figure C-26.

To reduce costs, the foil thickness should be a minimum. There are two factors to be considered in choosing the minimum usable thickness: the total percent of inductance change that the foil produces and the sensitivity of the inductance change between 2 and 1 mil and between 1 and 0.5 mil is small, less than 7 percent. However, there is a large decrease between 0.5 and 0.25 mil. The thickness of commercial foil is produced with a tolerance of ± 10 percent. Thus, local variations of 0.5-mil foil can produce — 0.03 and + 0.01 percent inductance change variations. The local thickness variations of 1-mil foil can produce — 0.01 and + 0.002 percent inductance change variations. It is hoped that the parallel coil technique will accurately detect pavement thickness variations of 0.25 in., the equivalent of an inductance variation of 0.05 percent. Therefore, 1-mil foil should be used under the pavement.

The coil parameters are as important as the foil parameters. An increase in the diameter of a coil increases the sensitivity of the coil inductance to coil-to-metal distance variations. Because sensitivity should be maximized, the coil diameter should be as large as possible. However, the diameter of the coils must be less than one-half the width of the foil strips so that the coils "see" an "infinite" sheet.

Another limit on the maximum coil size is that it be manageable. The spacing between the coil centers must be an integral multiple of the transverse wire spacing of the mesh so that both coils will always be over similar points with respect to the mesh grid pattern. For the percent ΔL signal to be symmetrical about the zero percent ΔL line, the coil centers must be spaced the same as the foil strip width. For a 6-in. by 12-in. grid mesh (12 in. longitudinally), a possible set of dimensions for the foil and coils is: foil strip and spacing width, 48 in.; coil diameter, 24 in.; foil thickness, 0.001 in.; coil spacing, 48 in.

To verify the preceding ideas, the full-scale model of a reinforced concrete pavement shown in Figure C-27 was used for experimentation. The model was composed of two 36-in. wide foil strips 36 in. apart, a 6-ft by 12-ft piece of 6-in. by 12-in. reinforcement mesh, and two 18-in. coils whose centers were 36 in. apart. The foil strips were taped vertically on a wall. The two coils were attached to a horizontal wooden bar and oriented parallel to the mesh. It was not necessary to use concrete in the model because both portland cement and bituminous materials are transparent to the magnetic field that produces the eddy currents. As before, the General Radio impedance comparator was used for inductance measurements. The coils were connected to it so that the output meter read the percent ΔL. A trimmer capacitor in series with one of the coils was used to equalize the coil impedance in the absence of the mesh and the foil.

The coils were moved horizontally, analogous to their movement along a pavement, and percent ΔL values were recorded every 2 in. for a distance of 5 ft. Figure C-28 shows the results for the following combinations of foil
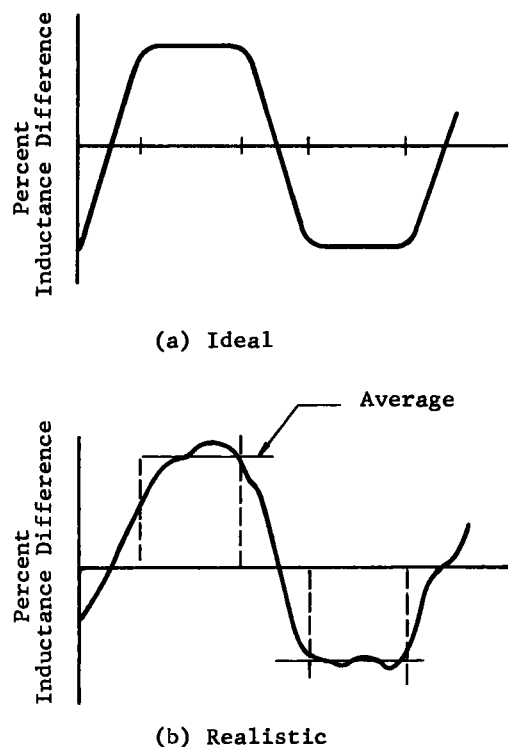

(a) Ideal

(b) Realistic

Figure C-25. Inductance variations along pavement.

and mesh distances: (a) the foil at $X_F = 9$ in. and no mesh present; (b) the mesh at $X_M = 4.5$ in. and no foil present; and (c) with the foil at $X_F = 8.5$, 9, 9.5 in. with the mesh at $X_M = 4.5$ in. Neither the mesh nor foil were perfectly flat or parallel to the coils. These irregularities were intentionally retained so as to better approximate the irregularities in an actual highway. If the foil and mesh were always parallel at the same X_M and X_F and contained no other irregularities, the percent ΔL curve for any combination of X_M and X_F would be similar to Figure C-25a. However, the foil and mesh curve in Figure C-28 shows many irregularities, most of which can be traced to the "foil only" or "mesh only" curves as mentioned in (a) and (b). The cusp at point A and the double hump at C appear in the mesh only curve, whereas the peak at B appears in the foil only curve. The rise in the mesh only curve between 20 and 30 in. imitates the curvature of the mesh. Variations of the foil-to-coil distance by 0.5 in. for a constant mesh-to-coil distance, gave peak-to-peak percent ΔL variations of at least 0.2.

For the parallel-coil technique, the peak inductance difference between the two coils is a function of the foil-to-coil distance, X_F, the average mesh-to-coil distance beneath the coils, $\overline{X}_M$, and the variations of the mesh-to-coil distance between the coils, dX_M/dl. Variations of average mesh distances, $\overline{X}_M$, do not have significant effects on the inductance measurements; i.e., if the mesh is parallel to the coils, variations of X_M of 1.5 in. have no detectable effect. The mesh is, of course, never perfectly parallel to the coils

and its depth may vary a couple of inches over a few feet. If the mesh is a different distance from each coil or is not parallel to the two coils, variations of its average distance can cause percent ΔL changes of the same amount as similar variations of the foil distance. For example, differential changes in mesh distance of 0.5 in. have caused inductance difference changes of 0.1, similar to foil distance variations of 0.5 in.

There is no reason to expect that variations in X_M will occur with any repetitive frequency. Thus, averaging a small number of foil cycles (approximately 10) should substantially reduce the dependence of the inductance changes on the mesh. Averaging also will reduce the effects of irregularities in the steel mesh and of steel mesh supporting rods on the foil depth measurement. Measurement accuracy will increase with the number of cycles averaged; however, the smaller the number of cycles averaged, the more localized is the measurement. The length of pavement included in one average can also be reduced by taking readings along different transverse locations instead of only at one as has been implied. Averaging at different transverse points has an additional advantage in that it will represent a two-dimensional area rather than one longitudinal line. The exact accuracy of this technique still must be determined; however, an accuracy of 0.25 in. at 10 in. may be possible.

General Feasibility Considerations

This report has only considered a cured concrete pavement, reinforced with 6-in. by 12-in. mesh. The measurement
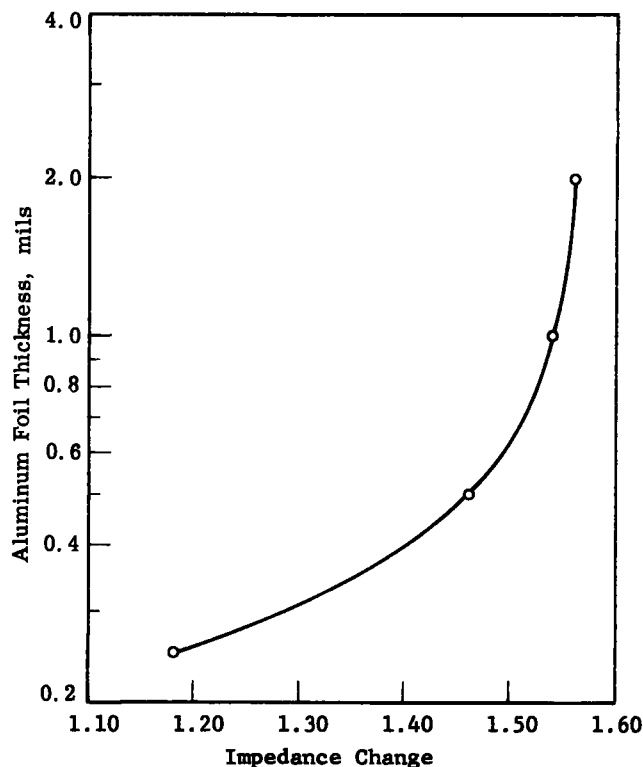
Figure C-26. Effect of foil thickness on inductance.
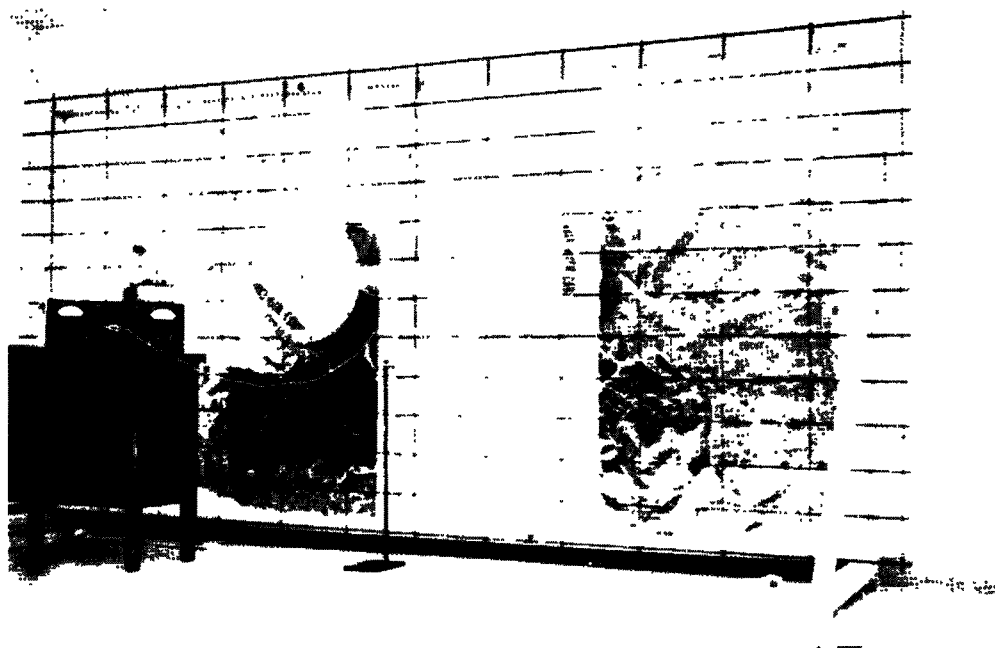
Figure C-27. Experimental setup for parallel-coil tests.
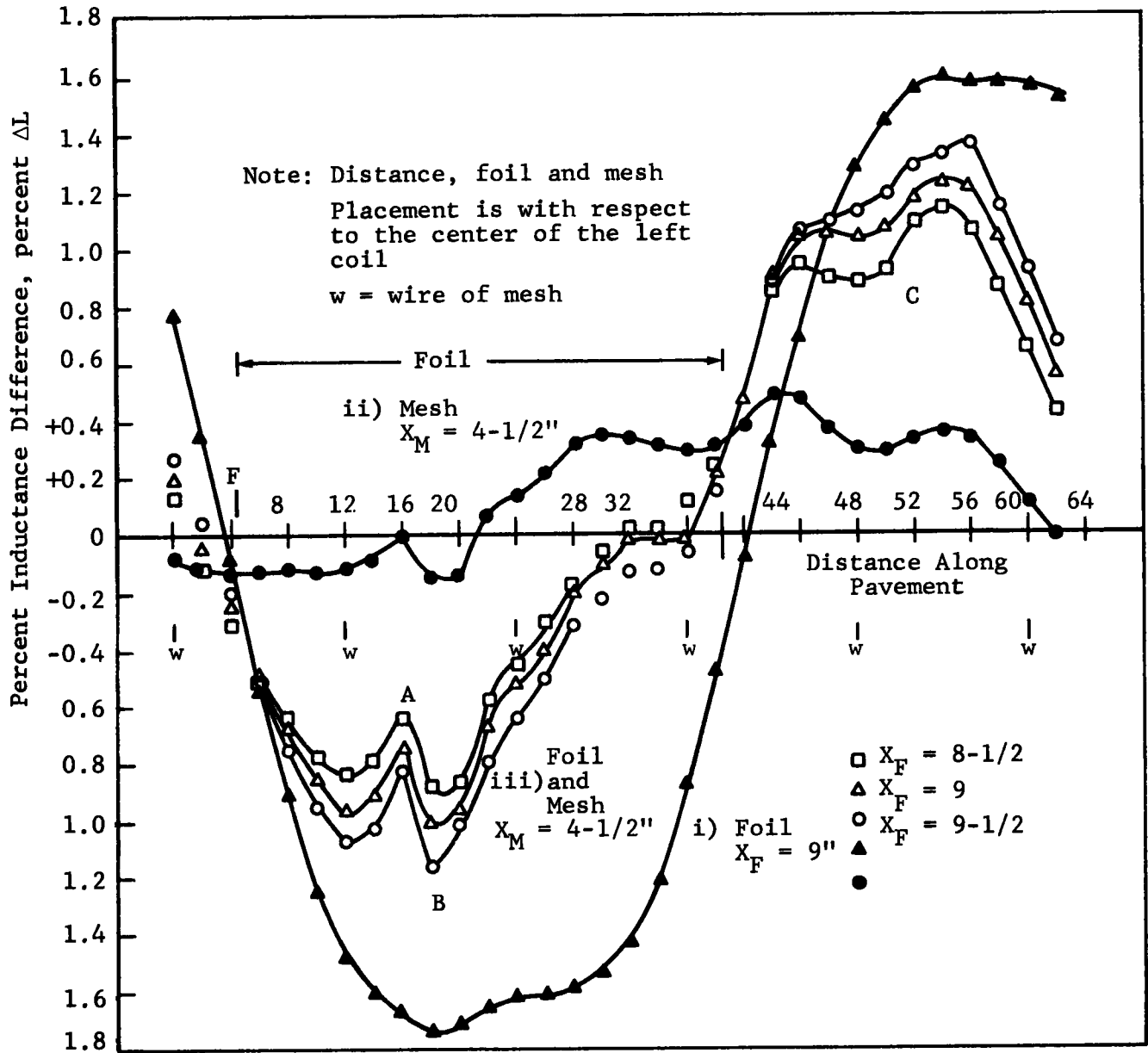
Figure C-28. Parallel-coil technique data.

techniques that were described earlier can be used just as accurately for pavements built with different materials.

For the parallel-coil technique, other grid sizes will require the use of different foil widths and coil spacings, but will not affect the accuracy of the measurements. Grid size, hopefully, will not affect the independent-coils technique. However, this should be experimentally verified.

Continuous bars, rather than mesh reinforcement, should allow more accurate measurements because the longitudinal and transverse bars are not welded at their intersections. Therefore, it should be more difficult for eddy currents to form. As a result, inductance measurements should be less sensitive to variations of $X_{1/}$. In addition, there should be smaller changes of inductance, because the variation of $X_{1/}$ is less for continuous reinforcement than for mesh.

Often, the mesh is simply placed on top of one layer of concrete with another layer poured over. For continuous reinforcement the transverse bars are constructed with steel legs, so that the bars are a predetermined height above the base. The longitudinal bars are also at a nearly constant height, because they are placed on top of transverse bars located 4 ft apart. There is little depth variation of the longitudinal bars between the transverse bars because the former are about 0.5 in. in diameter and do not bend.

Although all discussion has assumed that the pavement was cured concrete, this is not necessary. Any of the eddy

current techniques can be used immediately after paving because water is also transparent to the magnetic fields causing eddy currents. If measurements are made immediately after paving, any areas that are too thin could be corrected before the concrete sets.

Asphaltic pavements do not require the two-coil techniques because there is no steel reinforcement. Because asphalt is electrically transparent, an eddy current measurement only requires that foil be placed under the pavement. One coil is sufficient to determine the foil-to-coil distance.

Combined concrete and asphaltic pavements should be no more difficult to measure than concrete pavements. If the pavement to be measured is an asphalt layer on top of a concrete pavement, the foil must be placed below the layer to be measured. If the foil is placed between the asphalt and the concrete, the foil should not be a continuous sheet because this would stop the asphalt from binding to the concrete and would allow the asphalt to flow over the concrete. More investigation is needed on this problem.

The acceptability of the suggested techniques is as dependent on the cost as it is on the accuracy. The major cost, besides instrumentation, is the foil and its placement. Aluminum converter foil (1 mil) costs $0.53 per pound.* A 1-mile, 10-ft wide lane contains 52,800 sq ft. For the

---
* Kaiser Aluminum.

parallel-coil technique, 26,400 sq ft of the base must be covered with foil, at a foil cost of $197. To strengthen the foil and reduce the possibility of it tearing, the foil can be laminated to kraft paper. The foil and kraft will cost $246 per lane-mile. It is estimated that the placement of 48-in. wide strips, approximately 660 per mile, will take two men about 2 days per mile and cost about $200. Thus, foil in place will cost $450 per lane-mile. This cost can be compared with the present highway construction cost of $100,-000 per lane-mile and the cost of drilling core samples at $150 to $250 per core.

Electrical Technique Developed by Time Engineering Laboratory

It was brought to the attention of the research agency that Time Engineering Laboratories, in Chicago, had developed an electrical technique that required no pre-preparation of the pavement. Preliminary arrangements were made for agency personnel to visit the Time Engineering Laboratories. However, after several telephone calls made by the agency, the Time Engineering Laboratories were unable to arrange for the visit or to give any technical information concerning the device. Unfortunately, no evaluation of this technique has been possible.

APPENDIX D

BIBLIOGRAPHY

ACOUSTICS

AKASHI, T., "On the Measurement of Velocity and Loss of Ultrasonic Pulse in Concrete." *Proc. Third Internat. Conf. on Nondestructive Testing* (1961) pp. 574-578.

ANDREEU, G. A., and ZVEREU, V. A., "A Method for Investigating the Statistical Properties of Media Containing Random Inhomogeneities Using Frequency-Modulated Sound." *Soviet Phys. Acoustics*, Vol. 8, No. 1, pp. 29-36 (July-Sept. 1962).

ANDERSEN, J., and NERENST, P., "Summary of Expositions—International Symposium on Nondestructive Testing of Concrete." Internat. Union of Testing & Res. Labs. and Structures (RILEM), *Bull. No. 18* (Second Part), Summary 29 (June 1954).

ANDERSEN, J., and NERENST, P., "Wave Velocity in Concrete." *Proc. Am. Conc. Inst.*, Vol. 48, pp. 613-636 (Apr. 1952).

BACON, J. P., "New Developments in Ultrasonic Transducers and Their Application to Nondestructive Testing." *Nondestructive Test. Jour.*, Vol. 19, No. 3, pp. 184-187 (1961).

BACON, J. P., "New Developments in Ultrasonic Transducers and Their Application to Nondestructive Testing." *Periodical Monitor*, Vol. 1, No. 2 (Aug. 1961).

BARKHATOV, A. N., and CHERKASHIN, Y. N., "Measurement of the Back-Scattering of Sound by an Internal Wave." *Soviet Phys. Acoustics*, Vol. 8, No. 1, pp. 41-44 (July-Sept. 1962).

BATCHELDER, G. M., and LEWIS, D. W., "Comparison of Dynamic Methods of Testing Concretes Subjected to Freezing and Thawing." *Proc. ASTM*, Vol. 53, pp. 1053-1068 (1953).

BAWA, K. S., "General Discussion" (from "Effects of Concrete Characteristics on the Pulse Velocity—A Symposium, 1958"). *HRB Bull. 206* (1959).

BEAUZEE, M. C., "Errors of Measurement in the Determination of the Modulus of Elasticity by the Sonic Method." *Internat. Symposium on Nondestructive Testing of Materials and Structures*, Vol. 1, pp. 120-137.

BERNHARD, R. K., "Highway Investigation by Means of Induced Vibrations." *Bull. 49*, Eng. Exp. Station, Penn. State College (Oct. 1939).

BETZ, C. R., "Thickness Measurements by Ultrasonic Frequencies." *Elec. Mfg.*, Vol. 46, No. 2 (Aug. 1950).

BETZ, C. R., "Curved Crystal Developments in Ultrasonic Resonance Testing." *Nondestructive Test. Jour.*, Vol. 10, No. 4, pp. 28-31 (Apr. 1952).

BIOT, M. A., "Theory of Propagation of Elastic Waves in a Fluid Saturated Solid." *Jour. Acoust. Soc. Am.*, Vol. 28, p. 168 (1956).

BIOT, M. A., "Generalized Theory of Acoustic Propagation in Porous Dissipative Media." *Jour. Acoust. Soc. Am.*, Vol. 34, No. 9, p. 1254 (Sept. 1962).

BIRMANDREIS, C., "Nondestructive Testing of Bituminous Concrete: Relationship Between the Speed of Sound Propagation and the Temperature of the Concrete." *RILEM*, pp. 227-281 (1955).

BRADFIELD, G., and GATFIELD, E. N., "Determining the Thickness of Concrete by Mechanical Waves: Directed Beam Method." *Mag. of Conc. Res.*, Vol. 16, No. 46, pp. 49-53 (Mar. 1964).

BRADFIELD, G., and WOODROOFE, E. P. H., "Determining the Thickness of Concrete Pavements by Mechanical Waves: Diverging Beam Method." *Mag. of Conc. Res.*, Vol. 16, No. 46, pp. 45-48 (Mar. 1964).

BRADFIELD, G., "Dynamic Measurement of Elasticity Using Resonance Methods." *Brit. Jour. Appl. Phys.*, Vol. 11, p. 478 (Oct. 1960).

BRADFIELD, G., "Accurate Measurement of Dynamic Elastic Constants for Very Small Specimens." *Proc. Third Int. Congress on Acoustics*, p. 466 (1959).

BRADFIELD, G., "Accurate Assessment of Scatter from Singularities in Solids in Ultrasonic Flaw Detection." *Proc. Third Int. Congress on Acoustics*, p. 1255 (1959).

BRADFIELD, G., and GOODWIN, E. T., "A Note on Abnormalities in the Travel Time of a Wave Between Two Extensive Apertures." *Phil. Mag.*, Vol. 6, p. 1065 (Aug. 1961).

BRADFIELD, G. R., and WOODROOFE, E. P. H., "Determination of Thickness of Concrete Pavements Using Mechanical Waves." *Rep. No. PHYS/U5*, Teddington (England) Natl. Phys. Lab., Dept. of Scient. and Indus. Res., Gt. Britain (Feb. 1953).

BRADFIELD, G., "Ultrasonics in Solids." *Research*, Vol. 6, No. 2, pp. 68-79 (Feb. 1953).

BULLOCK, R. E., and WHITEHURST, E. A., "Effect of Certain Variables on Pulse Velocities Through Concrete." *HRB Bull. 206* (1958) pp. 37-42.

BUTLER, —, and VERNON, —, "Standing Wave Techniques of Thickness Measurements." *Jour. Acoust. Soc. Am.*, Vol. 18, p. 212 (1946).

CHATTERJEE, P. N., and SEN, B., "Use of Resonant Frequency Method as Standard for Nondestructive Testing of Concrete." *Jour. Inst. Eng.*, Vol. 39, No. 10, Part I, pp. 985-998 (June 1959).

CHEESMAN, W. J., "Dynamic Testing of Concrete with the Soniscope Apparatus." *Proc. HRB*, Vol. 29 (1949) pp. 176-181.

CHEESMAN, W. J., "Soniscope Studies of Concrete During Setting Period." *Hydro Res. News*, Vol. 3, No. 3, pp. 8-11 (July-Sept. 1951).

CHERNOV, —, "Correlation Properties of Waves in Randomly Inhomogeneous Media." *Jour. Acoust. Soc. Am.*, Vol. 28, p. 762 (1956).

COOK, —, "Thickness Measurements by Ultrasonic Resonance." *Jour. Acoust. Soc. Am.*, Vol. 27, p. 564 (1955).

DUFF, G. F. D., "On Wave Fronts and Boundary Waves." *Commun. on Pure and Appl. Math.*, Vol. 17, No. 2, pp. 189-227 (May 1964).

"Effects of Concrete Characteristics on the Pulse Velocity —A Symposium." *HRB Bull. 206* (1959) 74 pp.

ELVERY, R. H., "Discussion—Symposium on the Nondestructive Testing of Concrete. *RILEM* (1955) pp. 111-119.

ERDMAN, D., "Ultrasonic Pulse-Echo Techniques for Evaluating Thickness, Bonding and Corrosion." *Nondestructive Test. Jour.*, Vol. 18, No. 6, pp. 408-410 (1960).

ERWIN, W. S., "Ultrasonic Resonance Applied to Nondestructive Testing." *Rev. Sci. Inst.*, Vol. 18, No. 10, pp. 750-753 (Oct. 1947).

FACAVARU, I., and STANCULAESCU, G., "Influence of Shrinkage on the Variation of the Dynamic Modulus of Elasticity of Concrete with Rapid Setting Cement." *Jour. Am. Conc. Inst.*, Vol. 55, p. 825a (Jan. 1959).

FARRAR, N. S., "Vibration Waves in Concrete." *Eng.*, Vol. 206, pp. 378-380 (Sept. 1958).

FICKEN, "Sing-Around Method for Sound Velocities." *Jour. Acoust. Soc. Am.*, Vol. 28, p. 921 (1956).

"Field Soniscope Tests of Concrete." *Tech. Memo. No. 6-383*, U.S. Army Corps. of Engineers, Waterways Exper. Sta. (Apr. 1954).

FINAGIN, B. A., "Oscillations of a Piezoelectric Resonator at an Even Harmonic of the Thickness Resonance Oscillations." *Sov. Phys. Acoustics*, Vol. 8, No. 3, pp. 278-282 (Jan.-Mar. 1963).

FINAGIN, B. A., "Static Deformation of a Piezoelectric Plate Vibrating at Its Natural Frequency." *Sov. Phys. Acoustics*, Vol. 8, No. 4, pp. 356-360 (Apr.-June 1963).

FRIEDLANDER, F. G., "On the Radiation Field of Pulse Solutions of the Wave Equation. II." *Proc. Royal Soc.*, Series A, Vol. 279, No. 1378, pp. 386-395.

GASSMAN, F., "Elastic Waves Through a Packing of Spheres." *Geophys.*, Vol. 16, pp. 673-685 (Oct. 1951).

GATFIELD, E. N., "An Apparatus for Determining the Velocity of an Ultrasonic Pulse in Engineering Materials." *Electronic Eng.*, Vol. 24, No. 295, pp. 390-395.

GIBBS, F. T. W., "Determining Elastic Moduli of Materials by Resonance." *Metal Prog.*, Vol. 83, pp. 97-100 (Feb. 1963).

GLOTOV, V. P., "Coherent Scattering of Sound from Clusters of Discrete Inhomogeneities in Pulsed Emission." *Sov. Phys. Acoustics*, Vol. 8, No. 3, pp. 220-223 (Jan.-Mar. 1963).

GLOTOV, V. P., and LYSANOV, Y. P., "The Scattered Field for a Spherical Source Above a Plane Layer Con-

taining Discrete Inhomogeneities." *Sov. Phys. Acoustics,* Vol. 9, No. 2, pp. 142-147 (Oct.-Dec. 1963).

GOODELL, C. E., "Improved Sonic Apparatus for Determining Dynamic Modulus of Concrete Specimens." *Jour. Am. Concrete Inst.,* Vol. 22, No. 1, pp. 53-60 (Sept. 1950).

GULIN, E. P., "The Correlation of Amplitude and Phase Fluctuations in Sound Waves Reflected from a Statistically Rough Surface." *Sov. Phys. Acoustics,* Vol. 8, No. 4, pp. 335-340 (Apr.-June 1963).

GUMANYUK, M. N., "Method of Obtaining an Acoustic Contact Between Ultrasonic Transducers and Rocks." *Sov. Phys. Acoustics,* Vol. 9, No. 3, pp. 252-256 (Jan.-Mar. 1964).

HAMILTON, —, "Low Sound Velocity in Porosity Sediments." *Jour. Acoust. Soc. Am.,* Vol. 28, p. 16 (1956).

HARRIS, R. V., and BOBBIN, J. E., "Frequency-Dependent Effects in Ultrasonic Resonance Testing." *Nondestructive Test. Jour.,* Vol. 18, No. 5, pp. 327-332 (1960).

HASHMI, S. Z. R., "Application of Sing-Around Techniques to Ultrasonic Velocity Measurements in Large Samples of Solids." *Indian Jour. Pure Appl. Phys.,* Vol. 1, No. 4, pp. 159-160 (1963).

HEUKELOM, W., and FOSTER, C. R., "Dynamic Testing of Pavements." *Trans. ASCE,* Vol. 127, Part 1, pp. 425-457 (1962).

HOCHSHILD, R., "Applications of Microwaves in Nondestructive Testing." *Nondestructive Test. Jour.,* Vol. 21, No. 2 (Mar. 1963).

HOOK, J. F., "Generalization of a Method of Potentials for the Vector Wave Equation of Elasticity for Inhomogeneous Media." *Jour. Acoust. Soc. Am.,* Vol. 34, p. 354 (1962).

HOOK, J. F., "Green's Functions for Axially Symmetric Elastic Waves in Unbounded Inhomogeneous Media Having Constant Velocity Gradients." *Jour. Appl. Mech.,* Vol. 29E, No. 2, pp. 293-298 (1962).

HUGHES, —, "Velocity Dispersion of Elastic Waves in Solids." *Jour. Acoust. Soc. Am.,* Vol. 27, p. 1010 (1955).

"International Symposium on Nondestructive Testing of Materials and Structures." Internat. Union of Testing and Res. Labs. for Materials and Structures, Vol. 2.

JONES, R., and WHIFFEN, A. C., "A Survey of Dynamic Methods of Testing Roads and Runways." *HRB Bull. 277* (1960) pp. 1-7.

JONES, R., "A Vibration Method for Measuring the Thickness of Concrete Road Slabs in Situ." *Mag. of Conc. Res.,* pp. 97-101 (July 1955).

JONES, R., "Following Changes in the Properties of Road Bases and Subbases by the Surface Wave Propagation Method." *Civil Eng. and Pub. Wks. Rev.,* Vol. 58, No. 682, pp. 613-617 (May 1963); No. 683, pp. 777-780 (June 1963).

JONES, R., "Measurement and Interpretation of Surface Vibrations on Soil and Roads." *HRB Bull. 277,* pp. 8-29 (1960).

JONES, R., "Measurement of the Thickness of Concrete Pavements by Dynamic Methods: A Survey of the Difficulties." *Mag. of Conc. Res.,* pp. 31-34 (Jan. 1949).

JONES, R., and WRIGHT, P., "Some Problems Involved in Destructive and Nondestructive Testing of Concrete." *Roads and Road Constr.,* Vol. 32, No. 380, 249-251 (1954).

JONES, R., "Surface Wave Technique for Measuring the Elastic Properties and Thickness of Roads: Theoretical Development." *Brit. Jour. Appl. Phys.,* Vol. 13, No. 1, pp. 21-29 (1962).

JONES, R., "Testing of Concrete By Ultrasonic Pulse Technique," *Proc. HRB,* Vol. 32 (1953) pp. 258-275.

JONES, R., "Testing Concrete by Ultrasonic Pulse Techniques. II." *RILEM Bull.* 1 (Oct. 1954) pp. 75-93.

JONES, R., "The Application of Ultrasonics to the Testing of Concrete." *Research,* pp. 383-384 (May 1948).

JONES, R., "The Dynamic Testing of Concrete by a Supersonic Method." *Publ. Int. Assn. of Bridge Struct. Eng.,* pp. 227-240 (1948).

JONES, R., "Nondestructive Method of Testing Concrete During Hardening." *Conc. and Constr. Eng.,* Vol. 44, No. 4, pp. 127-129 (Apr. 1949).

JONES, R., "The Nondestructive Testing of Concrete." *Mag. of Conc. Res.,* pp. 67-76 (June 1949).

JONES, R., *Nondestructive Testing of Concrete.* Cambridge Univ. Press (1962).

JONES, R., "The Ultrasonic Testing of Concrete." *Ultrasonics,* Vol. 1, pp. 78-82 (Apr.-June 1963).

KAPLAN, M. F., "Recent Developments in Nondestructive Method of Testing Concrete with Particular Reference to Ultrasonic Pulse Technique." *Trans. S. African Inst. Civil Eng.,* Vol. 5, No. 8, pp. 243-252 (Aug. 1955).

KAPLAN, M. F., "The Effects of Age and Water/Cement Ratio upon the Relation Between Ultrasonic Pulse Velocity and Compressive Strength of Concrete." *Mag. of Conc. Res.,* Vol. 11, No. 32, pp. 85-91 (July 1959).

KOLSKY, H., "Stress Waves in Solids." *Jour. Sound and Vibration,* Vol. 1, No. 3, pp. 88-110 (July 1964).

KOZAN, G. R., "Investigation of Electronic Interval Timer for Rigid Pavement Evaluation." *Hwy. Res. Abstr.,* Vol. 24, No. 11, pp. 33-34 (Dec. 1954).

KOZAN, G. R., "Nondestructive Testing of Concrete Pavements." *Proc. HRB,* Vol. 34 (1955) pp. 368-378.

KNOPOFF, L., "Seismic Wave Velocities in Western Granite." *Trans. Am. Geophys. Union,* Vol. 3S, pp. 969-978 (Dec. 1954).

KRASILNIKOV, V. N., "Refraction of Flexure Waves." *Soviet Phys. Acoustics,* Vol. 8, No. 1, pp. 58-62 (July-Sept. 1962).

KRAUTKRAMER, J., "Determination of Size of Defects by Ultrasonic Impulse Echo Method." *Brit. Jour. Appl. Phys.,* Vol. 10, No. 6 (June 1959).

KURYANOV, B. F., "The Scattering of Sound at a Rough Surface with Two Types of Irregularity." *Sov. Phys. Acoustics,* Vol. 8, No. 3, pp. 252-258 (Jan.-Mar. 1963).

LAMB, D. R.,"A New Soniscope—The Elastiscope." *Proc. HRB*, Vol. 35 (1956) pp. 418-423.

LAPIN, A. D., "Note on the Scattering of a Plane Wave on a Periodically Uneven Surface." *Sov. Phys. Acoustics*, Vol. 8, No. 4, pp. 347-350 (Apr.-June 1963).

LEROLLAND, M., "Use of the Pendulum for the Study of Elastic Properties of Solids." *Nondestructive Test. Jour.*, Vol. 8, No. 4, pp. 16-19 (1950).

LESLIE, J. R., and CHEESMAN, W. J., "Ultrasonic Method of Studying Deterioration and Cracking in Concrete Structures." *Jour. Am. Conc. Inst.*, pp. 17-36 (Sept. 1949).

LESLIE, J., "Pulse Techniques Applied to Dynamic Testing." *Proc. ASTM*, Vol. 50, pp. 1314-1323 (1950).

LOCHNER, J. P., and DE V. KEET, W., "A Simple Method of Measuring the Dynamic Young's Modulus of Concrete." *Jour. Sci. Instr.*, Vol. 32, pp. 296-299.

LONG, B. G., KURTZ, H. F., and SANDENAW, T. A., "An Instrument and Technique for Field Determination of the Modulus of Elasticity and Flexural Strength of Concrete (Pavements)." *Proc Am. Conc. Inst.*, Vol. 41, No. 3, p. 217 (Jan. 1945).

MANKE, P., and HEMPHILL, L., "Nondestructive Thickness Tests for Highway Pavements." *Res. Publ. No. 14*, School of Civil Eng. Oklahoma State Univ.

MARKHAM, F., ET AL., "Measurement of Elastic Constants by the Ultrasonic Pulse Method." In "Physics of Nondestructive Testing." *Brit. Jour. Appl. Phys.*, Supplement No. 6, pp. 56-63 (1957).

MAXWELL, A. A., "Nondestructive Testing of Pavements." *HRB Bull.* 277 (1960) pp. 30-35.

"Measurements of Vibration Wave Velocities Through Concrete Structures." *Mat Lab. Rep. No. C-468*, U.S. Bureau of Reclamation (Nov. 1949).

MERKULOV, L. G., and YABLONIA, L. M., "Operation of a Damped Piezoelectric Transducer Containing a Number of Intermediate Layers." *Sov. Phys. Acoustics*, Vol. 9, No. 4, pp. 365-373 (Apr.-June 1964).

MEYER, E., "Transmission of Supersonic Sound in Setting Cement." *Electroacoustics*, Oxford Press, pp. 23-25 (1939).

MEYER, R. C., "Dynamic Testing of Concrete Pavements with the Soniscope." *Proc. HRB*, Vol. 31 (1952) p. 234-245.

MORSE, —, "Sound Propagation in Granular Media." *Jour. Acoust. Soc. Am.*, Vol. 24, p. 456 (1952).

MORSE, —, "Acoustic Propagation in Granular Media." *Jour. Acoust. Soc. Am.*, Vol. 24, p. 696 (1952).

MORSE, —, "Sound Propagation in the Ground." *Jour. Acoust. Soc. Am.*, Vol. 26, p. 940 (1954).

MUENOW, R., "A Sonic Method to Determine Pavement Thickness." Portland Cement Assn.

MUSGRAVE, M. J. P., "Elastic Waves in Anisotropic Media." *Proc. Solid Mechs.*, Vol. 11, p. 63 (1961).

MUSGRAVE, M. J. P., "Reflexion and Refraction of Plane Elastic Waves at a Plane Boundary Between Aeolotropic Media." *Geophys. Jour. Roy. Soc.*, Vol. 3, p. 406 (1960).

NERENST, P., "The Nondestructive Testing of Concrete with Special Reference to the Wave Velocity Method." *Building Res. Rep. No. 3*, Danish Nat. Inst. of Building Research, Copenhagen (1950).

"Nondestructive Testing of Concrete." *HRB Bibl. 33* (1963).

NIJBOER, L. W., and METCALF, C. T., "Dynamic Testing at the AASHO Road Test." *Proc. Internat. Conf. on Struct. Design of Asphalt Pavements*, Univ. of Michigan, pp. 713-721 (Aug. 1962).

NIJBOER, L. W., "Dynamic Investigations of Road Constructions." *Shell Bitumen Monograph No. 2* (1955).

NIJBOER, L. W., and VAN DER POEL, C., "A Study of Vibration Phenomena in Asphaltic Road Constructions." *Proc. Assn. Asphalt Pav. Tech.*, Vol. 22, (1953) pp. 197-231.

NISBET, R. T., "Measuring Wall Thickness by Pulse Echo Technique." *Mater. Protec.*, Vol. 2, No. 6, pp. 66-68 (1963).

"Nondestructive Tests on Road Concretes." *RILEM Bull. No. 17* (Apr. 1954).

NYBORG, —, and RUDNIK, —, "Acoustic Absorption in Sand and Soil." *Jour. Acoust. Soc. Am.*, Vol. 20, p. 597 (1948).

PARKER, W. E., "Pulse Velocity Testing of Concrete." *Proc. ASTM*, Vol. 53, pp. 1033-1042 (1953).

PENDERED, J. W., and BISHOP, R. E. D., "A Critical Introduction to Some Industrial Resonance Testing Techniques." *Jour. Mech. Eng. Sci.*, Vol. 5, No. 4, pp. 345-367 (Dec. 1963).

PETERSON, P. H., "Relation of Rebound-Hammer Test Results to Sonic Modulus and Compressive Strength Data." *Proc. HRB*, Vol. 34 (1955) pp. 387-399.

PICKETT, G., "Dynamic Testing of Pavements." *Jour. Am. Conc. Inst.*, Vol. 16, No. 5, pp. 473-488 (Apr. 1945).

PIHLAJAVAARA, S. E., "Introductory Bibliography for Research on Drying of Concrete. Transfer Phenomena, Measurement Methods, Structure, and Properties of Matter." The State Inst. of Tech. Res., Helsinki (1962).

PLOWMAN, J. M., "Young's Modulus and Poisson's Ratio of Concrete Cured at Various Humidities." *Mag. Conc. Res.*, Vol. 15, No. 44, pp. 77-82 (1963).

"Portable Ultrasonic Concrete Testing Apparatus." *Mag. Conc. Res.*, Vol. 7, No. 21, pp. 161-164 (Nov. 1955).

POTTER, —, "On Wave Propagation in a Random Inhomogeneous Medium." *Jour. Acoust. Soc. Am.*, Vol. 29, p. 197 (1957).

POWERS, T. C., "Measuring Young's Modulus of Elasticity by Means of Sonic Vibrations." *Proc. ASTM*, Vol. 38, Part II, pp. 460-469 (1938).

"Propagation of Surface Waves on an Inhomogeneous Plane Layer." *Rep. No. 1382-2*, Ohio State Univ. Res. Foundation (Feb. 1962).

"Proposed Tentative Method of Test for the Measurement of Pulse Velocity of Propagation of Elastic Waves in Concrete." *ASTM Bull. No. 204*, pp. 19-22 (Feb. 1955).

PROUD, —, "Propagation of Sound Pulses in a Dispersive Medium." *Jour. Acoust. Soc. Am.*, Vol. 28, p. 80 (1956).

REDWOOD, M., "Generation of Secondary Signals in Propagation of Ultrasonic Waves in Bounded Solids." *Proc. Phys. Soc.*, Vol. 72, No. 467, pp. 841-853 (Nov. 1958).

ROBINSON, A., "Wave Propagation in a Heterogeneous Elastic Medium." *Jour. Math. Phys.*, Vol. 36, pp. 210-222 (Oct. 1957).

SHANKAR, N. K., "Nondestructive Testing of Concrete by Ultrasonic Methods." *Indian Conc. Jour.*, Vol. 37, No. 7, p. 262, (1963).

SHCHUKIN, V. A., and YAKOVLEV, L. A., "Influence of Coupling Layers on the Accuracy of Velocity of Sound Measurements in Solids." *Sov. Phys. Acoustics*, Vol. 9, No. 3, pp. 315-318 (Jan.-Mar. 1964).

SHEVCHENKO, V. V., "Transmission of a Surface Wave over a Nonuniform Part of a Plane Impedance Surface." *Sov. Phys. Acoustics*, Vol. 9, No. 3, pp. 283-289 (Jan.-Mar. 1964).

SHILSTONE, C. M., and SHILSTONE, J. M., "Ultrasonic Inspection of Hardened Concrete." *Nondestructive Test. Jour.*, Vol. 19, No. 1, pp. 39-44 (1961).

SHIROKOVA, T. A., "The Variation in the Form of a Pulse Caused by the Effect of Random Inhomogeneities in a Medium." *Soviet Phys. Acoustics*, Vol. 9, No. 1, pp. 78-81, (July-Sept. 1963).

SPINNER, S., and TEFFT, W. E., "A Method for Determining Mechanical Resonance Frequencies and for Calculating Elastic Moduli from these Frequencies." *Proc. ASTM*, Vol. 61, pp. 1221-1238.

STONE, R. G., and MINTZER, D., "Experimental Study of High-Frequency Sound Propagation in a Randomly Inhomogeneous Medium." *Jour. Acoust. Soc. Am.*, Vol. 34, p. 735 (1962).

SWAIN, R. J., "Recent Techniques for Determination of in Situ Elastic Properties and Measurement of Motion Amplification in Layered Media." *Geophys.*, Vol. 27, No. 2, pp. 237-241 (Apr. 1962).

"Symposium on Vibration Testing of Roads and Runways." Held at Koninklijke/Shell-Laboratorium, Amsterdam.

TAHSIN, S. I., and SPENCE, R. D., "The Propagation of a Sound Pulse in a Medium with a Complex Elastic Modulus." *Phys. Rev.*, Vol. 94, p. 1442 (1954).

TEUMIN, I. I., "Measuring the Power of Elastic Vibrations Applied to a Load." *Sov. Phys. Acoustics*, Vol. 8, No. 3, pp. 291-293 (Jan.-Mar. 1963).

TYUTEKIN, V. V., "Reflection and Refraction of Flexure Waves at the Boundary of Separation Formed by Two Plates." *Soviet Phys. Acoustics*, Vol. 8, No. 2, pp. 180-184 (Oct.-Dec. 1962).

VAN DER POEL, C., "Vibration Research on Road Constructions." Symposium on Dynamic Testing of Soils, *ASTM Spec. Tech. Pub. No. 156*, pp. 174-185 (1953).

"Vibration Testing of Concrete." *RILEM Bull. No. 15* (Aug. 1953).

VIKTOROV, I. A., and ZUBOVA, O. M., "Directivity Diagrams of Radiators of Lamb and Rayleigh Waves." *Sov. Phys. Acoustics*, Vol. 9, No. 2 (Oct.-Dec. 1963).

VIKTOROV, I. A., "Rayleigh Waves in the Ultrasonic Range." *Sov. Phys. Acoustics*, Vol. 8, No. 2, pp. 118-130 (Oct.-Dec. 1962).

VIKTOROV, I. A., ET AL., "An Investigation of the Propagation of Ultrasonic Surface Waves at the Boundary Between a Solid and a Liquid." *Sov. Phys. Acoustics*, Vol. 9, No. 2, pp. 131-138 (Oct.-Dec. 1963).

VIKTOROV, I. A., "Effects of a Second Approximation in the Propagation of Waves Through Solids." *Sov. Phys. Acoustics*, Vol. 9, No. 3, pp. 242-246 (Jan.-Mar. 1964).

WALTER, L., "Progress in Nondestructive Testing of Concrete—The Use of Ultrasonics." *Indian Conc. Jour.*, Vol. 32, No. 2, pp. 50-52.

WEST, H. H., "Determination of Young's Modulus of Elasticity for Concrete by a Velocity Method." *Rep. No. C-322*, Mat. Lab., U.S. Bur. of Reclamation (1946).

WEST, H. H., "Measurements of Vibration Wave Velocities Through Concrete Structures." *Rep. No. C-468*, Mat. Lab., U.S. Bur. of Reclamation (Nov. 10, 1949).

WEST, H. H., "Determination of Young's Modulus of Elasticity for Concrete by a Velocity Method." *Rep. No. C-468*, Mat. Lab., U.S. Bur. of Reclamation (Nov. 10, 1949).

WHITEHURST, E. A., "Pulse Velocity Techniques and Equipment of Testing Concrete." *Proc. HRB*, Vol. 33 (1954) pp. 226-242.

WHITEHURST, E. A., "Effect of Variations in Mix Design or Curing Conditions on a Pulse Velocity-Strength Relationship." *HRB Bull.* 206 (1959) pp. 57-63.

WHITEHURST, E. A., "Soniscope Tests on Concrete Structures." *Jour. Am. Conc. Inst.*, p. 433 (Feb. 1951).

WHITEHURST, E. A., "Use of the Soniscope for Measuring Setting Time of Concrete." *Proc. ASTM*, Vol. 51, p. 1166 (1951).

WHITEHURST, E. A., "Pulse Velocity Techniques and Equipment for Testing Concrete." *Proc. HRB*, Vol. 33, pp. 226-241 (1954).

WORLTON, D. C., "Ultrasonic Testing with Lamb Waves." *Nondestructive Test. Jour.*, Vol. 15, No. 4, pp. 218-222 (1957).

WYLLIE, M. R. J., ET AL., "An Experimental Investigation of Factors Affecting Elastic Wave Velocities in Porous Media." *Geophys.*, Vol. 23, pp. 459-493 (July 1958).

NUCLEAR

American Institute of Physics Handbook." McGraw-Hill (1957) pp. 8-104.

BAKER, P. E., "Density Logging with Gamma Rays." *Petrol. Trans. AIME*, Vol. 210, pp. 289-294 (Oct. 1957).

BOURGEOIS, J., ERTAUD, A., and JACKSQUESS, T., "Investigation of Several Special Shielding Concretes." *Jour. Phys. Radium*, Vol. 14, pp. 317-322 (May 1953).

CAREY, W. N., JR., and REYNOLDS, J. F., "Some Refinements in Measurement of Surface Density by Gamma Ray Absorption." *HRB Spec. Rep. 38* (1958) pp. 1-23.

COLE, E. K., and DAVIS, R. G., "Backscatter Measuring Gauges." Brit. Pat. No. 814,286 (June 3, 1959).

FEARON, R. E., "Gamma-Ray Well Logging." *Nucleonics,* Vol. 7, No. 4, pp. 67-75 (Apr. 1949).

GATLIN, C., *Petroleum Engineering.* Prentice-Hall (1960).

GRODSTEIN, G. W., "X-Ray Attenuation Coefficients from 10 kev to 100 Mev," *Nat. Bur. Stand. Circ. 583,* U.S. Govt. Printing Off., Washington, D.C. (Apr. 30, 1957) 50 pp.

HART, H., and KARSTENS, E., "Radioactive Isotopes in Thickness Measurement." *Vieb Vierial Tech.* (Berlin) (1958).

MANKE, P. G., and HEMPHILL, L., "Nondestructive Thickness Tests for Highway Pavements." *Res. Pub. No. 14,* School of Civil Eng., Oklahoma State Univ., pp. 9-24 (Bibliography of nuclear methods).

MAZARI, M., "Coefficients of Linear Absorption of Fast Neutrons in Concrete." *Rev. Mex. Fix.,* Vol. 6, pp. 1-8 (1957).

"New Logging Technique Measures Density, Porosity." *World Oil,* Vol. 139, No. 7, pp. 142, 144, 156 (Dec. 1954).

PLACZEK, G., "The Functions $E_n(X)$." *Rep. NRC No. 1547,* Div. of Atomic Energy, Nat. Res. Council of Canada (Dec. 1946).

PURTNAM, J. L., "Development Control and Automation." Vol. 2, No. 11, pp. 417-421 (Nov. 1955).

TOLAN, J. H., and McINTOSH, W. T., "Investigations of Applications of Compton Backscatter." *Rep. NR-88,* Lockheed Nuclear Products, Marietta, Ga. (July 1960).

ELECTRICAL

BALACHANDRAN, M., "Measurements of Dielectric Constants and Loss Tangents of Building Materials." (in German) *Zeits. für Angerwandte Phys.,* Vol. 7, No. 12, pp. 588-593 (Nov. 1955).

COHN, G. I., and EBSTEIN, B., "A Microwave Non-Contacting Tracing Technique for Automatic Contour-Following Machines." *Proc. Nat. Electron. Conf.* (Oct. 1956).

CUMING, W. A., "Materials for RF Shielded Chambers and Enclosures." Digest of Fourth Nat. Symp. on Radio Frequency Interference (June 1962).

HAMMOND, E., and ROBSON, T. D., "Comparison of the Electrical Properties of Various Kinds of Cement and Concrete." *The Engineer,* Vol. 199, 5165 (Jan. 21, 1955) pp. 78-80; No. 5166 (Jan. 28, 1955) pp. 114-115.

REED, H. R., "Propagation Data for Interference Prediction. *RADC-TN-59-218,* Vol. 11, pp. 55-109, DDC No. AD 233-387 (Jan. 1960).

Reference Data for Radio Engineers. American Book—Stratford Press, N.Y., 4th Ed. (1956).

Published reports of the

NATIONAL COOPERATIVE HIGHWAY RESEARCH PROGRAM

are available from:

Highway Research Board
National Academy of Sciences
2101 Constitution Avenue
Washington, D.C. 20418

* Highway Research Board Special Report 80.